

Inhibition of the MDM2/p53 Interaction

Design, Synthesis and Evaluation of MDM2 Inhibitors

Mariell Pettersson



UNIVERSITY OF GOTHENBURG

Department of Chemistry and Molecular Biology

University of Gothenburg

2015

DOCTORAL THESIS

Submitted for fulfilment of the requirements for the degree of

Doctor of Philosophy in Chemistry

Inhibition of the MDM2/p53 Interaction

Design, Synthesis and Evaluation of MDM2 Inhibitors

Mariell Pettersson

Cover illustration: Model of a spiro-2,5-diketopiperazine bound to MDM2.

© Mariell Pettersson

ISBN: 978-91-628-9313-2

<http://hdl.handle.net/2077/37905>

Department of Chemistry and Molecular Biology

SE-412 96 Göteborg

Sweden

Printed by Ineko AB

Källered, 2015

Abstract

Numerous essential cellular processes are regulated by protein-protein interactions (PPIs) and PPIs have therefore been recognised as potential new drug targets. The transcription factor p53 is often referred to as the guardian of the genome due to its involvement in DNA repair, induction of cell cycle arrest and cellular apoptosis. The amount of p53 in a cell is mainly controlled by the negative regulator MDM2, which upon complex formation with p53 leads to an overall reduction of the p53 level. Consequently, inhibition of the MDM2/p53 interaction has emerged as a promising new therapeutic strategy for the treatment of cancers retaining wild-type p53.

This thesis describes the design, synthesis and evaluation of β -hairpins, 8-(triazolyl)purines and 2,5-diketopiperazines as MDM2/p53 interaction inhibitors.

β -Hairpin derivatives were synthesised using automated solid phase peptide synthesis followed by a head to tail cyclisation in solution. Evaluation of the MDM2 inhibitory activity of the β -hairpin derivatives together with solution conformational analysis using NAMFIS calculations revealed that molecular flexibility is important to gain highly potent MDM2 inhibitors. Two series of 8-(triazolyl)purines and 2,5-diketopiperazines (2,5-DKPs) were evaluated as MDM2 inhibitors. The first series were designed to directly mimic an α -helical region of the p53 peptide, containing key residues in the i , $i+4$ and $i+7$ positions. Conformational analyses indicated that both 8-(triazolyl)purines and 2,5-DKP derivatives were able to place substituents in the same spatial orientation as an α -helical template. The second series were designed primarily based on structure-based docking studies. The most potent inhibitors identified were from the latter series and displayed micromolar IC_{50} -values in a biochemical fluorescence polarization assay. Binding to MDM2 was confirmed by WaterLOGSY experiments. Efficient synthetic protocols for the synthesis of both tetrasubstituted 8-(triazolyl)purines and tetrasubstituted 2,5-DKPs have been developed. Furthermore, an efficient bromination protocol for 8-bromination of electron rich purines utilising pyridiniumtribromide was developed. The fluorescent properties of the 8-(triazolyl)purines were determined and it was found that the regioisomerism of the triazole has an important impact on the quantum yield.

Keywords: Protein-protein interaction, MDM2/p53 interaction, MDM2 inhibitors, α -helix mimetics, β -hairpin, 2,5-diketopiperazine, spiro-2,5-diketopiperazine, purine, 8-(triazolyl)purine, solution conformational analysis, NAMFIS, fluorescence.

List of publications

This thesis is based on the following papers and manuscripts, which are referred to in the next by their Roman numerals.

- I **Flexibility is a Key Feature for Inhibition of the MDM2/p53 Protein-Protein Interaction by Cyclic Peptidomimetics**
Emma Danelius, Mariell Pettersson, Matilda Bred, Jaeki Min, R. Kiplin Guy, Morten Grøtli, Mate Erdelyi
Manuscript
- II **8-Triazolylpurines: Towards Fluorescent Inhibitors of the MDM2/p53 Interaction**
Mariell Pettersson*, David Bliman*, Jimmy Jacobsson, Jesper Nilsson, Jaeki Min, Luigi Iconaru, R. Kiplin Guy, Richard W. Kriwacki, Joakim Andréasson, Morten Grøtli
Submitted Manuscript
- III **8-Bromination of 2,6,9-Trisubstituted Purines with Pyridinium Tribromide**
David Bliman*, Mariell Pettersson*, Mattias Bood, Morten Grøtli
Tetrahedron Lett. **2014**, *55*, 2929-2931
- IV **Design, Synthesis and Evaluation of 2,5-Diketopiperazines as Inhibitors of the MDM2/p53 Interaction**
Mariell Pettersson, Maria Quant, Jaeki Min, Luigi Iconaru, R. Kiplin Guy, Richard W. Kriwacki, Kristina Luthman, Morten Grøtli
Manuscript

* Equally contributing authors

Contribution to Papers I-IV

- I Formulated the research problem together with ED. Performed or supervised parts of the synthesis, contributed to the interpretation of the results and the conformational analysis, wrote the manuscript together with ED. Performed parts of the fluorescent polarisation measurements together with JM.
- II Formulated the research problem with DB. Also performed or supervised the experimental work, interpreted the results and wrote the manuscript together with DB and contributed to the photophysical characterisation. Performed parts of the fluorescent polarisation measurements together with JM.
- III Formulated the research problem, performed or supervised parts of the experimental work, contributed to interpretation of the results and wrote the manuscript together with DB.
- IV Contributed significantly to formulation of the research problem, performed or supervised the experimental work, interpreted the results and wrote the manuscript. Performed parts of the fluorescent polarisation measurements together with JM.

List of Abbreviations

AA	Amino acid
Bn	Benzyl
Boc	<i>tert</i> -Butyloxycarbonyl
<i>t</i> Bu	<i>tert</i> -Butyl
CDI	Carbonyldiimidazole
Cmp	Compound
Conc	Concentrated
CuAAC	Copper catalysed azide-alkyne cycloaddition
DCM	Dichloromethane
DIPEA	<i>N,N</i> -Diisopropylethylamine
2,5-DKP	2,5-Diketopiperazine
DIAD	Diisopropyl azodicarboxylate
DMAP	4-Dimethylaminopyridine
DMEDA	<i>N,N'</i> -Dimethylethylenediamine
DMF	Dimethylformamide
DMSO	Dimethylsulfoxide
DNA	Deoxyribonucleic acid
eq.	Equivalent(s)
FDA	Food and Drug Administration
Fmoc	9-Fluorenylmethoxycarbonyl
FP	Fluorescence polarisation
GPCR	G protein coupled receptor
h	Hours
HATU	1-[Bis(dimethylamino)methylene]-1 <i>H</i> -1,2,3-triazolo[4,5- <i>b</i>]pyridinium-3-oxide hexafluorophosphate
HPLC	High performance liquid chromatography
HRMS	High resolution mass spectroscopy
HTS	High throughput screening
IC ₅₀	Inhibitor concentration required to inhibit an enzyme by 50%
LCMS	Liquid chromatography
Leu	Leucine
LG	Leaving group
MDM2	Mouse Double Minute 2 Homolog
MW	Microwave
NAMFIS	NMR analysis of molecular flexibility in solution

n.d	Not determined
NOE	Nuclear Overhauser effect
NOESY	Nuclear Overhauser effect spectroscopy
NMR	Nuclear magnetic resonance
nr	No reaction
o.n	Over night
p53	Tumour protein p53
PDB	Protein Data Bank
PG	Protecting group
Phe	Phenylalanine
ppm	Parts per million
PPI	Protein-protein interaction
Pro	Proline
PyBOP	Benzotriazol-1-yl-oxytripyrrolidinophosphonium hexafluorophosphate
Pyr	Pyridinium
RMSD	Root-mean-square cutoff
RNA	Ribonucleic acid
r.t.	Room temperature
SPPS	Solid phase peptide synthesis
SPR	Surface plasmon resonance
TBTU	<i>N</i> -[(1 <i>H</i> -Benzotriazol-1-yl)(dimethylamino)methylene]- <i>N</i> - methylmethanaminium hexafluorophosphate <i>N</i> -oxide
TFA	Trifluoroacetic acid
THF	Tetrahydrofuran
TIPS	Triisopropylsilane
TLC	Thin layer chromatography
TMS	Trimethylsilyl
Trp	Tryptophane
WaterLOGSY	Water-Ligand Observed via Gradient Spectroscopy

Table of Contents

1	Introduction	1
1.1	Protein-protein interaction.....	1
1.2	The MDM2/p53 interaction.....	3
1.3	MDM2/p53 interaction inhibitors.....	6
1.3.1	Type I inhibitors.....	7
1.3.2	Type II inhibitors.....	8
1.3.3	Type III inhibitors.....	9
2	Methods Used for Biological Evaluation	13
2.1	Fluorescence polarisation assay.....	13
2.2	Surface plasmon resonance assay.....	14
2.3	Water-ligand observed <i>via</i> gradient spectroscopy.....	15
3	Aims of the Thesis	19
4	β-Hairpins as Inhibitors of the MDM2/p53 PPI (Paper I)	21
4.1	β -Hairpins.....	21
4.1.1	Design of stable β -hairpins.....	22
4.2	Solid phase peptide synthesis.....	22
4.3	Conformational studies of β -hairpins.....	26
4.3.1	NMR analysis of molecular flexibility in solution.....	26
4.4	β -Hairpins as MDM2 inhibitors (Paper I).....	28
4.4.1	Design of β -hairpins.....	29
4.4.2	Synthesis of β -hairpins.....	30
4.4.3	Conformational analysis of peptides I and 1-3.....	33
4.4.4	Evaluation of β -hairpins as MDM2 inhibitors.....	36
4.5	Summary paper I.....	37
5	8-(Triazolyl)purines as Inhibitors of the MDM2/p53 PPI (Paper II and III)	39
5.1	Purines.....	39
5.2	8-(Triazolyl)purines as MDM2 inhibitors (Paper II).....	41
5.2.1	Design of 8-(triazolyl)purines as type III inhibitors.....	41
5.2.2	Synthesis of 8-(triazolyl)purines.....	42

5.2.3	Synthesis of 8-(triazolyl)purines as type III inhibitors	43
5.2.4	Evaluation of the purine type III mimetics as MDM2 inhibitors	47
5.2.5	Conformational analysis of 13a and 14a	47
5.2.6	Design of a second series of 8-(triazolyl)purines	49
5.2.7	Synthesis of 8-(triazolyl)purines as type II mimetics.....	50
5.2.8	Evaluation of the 8-(triazolyl)purines type II mimetics as MDM2 inhibitors.....	53
5.2.9	Photophysical characterisation of 8-(triazolyl)purines.....	54
5.3	8-Bromination of purines (Paper III)	57
5.4	Summary of papers II and III.....	60
6	2,5-Diketopiperazines as Inhibitors of the MDM2/p53 PPI (Paper IV)	61
6.1	2,5-Diketopiperazines	61
6.1.1	Synthesis of 2,5-DPKs.....	62
6.2	2,5-DKPs as MDM2 inhibitors (Paper IV).....	65
6.2.1	Design of 2,5-DKPs as type III mimetics	65
6.2.2	Synthesis of 2,5-DKPs as type III mimetic	67
6.2.3	Biological evaluation of 2,5-DKPs as type III inhibitors	71
6.2.4	Design of 2,5-DKPs as type II inhibitors.....	71
6.2.5	Synthesis of 2,5-DKPs as type II inhibitors	73
6.2.6	Biological evaluation of 2,5-DKPs as type II inhibitors.....	85
6.3	Summary of paper IV.....	87
7	Concluding Remarks and Future Perspectives	89
8	Acknowledgement	91
9	Appendices	93
10	References	101

1 Introduction

For the development of novel drug treatments additional drug targets need to be identified. Today there are ca 3,000 proteins identified for which the activity is expected to be controlled by drugs.¹ Only a small fraction of these proteins (ca 10%) has been explored as therapeutic targets. Most of the explored protein targets belong to few protein families, such as the G protein coupled receptors (GPCRs), enzymes, ion channels, or nuclear hormone receptors.² The majority of these proteins are regulated by the binding of an endogenous small molecule as a substrate/ligand or a co-factor. However, protein-protein complex formation also modulates protein activity. It has been estimated that there are between 130,000 – 650,000 protein-protein interactions (PPIs) in human cells of which only a few are known.³ As several important cellular processes are regulated by PPIs they have been recognised as potential drug targets.⁴ This thesis focuses on the development of compounds that interrupts PPIs.

1.1 Protein-protein interaction

A protein-protein interaction (PPI) is defined as “*an interaction of two identical or dissimilar proteins at their domain interfaces that regulates the function of the protein complex (interactions involving enzyme active sites are not termed PPIs in drug discovery)*”.⁵

PPIs are involved in the regulation of numerous essential cellular processes including cell growth, DNA replication, transcriptional activations and transmembrane signal transduction and play a central role in disease development.⁶ Every PPI associated with a disease is a potential new drug target. Consequently, modulating PPIs is a

promising approach to gain valuable information and understanding associated with pathophysiology and hence development of new therapeutics.⁵

Targeting PPIs is considered to be more challenging compared to more conventional protein targets such as enzymes or GPCRs.⁷⁻⁹ The protein interaction sites are often shallow, solvent exposed and cover a large surface area ($\sim 1500-3000 \text{ \AA}^2$) compared to enzymes/receptors that typically bind small molecules in smaller ($\sim 300-500 \text{ \AA}^2$) well-defined binding pockets that are less exposed to solvent. In addition, PPIs involve a large number of weak, often hydrophobic, interactions and there are generally no small molecule substrates/ligands that can be used as starting points for the design of modulators targeting PPIs.¹⁰

In this thesis, inhibitors targeting the protein-protein interface will be discussed. In addition to the PPI interface, there are examples of small molecules that target allosteric sites that upon binding induce a conformational change and thereby prevent the PPI. Another example is the so called interfacial binders that form ternary or higher order complexes, locking the proteins in a non-productive conformation.⁴ The two latter will not be discussed in this thesis.

The amino acid residues at the protein-protein interface do not contribute equally to the formation of the protein-protein complex. A small subset of residues has a higher contribution to the binding free energy and these are referred to as “hot spot” residues.¹¹⁻¹³ The energy contribution of individual residues in a PPI have been identified by the use of alanine scans and a hot spot residue is defined as a residue that when exchanged to alanine shows a decrease in $\Delta\Delta G$ of $\geq 2 \text{ kcal/mol}$.¹⁴⁻¹⁵ Although informative, alanine scanning experiments are time-consuming and expensive, furthermore, alanine mutations can destabilise and change the protein conformation preventing the PPI. Other techniques that have been used to identify hot spots include

NMR spectroscopy and x-ray crystallography.¹⁶⁻¹⁸ Computational methods have also been developed for prediction of hot spots at protein-protein interfaces.¹⁹ Although the term hot spot often refers to single residues, it can also be used to describe regions (sometimes also called hot regions) that are comprised of a set of hot spot residues. PPIs with hot spot regions that adopt a well-defined secondary structure such as an α -helix, β -sheet or loop conformation have been identified as particularly interesting drug targets.¹⁹⁻²⁰ In this thesis PPIs having an α -helix at the interface is of particular interest.

As many as 62% of all PPIs in the Protein Data Bank (PDB) have an α -helix at the interface.²¹⁻²² A general α -helix is defined by the torsion angles $\Phi = -60^\circ$ and $\Psi = -45^\circ$. The α -helix has a rise of 1.5 Å/residue or 5.4 Å/turn resulting in around 3.4 amino acid residues per turn.²³ In this thesis a specific α -helix is investigated that interacts with its protein partner mainly with the i , $i+4$ and $i+7$ residues located on the same face of the helix (see section 1.2). A mimic that can reproduce the key interactions of the α -helix should be able to bind to the target site of the α -helix and inhibit the PPI.²¹

Despite the challenges with targeting PPIs, there have been some successes with hot spot-based design of small molecules PPI inhibitors. There are examples that have reached clinical trials for the treatment of cancer²⁰ including inhibitors of the MDM2/p53²⁴ and Bcl-2/Bax PPIs.²⁵⁻²⁶ Besides small molecules, protein-based PPI modulators such as monoclonal antibodies have also been reported.²⁷⁻²⁹

1.2 The MDM2/p53 interaction

The MDM2/p53 interaction has been identified as an attractive target for the development of drugs used for cancer treatment.³⁰ The transcription factor p53 plays

an essential role in preventing tumour development due to its involvement in DNA repair, cell cycle arrest, cellular apoptosis and cell senescence.

Stress signals caused primarily by DNA damage, but also hypoxia and heat shock, activate p53 by post-translational modifications such as phosphorylation or acetylation, ultimately resulting in apoptosis or cell cycle arrest.³¹⁻³² These modifications affect the p53 protein in two ways, first the half-life is prolonged from minutes to hours and the concentrations of p53 in the cell is increased up to 10 fold. Secondly, the ability of p53 to promote transcription is improved as these modifications facilitate binding of specific DNA sequences.³³

Dysfunctional p53 is present in most, if not all, human cancers. Inactivation of p53 can be caused by mutations in the TP53 gene (the gene coding for p53).³⁴ The p53 activity is also regulated by a number of negative and positive feedback loops where the most important involves the negative regulator MDM2 (Figure 1).^{33,35} The function of MDM2 is to control p53 activity primarily by keeping the p53 levels low in unstressed cells and switching off p53 after a stress induced activation.³³ However, overexpression of MDM2 leads to rapid degradation of wild type p53.³¹

Three events take place upon binding of MDM2 to p53: (1) MDM2 functions as an E3 ligase and ubiquitinates p53 which leads to proteasomal degradation of p53. (2) MDM2 binds to the N-terminal transactivation domain of p53 and prevents p53 from direct binding to DNA and hence to work as a transcription factor. (3) MDM2 promotes export of p53 out from the cell nucleus.

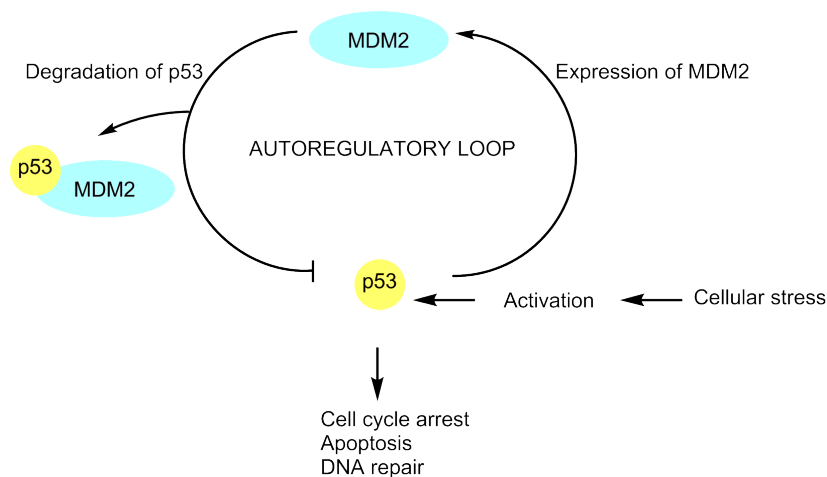


Figure 1. Schematic representation of the autoregulatory feedback loop for the inhibition of p53 by MDM2. Upon cellular stress p53 is activated which in turn activates expression of MDM2 and transcriptional activity (cell cycle arrest, apoptosis and DNA repair). MDM2 binds to p53 and forms a complex which leads to deactivation of p53.

Consequently, inhibition of the MDM2/p53 interaction has potential as treatment of human cancers which have retained wild type p53, by restoring the tumour suppressor activity of wild type p53.³⁰ An overexpression of MDM2 is in certain cases associated with a lower survival rate as a result of decreased response to therapeutic treatment, increased recurrence and metastasis.³⁶⁻³⁷ Mutant p53 is often resistant to degradation promoted by MDM2 and therefore inhibition of the MDM2-p53 interaction would have no therapeutic effect in these cases.^{31,38}

The crystal structure of the MDM2/p53 complex revealed that the amino acid residues 15–29 of p53 interact with MDM2 and residues Phe19 to Leu29 form an α -helix in the complex (Figure 2). Three hot spot residues in the i , $i+4$ and $i+7$ position of the p53 helix have been identified, Phe19, Trp23 and Leu29, of which the side chains bind to a hydrophobic cleft of MDM2.³⁹ In this thesis, the hydrophobic cleft of

MDM2 will be divided into three pockets that will be referred to as the Phe-, Trp- and Leu-pocket, respectively.

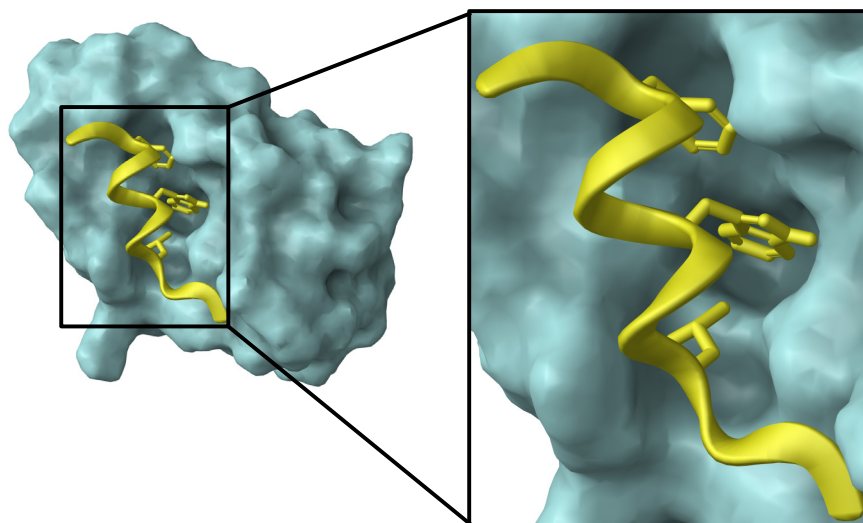


Figure 2. Crystal structure of p53 (yellow) bound to MDM2 (turquoise), the side chains of the hot spot residues Phe19, Leu29, Trp23 (from the top and downwards) are shown (PDB code: 1YCR).

1.3 MDM2/p53 interaction inhibitors

The fact that p53 interacts *via* an α -helical segment (see section 1.2) makes it possible to use the α -helix as a starting point and design α -helix mimetics as MDM2/p53 interaction inhibitors. A number of examples of α -helix mimetics that inhibit the MDM2/p53 interaction have been published.⁴⁰ The inhibitors are often divided into three groups, type I, II and III.⁴¹ The different types have in common that they consist of a scaffold that can place substituents in the same spatial orientation as the i , $i+4$ and $i+7$ side chains of the p53 helix (Figure 3).

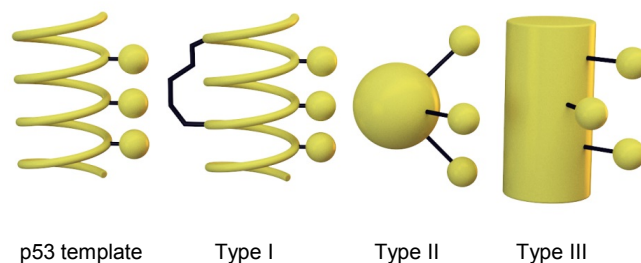


Figure 3. Schematic representation of the different types of α -helix mimetics, the p53 peptides is used as a template for the design of the mimetics. The mimetics have the ability to place the side chains or substituents (illustrated as yellow spheres) in the same spatial orientation as the important side chains (i , $i+4$ and $i+7$) of p53. Type I mimetics, often called synthetic peptides, consist of stabilised peptides. Type II and III mimetics are often non-peptidic small molecules, where type III is designed to mimic the topography of an α -helix whereas type II are not. Type II inhibitors have traditionally been identified in HTS campaigns and as a result vary widely in structure.

1.3.1 Type I inhibitors

Type I inhibitors are synthetic peptides that mimic the conformation of the p53 helix. There are synthetic linear peptides that can adopt a helical conformation and inhibit the MDM2/p53 interaction.⁴¹ However, the use of linear peptide sequences as drugs is associated with some drawbacks, for instance they often adopt random conformations in solution.⁴² Furthermore, they often suffer from low cell permeability and are proteolytically unstable as proteases are known to bind their substrates in an extended conformation.⁴³ This can be overcome by the use of stabilised peptides and a number of methods for stabilising α -helix structures of short peptides have been reported.^{42,44} One example is to use hydrocarbon stapling methods, where incorporation of a hydrocarbon linker holds the peptide in a helical conformation.⁴⁵ SAH-p53-8 is an example of a stabilised peptide used as an inhibitor of MDM2 showing activity both *in vitro* with an IC_{50} of 216 nM in a biochemical assay and *in vivo* (Figure 4).⁴⁶

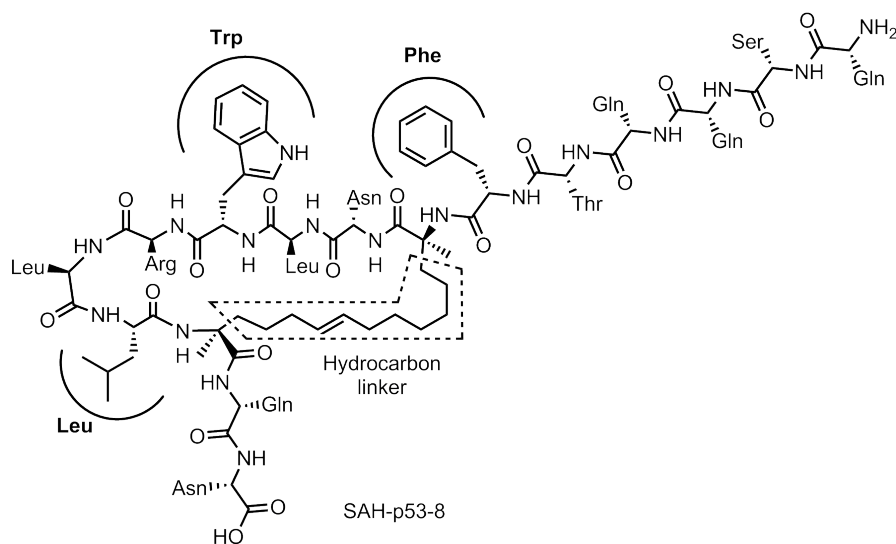


Figure 4. Structure of SAH-p53-8, a type I inhibitor of MDM2, the curved lines represent the Phe-, Trp- and Leu-pockets of MDM2.

Crystal structures of SAH-p53-8 bound to MDM2 show that the hydrocarbon chain stabilises the helical conformation and facilitates binding of the Leu, Trp, and Phe residues in the correct MDM2 pockets.⁴⁷

1.3.2 Type II inhibitors

Small non-peptide scaffolds that place substituents in the same spatial orientation as the p53 helix, but are not designed to mimic the α -helix topography are referred to as type II inhibitors or functional mimetics.⁴¹ These inhibitors have traditionally been identified in high throughput screening (HTS) campaigns. Using HTS, Hoffmann-La Roche discovered the nutlins as the first small molecule inhibitors of the MDM2/p53 interaction. The most potent compound was nutlin-3 with an IC_{50} of 90 nM in a biochemical assay (Figure 5). Nutlin-3 bound to MDM2 was the first example of a crystal structure with a non-peptidic small molecule bound to MDM2.⁴⁸ Nutlin-3 is today routinely used as a tool compound to study p53 biology. Other small molecule

inhibitors of the MDM2/p53 interaction identified by HTS include benzodiazepinedione ($K_d = 80 \text{ nM}$)⁴⁹ and chromenotriazolopyrimidine ($IC_{50} = 1.23 \text{ }\mu\text{M}$)⁵⁰ derivatives (Figure 5).

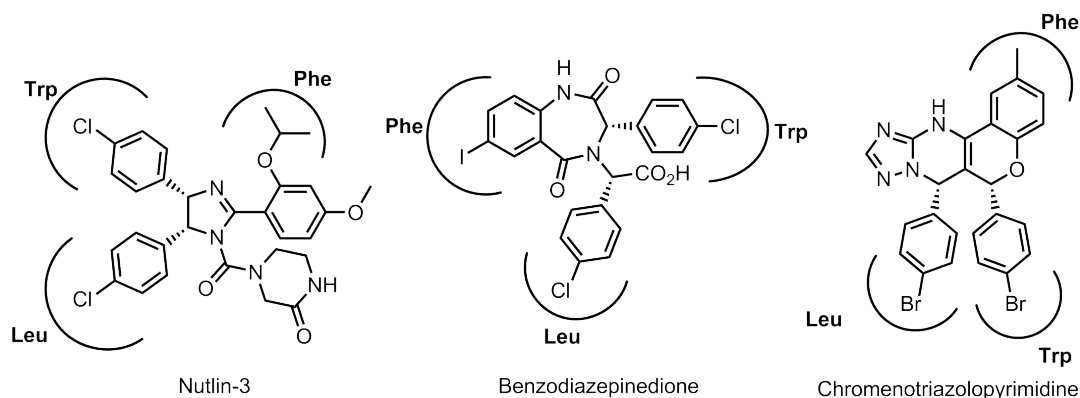


Figure 5. Examples of type II mimetics as MDM2 inhibitors, curved lines represent the Phe-, Trp- and Leu-pockets of MDM2.

1.3.3 Type III inhibitors

Type III inhibitors or α -helix mimetics consist often of non-peptidic scaffolds that mimic the topography of an α -helix and can position the substituents in the same spatial orientation as the i , $i+4$ and $i+7$ amino acid side chains of the p53 helix.⁴¹ In comparison to type II, which do not mimic the helical conformation of the backbone, the type III inhibitor scaffolds are generally more extended.

Hamilton and co-workers identified the first type III mimetics, the terphenyl derivatives (Figure 6).⁵¹ They recognised that a terphenyl scaffold in a staggered conformation places the *ortho* substituents to mimic the i , $i+3(4)$ and $i+7$ residues of an α -helix and terphenyl-1 has a $K_i = 0.182 \text{ }\mu\text{M}$ against MDM2 (Figure 6).⁵² Inspired by the terphenyl scaffold, a number of type III mimetics has been reported.^{41,53} Wilson and co-workers have reported the oligobenzamide scaffold as useful MDM2 inhibitors

($IC_{50} = 1.0 \mu\text{M}$).⁵⁴ Additional type III mimetics include pyrrolopyrimidine ($K_i = 0.62 \mu\text{M}$)⁵⁵ and spirooligomer ($K_d = 0.4 \mu\text{M}$) derivatives.⁵⁶ Fasan *et al.* have reported β -hairpin-based MDM2 inhibitors.⁵⁷ It was identified that a β -hairpin could function as a scaffold and hold amino acid side chains in the correct relative positions mimicking the α -helix of p53. The most potent derivative found had an IC_{50} of 140 nM (Figure 6).⁵⁸ β -Hairpins do not per definition fit into this group as type III mimetic scaffolds often are non-peptidic, but they can be placed in this group since the β -hairpin can place the Leu, 6CITrp and Phe residues in the same spatial orientation as the i , $i+4$ and $i+7$ residues in an α -helix (Figure 6).

The type III mimetics have the possibility to be used against different PPIs having an α -helix at the interface just by exchanging substituents. This has been illustrated by terphenyl derivatives disrupting the Bcl-x_L/Bax interaction in addition to the MDM2/p53 interaction.⁵⁹

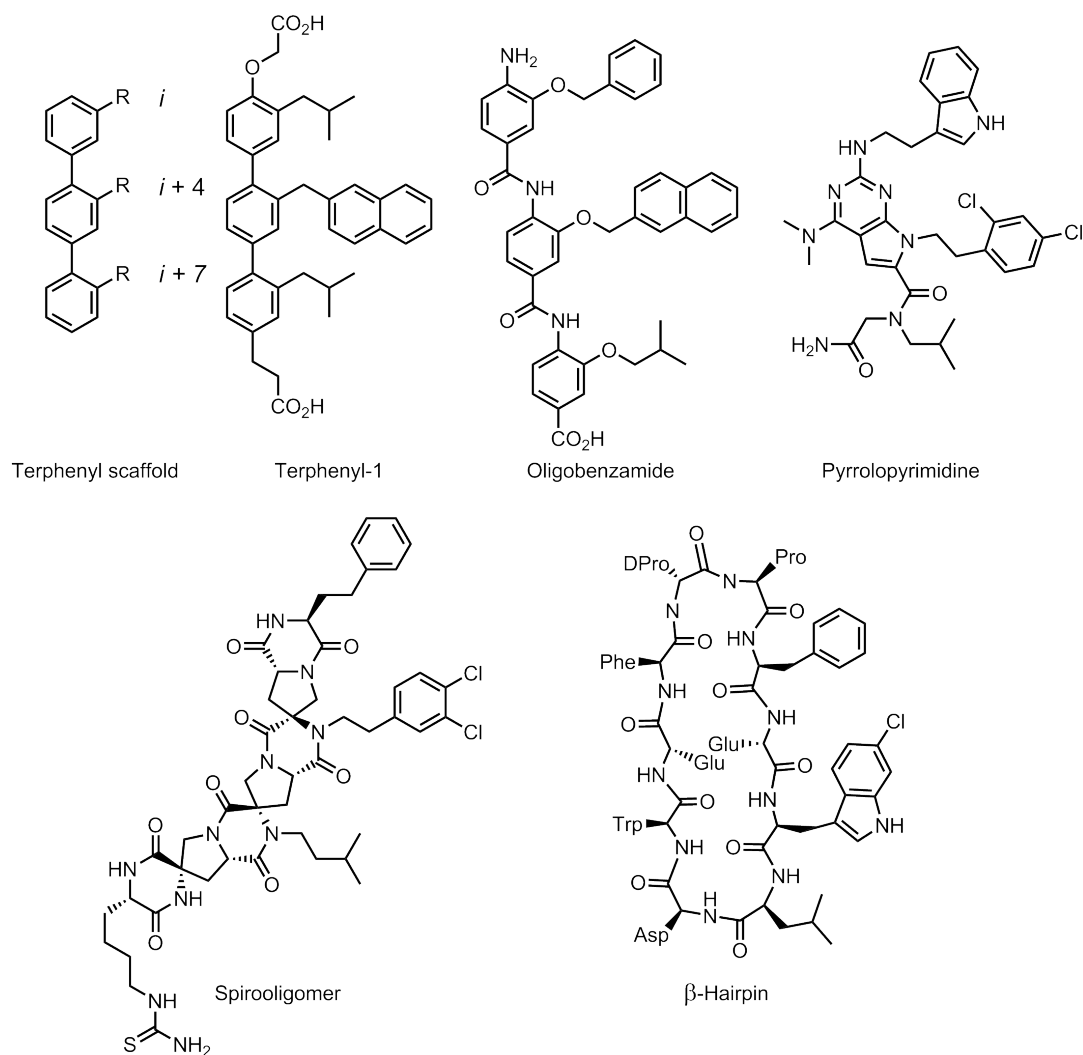


Figure 6. Examples of type III mimetics as inhibitors of MDM2.

There are currently seven small molecule MDM2/p53 interaction inhibitors in clinical trials and representative examples are shown in Figure 7.²⁴ All these can be classified as type II mimetics. Hoffman-La Roche has two MDM2 inhibitors in clinical trials (RG7112 and RG7388). RG7112 has been evaluated against different cancers including sarcoma, myelogenous leukemia and hematologic neoplasm.^{24,60} RG7388 is a second generation MDM2/p53 inhibitor, more potent and selective than RG7112 and

is investigated against solid and hematological tumours.⁶¹ Additional MDM2/p53 interaction inhibitors in clinical trials include MI-77301²⁴ and AMG 232⁶² (Figure 7).

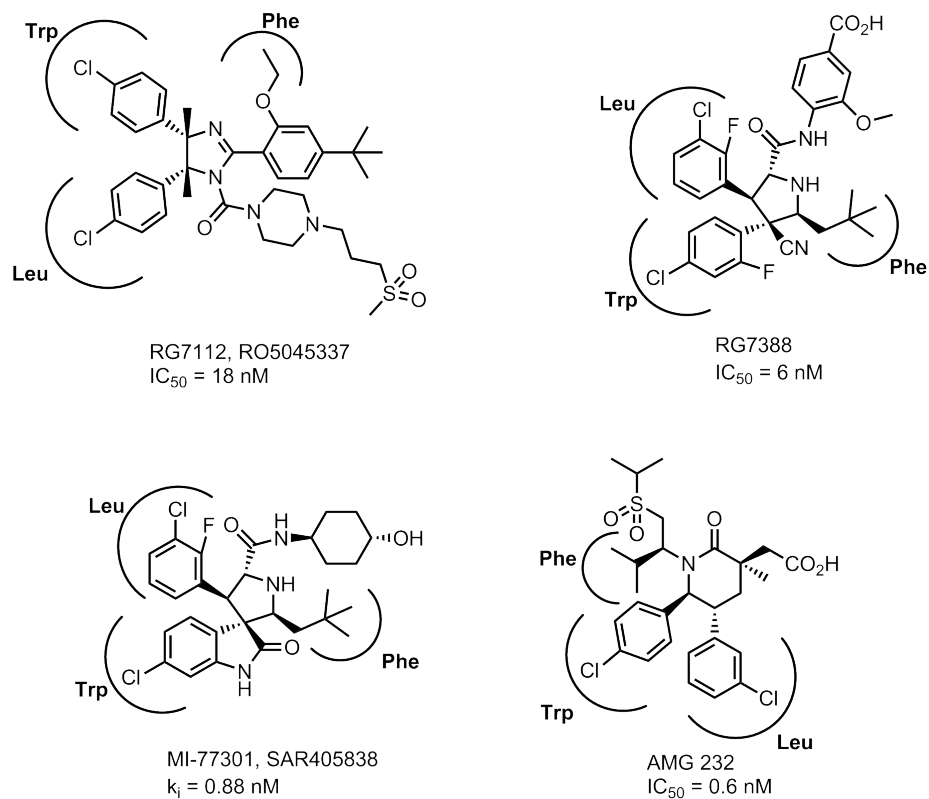


Figure 7. MDM2 inhibitors in human clinical trials, the curved lines represent the Phe-, Trp- and Leu-pockets of MDM2.

2 Methods Used for Biological Evaluation

There are different methods available to evaluate small molecules as inhibitors for PPIs. In the following section principles for the biochemical methods used in this thesis are presented.

2.1 Fluorescence polarisation assay

When a fluorescently labelled ligand is excited by polarised light the emitted light will have a polarisation that is inversely proportional to the rate of tumbling in solution.⁶³⁻⁶⁴ The fluorescence polarisation (FP) assay takes advantage of this observation. A schematic illustration of the principles of the FP-assay is outlined in Figure 8. When a fluorescently labelled peptide-protein complex is excited by light the emitted light will be mainly polarised as an effect of the slow tumbling of the complex in solution. In comparison, when an unbound fluorescent peptide is excited the faster tumbling in solution will result in depolarisation of the emitted light.

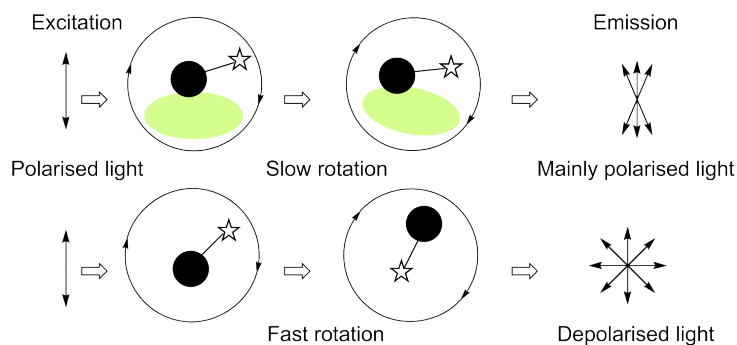


Figure 8. Schematic illustration of the FP-assay, ☆ = fluorophore, ● = a peptide or nucleic acid, ● = protein.

In drug discovery the FP assay is routinely used in HTS, often as a competitive assay where a decrease of the FP signal indicates binding of an unlabelled ligand to the protein. The FP technique has been used to study a range of different molecular interactions such as protein-protein, protein-DNA and protein-ligand interactions.

2.2 Surface plasmon resonance assay

In the surface plasmon resonance (SPR) a protein is immobilised on a functionalised gold surface.⁶⁵⁻⁶⁶ When the surface is illuminated with polarised light, the light will be reflected by the gold surface acting as a mirror. The basic principles of the SPR assay are illustrated in Figure 9. Changing the angle of the illuminated light the reflected light intensity will change and will eventually pass through a minimum (Figure 9B). At that angle, called the SPR angle, the light will excite so called surface plasmons, inducing surface plasmon resonance. In an SPR measurement the SPR angle is measured first with only the protein immobilised on the surface (Figure 9A). The SPR angle is dependent on changes in the refractive indexes on both sides of the gold surface and a change in angle is directly proportional to the amount of material located on the surface. The change is measured in resonance units (RU), where 1 RU = 1 pg/mm². The refractive index on the same side as the light source will not change but the refractive index on the other side changes upon binding of e.g. a ligand to the immobilised protein (Figure 9AII). When the ligand is washed away the SPR angle will decrease (Figure 9AIII). The change in angle can be observed in a sensogram (Figure 9C). The changes in SPR angle can be measured in real time and the on-rate (k_{on} (M⁻¹ s⁻¹)) and off-rate (k_{off} (s⁻¹)) constants can be obtained. The dissociation constant (K_{D} (M)) can be obtained from the ratio of k_{off} and k_{on} or by plotting the response obtained against the concentrations.

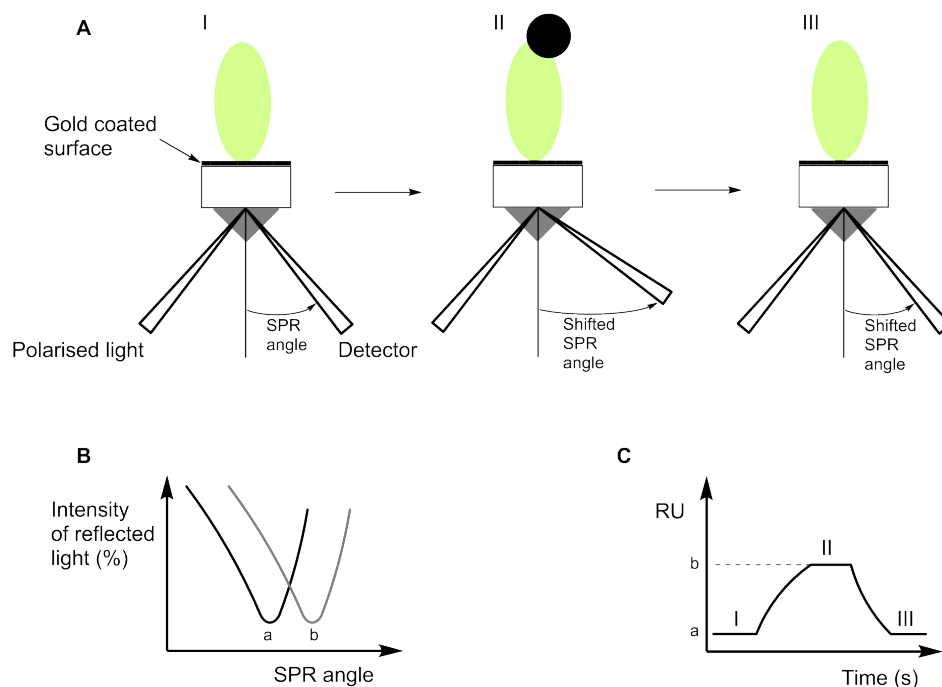


Figure 9. Schematic illustration of SPR, ● = immobilised protein, ● = ligand. **(A)** I. The SPR angle is measured of the immobilised protein in the absence of ligand. II. Upon binding of the ligand the SPR angle increases. III. Removal of the ligand by washing decreases the angle; **(B)** The SPR angle changes from a to b upon binding of a ligand; **(C)** Sensogram of a typical SPR measurement of one concentration (RU = resonance units (pg/mm^2)).

2.3 Water-ligand observed *via* gradient spectroscopy

Water-Ligand Observed *via* Gradient Spectroscopy (WaterLOGSY) is a 1D-NMR spectroscopic technique based on the NOESY experiment used for detecting ligand-protein interactions.⁶⁷⁻⁶⁹ In the WaterLOGSY experiment, bulk water is excited and during a mixing time (up to several seconds) the magnetisation is transferred to the ligand *via* the protein-ligand complex (Figure 10).

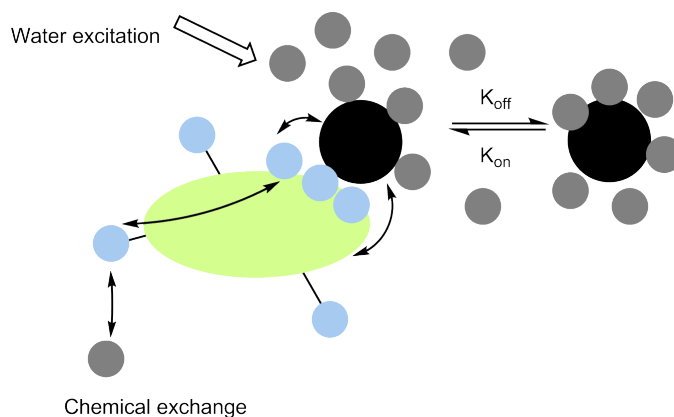


Figure 10. Schematic illustration of the principles of water-ligand observed via gradient spectroscopy (WaterLOGSY). ● = ligand, ● = protein and ● = bulk water. ● = water molecules at the protein-ligand interface or labile protein protons that have been exchanged with protons from the excited water. Example of the different cross-relaxation pathways are shown as black double headed arrows.

The magnetisation is transferred *via* ^1H - ^1H cross relaxation and there are two major relaxation pathways. The first is direct cross relaxation from water molecules at the protein-ligand interface and the second *via* chemical exchange of protons from the excited water with exchangeable protein protons such as NH and OH protons. As a result ligands that bind to the protein will have the same NOE as the protein. Opposite signs for ligands that bind to the protein and nonbinding ligands are observed. In WaterLOGSY the binding ligands are commonly reported as positive signals and the nonbinding are reported as negative signals in the WaterLOGSY spectra (Figure 11).

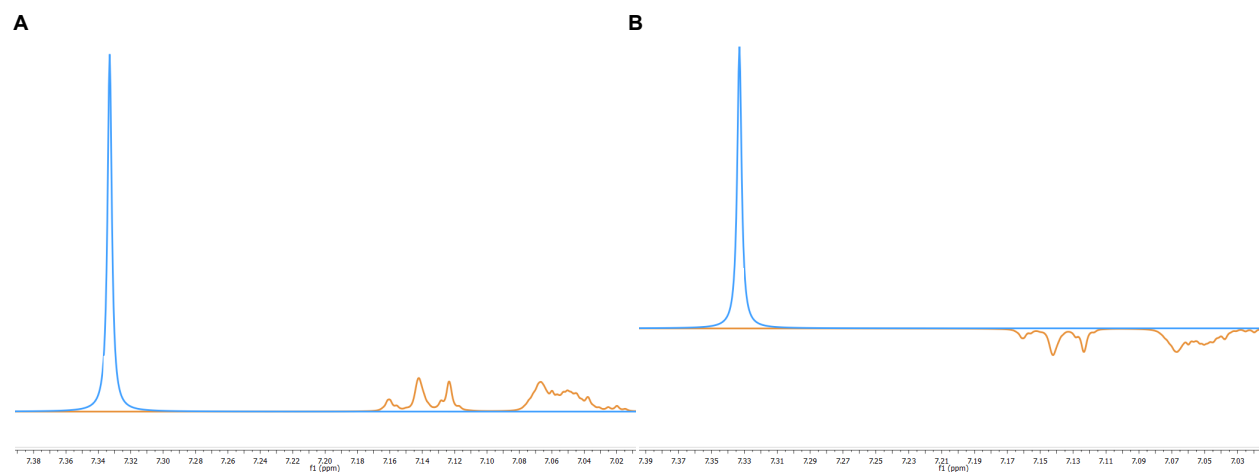


Figure 11. Schematic representation of a WaterLOGSY experiment. **(A)** ^1H NMR spectra of two compounds x (blue) and y (orange); **(B)** WaterLOGSY spectra of x and y, where a positive signal from x (blue) indicates binding to protein and negative signal from y (orange) indicates no binding to the protein.

3 Aims of the Thesis

The overall aim of this thesis was to investigate whether 8-(triazolyl)purine and 2,5-diketopiperazine could act as scaffolds for novel α -helix mimetics, and if derivatives of these and β -hairpin peptides could act as inhibitors of the MDM2/p53 protein-protein interaction.

The specific objectives of the thesis were to:

- Investigate the β -hairpin motif as a scaffold for MDM2 inhibitors. Evaluate if a higher population of β -hairpin conformation in solution improves the inhibitory activity of MDM2/p53 interactions. Investigate the preferred conformations in solutions by a NAMFIS analysis, i.e. a combined NMR spectroscopic and computational technique.
- Design, synthesise and biochemically evaluate 8-(triazolyl)purine as a scaffold for α -helix mimetics acting as MDM2 inhibitors. In addition, determine the photophysical properties of the obtained compounds.
- Design, synthesise and biochemically evaluate 2,5-diketopiperazine as a scaffold for α -helix mimetics acting as MDM2 inhibitors.

4 β -Hairpins as Inhibitors of the MDM2/p53 PPI (Paper I)

4.1 β -Hairpins

The β -hairpin motif in a peptide is constructed by two antiparallel β -strands connected by a loop or a turn. The β -hairpin motif is present in numerous biomolecules and is important for the recognition and interaction with their targets.⁷⁰ Furthermore, β -hairpin motifs have been used as model substrates for understanding early stage protein folding⁷¹ and have also been investigated as peptidomimetics targeting e.g. PPIs such as the MDM2/p53 interaction (see Figure 6, section 1.3.3), proteases and bacteria where the main mechanism of action involves lysis of the bacterial cell membrane.⁷²⁻⁷³

There are different types of β -turns and they are defined by the Φ and Ψ dihedral angles of the $i+1$ and $i+2$ amino acids in the turn (Figure 12). In this thesis only the type I' and II'' turns will be considered. They consist of four amino acid residues (i , $i+1$, $i+2$ and $i+3$) and are defined by $\Phi(i+1) = 60^\circ$, $\Psi(i+1) = 30^\circ$, $\Phi(i+2) = 90^\circ$, $\Psi(i+2) = 0^\circ$, and $\Phi(i+1) = 60^\circ$, $\Psi(i+1) = -120^\circ$, $\Phi(i+2) = -80^\circ$, $\Psi(i+2) = 0^\circ$, respectively.⁷⁴

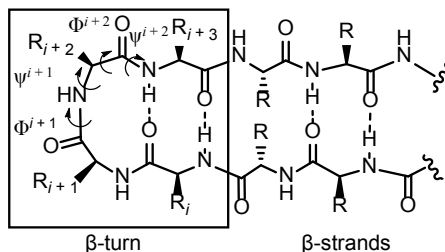


Figure 12. Schematic representation of a β -hairpin structure, the β -turn is shown in the square together with the dihedral angles defining the turn structure.

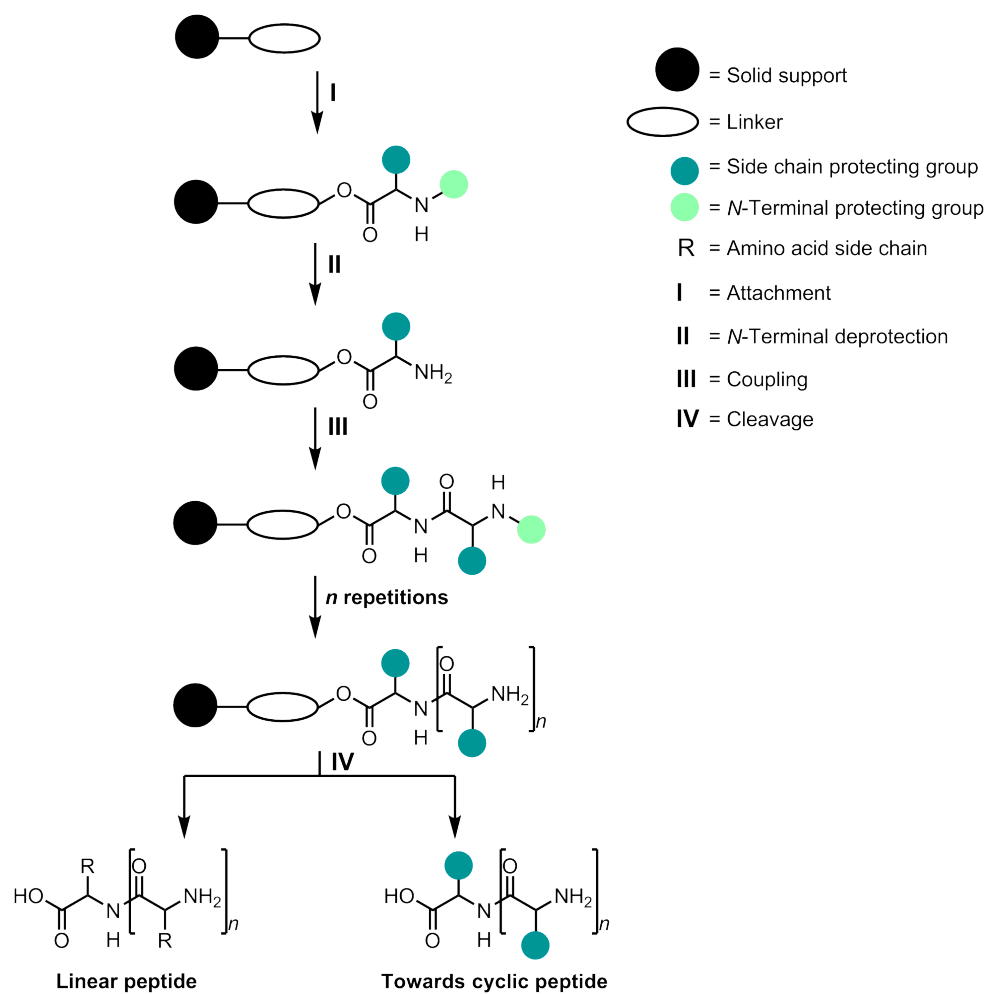
4.1.1 Design of stable β -hairpins

When designing a stable β -hairpin there are some important factors to consider such as turn sequence, interactions between side chains and intramolecular hydrogen bonding.⁷⁵ Popular turn sequences that promote β -hairpin folding include D-Pro-Gly, Asp-Gly and D-Pro-Pro.^{72,75} Side chain interactions such as aromatic, hydrophobic and hydrogen bonding between side chains enhance the stability. Typically interstrand interactions refer to interactions between residues directly opposite to each other in the hairpin e.g. Trp-zippers (Trp-Trp interstrand interactions).⁷⁶ β -Branched amino acids e.g. Val have been shown to extend the β -strand backbone conformation which in turns also stabilizes the β -hairpin conformation.⁷⁷ Interstrand hydrogen bonding from both the backbone (carbonyl oxygen and amide hydrogen) and side chain interactions⁷⁸ also promotes β -hairpin folding.⁷⁵ Moreover, cyclisation also facilitates β -hairpin folding.⁷⁹

4.2 Solid phase peptide synthesis

Solid phase peptide synthesis (SPPS) was first reported by R. B. Merrifield and is the standard method for preparing peptides.⁸⁰ SPPS uses a solid support on which a peptide can be synthesised in a sequential process in the *C*-terminal to *N*-terminal direction. The general principles for SPPS are outlined Scheme 1 and consist of four basic steps.⁸¹⁻⁸² The first step involves attachment (I) of the first amino acid *via* the carboxylic acid to the resin (solid support and linker). This step is however often not needed due to the large number of commercially available resins on which the first amino acids is already attached. The linker can be attached to both the *C*- and *N*-terminal of the amino acid, but attachment to the *C*-terminal is most often used. Second, deprotection of the *N*-terminal (II) followed by the coupling step (III), where

one amino acid is coupled to the growing peptide using a peptide coupling reagent. Steps II and III are repeated n times for an $n+1$ amino acid long peptide. The fourth and final step is cleavage of the peptide from the solid support (IV) to provide the free peptide.



Scheme 1. Schematic illustration of the principle steps in solid phase peptide synthesis (SPPS).

Depending on whether the final product is a linear or cyclic peptide the side chain protecting groups can be cleaved simultaneously with the linker or as a separate step, respectively. Every coupling can be driven to completion by the use of excess reagents which typically gives higher yields. In between each step, excess reagents and possible

soluble side products can be easily separated from the growing peptide by filtration and washing. Essential issues to consider for SPPS are protecting groups for the *N*-terminal and the side chain functional groups, the solid support, the linker and choice of peptide coupling reagent.

The choice of the protecting groups in SPPS is crucial for the reaction outcome and the *N*-terminal protecting group decides the overall synthetic strategy.⁸³ The *N*-terminal and side chain protecting groups need to be orthogonal and/or compatible.⁸⁴ Orthogonal protecting groups are cleaved using different conditions (e.g. basic or acidic) in contrast to compatible protecting groups which are cleaved by the same conditions but often with different rates. The two major protecting group strategies used in SPPS are the Boc/Bn or the Fmoc/*t*Bu strategies (Figure 13), where Boc and Fmoc are the *N*-terminal and Bn and *t*Bu are the side chain protecting groups.

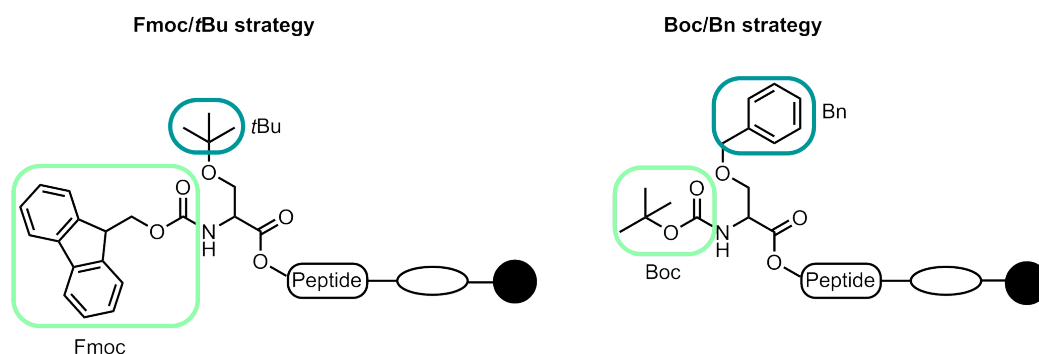


Figure 13. Protecting group strategies used in SPPS, serine is used as an example, ●—○ = resin.

Fmoc and *t*Bu are orthogonal protecting groups as the Fmoc group is cleaved under basic conditions and the *t*Bu under acidic. The Fmoc/*t*Bu strategy has been used in the thesis and will therefore be the only strategy discussed further.

For routine SPPS crosslinked polystyrene (PS)-based resins are used as solid support.⁸¹ When more hydrophilic resins are required crosslinked polyamide-based resins and

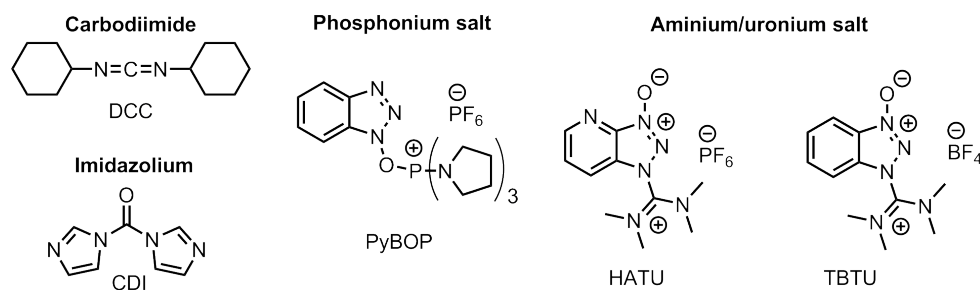


Figure 14. Examples of commonly used peptide coupling reagents.

4.3 Conformational studies of β -hairpins

Techniques available for studies of β -hairpin conformation include NMR, CD and IR spectroscopy.⁷¹ In this thesis NMR analysis of molecular flexibility in solution (NAMFIS) has been utilised for conformational studies. The method is based on geometrical constrains (interproton distances and dihedral angles) obtained from NMR spectra.⁸⁷ The obtained constrains are then converted to an ensemble of three-dimensional structures.

4.3.1 NMR analysis of molecular flexibility in solution

NAMFIS is a combined NMR spectroscopic and computational technique and can be used to determine the conformational ensemble of a compound in solution.⁸⁷ NAMFIS has previously been used to determine the solution conformations of both peptides^{78,88-89} and small molecules.⁹⁰⁻⁹¹

Two variables are used as input data in the NAMFIS analysis (Figure 15), first the experimentally obtained dihedral angles ($\Phi_{\text{H-N-C}\alpha\text{-H}}$) and interproton distances derived from $^3J_{\text{CH}\alpha,\text{NH}}$ coupling constants and NOE-correlations, respectively. The second

variable is the back-calculated distances and dihedral angles of a theoretical ensemble derived by a constraints free Monte Carlo conformational search. The $^3J_{\text{CH}\alpha,\text{NH}}$ coupling constants are related to the conformation through the dihedral angles which are obtained using the Karplus equation. For the study of peptides a Karplus equation especially developed for peptides is utilised.⁹²⁻⁹³ The NOE correlations are obtained from NOESY build-up experiments.

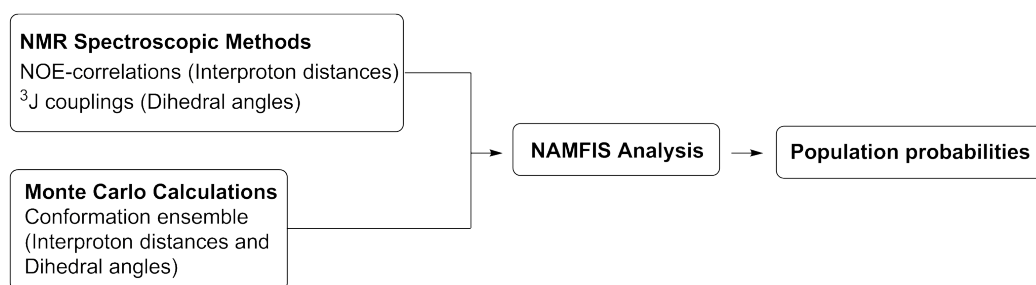


Figure 15. Schematic illustration of the NAMFIS analysis

NAMFIS analysis deconvolutes experimental, time-averaged data using the theoretically available conformations to identify the conformational ensemble that best fits to all experimentally obtained data (NOE and $^3J_{\text{CH}\alpha,\text{NH}}$) simultaneously. NAMFIS computes the probability of the theoretically available conformations (Figure 15).⁸⁷ The quality of the fit of the experimental and computed data is expressed as the sum of square differences (SSD), for which a lower value represents a better fit between the data.⁹⁴

4.4 β -Hairpins as MDM2 inhibitors (Paper I)

Fasan *et al.* have reported β -hairpins as inhibitors of MDM2/p53 interactions, from a series of 78 investigated peptides inhibitor **I** shown in Figure 16A was most active.⁵⁷⁻⁵⁸ β -hairpin, **I**, can place the Leu7, 6ClTrp8 and Phe10 residues in analogy with the i , $i+3(4)$ and $i+7$ residues of the p53 helix. A crystal structure of **I** with MDM2 confirmed that Leu7, 6ClTrp8 and Phe10 of **I** bind to the MDM2 pockets and showed that the bioactive conformation of peptide **I** can be a β -hairpin conformation.⁵⁸

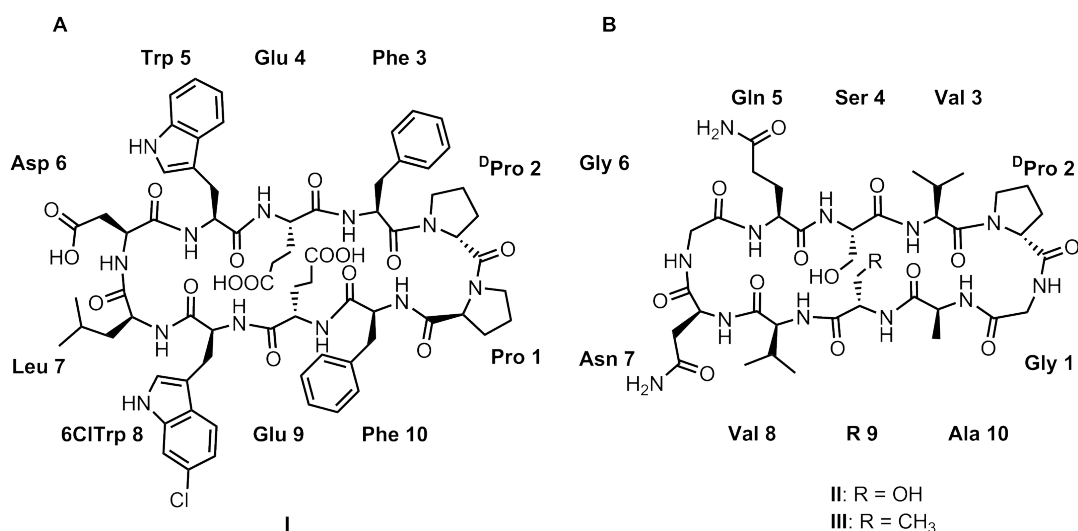


Figure 16. (A) A previously published β -hairpin inhibitor of the MDM2/p53 interaction, with the numbering of amino acids used in this thesis; (B) Structure of cyclic β -hairpins used for the investigation of interstrand hydrogen bonding. R = CH₃ or OH.

Danielius *et al.* have found that interstrand hydrogen bonding facilitates β -hairpin formation in solution.⁷⁸ Peptides **II** and **III** were used as model substrates, where **II** (R = OH) has the ability to form an interstrand hydrogen bond whereas **III** (R = CH₃) does not (Figure 16). NAMFIS analysis of the two peptides revealed that an interstrand hydrogen bond facilitates β -hairpin folding in solution and a clear difference of peptides **II** (R = OH) and **III** (R = CH₃) could be observed where the

former exhibits 88% probability of folded conformation in solution compared to 50% folding in the absence of the interstrand hydrogen bond.

Based on these findings it was decided to further investigate β -hairpins as MDM2 inhibitors and evaluate if a higher β -hairpin population in solution would increase the binding affinity to MDM2.

4.4.1 Design of β -hairpins

Peptide **I** was used as a starting point and low energy conformations of a series of peptides were explored with conformational analysis by Monte Carlo Multiple Minimum (MCMM) in MacroModel.⁹⁵ OPLS-2005 was used as force field together with the Born water solvation model. Estimated β -hairpin populations were predicted from the identified low energy conformations and peptides **1-3** were selected for further investigation. The following modifications of **I**, aiming for a more stable β -hairpin were performed to obtain **1** (Figure 17). First the turn sequence was formed by Gly1-D-Pro2 instead of Pro1-D-Pro2, as it is a known turn inducing sequence and has proven successful for peptides **II** and **III** (Figure 16B).⁷⁸ In order to make the interstrand hydrogen bonding interaction between side chains possible the glutamic acids (Glu4 and Glu9) in **I** were replaced by serines (Ser4 and Ser9) in **1**. Peptides **2** and **3** were designed in order to investigate the possibility of halogen bonding in the binding pocket of MDM2 by introduction of a 4-chlorophenylalanine (4ClPhe8) and 4-bromophenylalanine (4BrPhe8), respectively (Figure 17). In addition, 4-chloro- and 4-bromophenyl could serve as alternatives to the 6-chloroindole moiety of **1**. An additional carboxylic acid containing residue was introduced in peptides **2** and **3** (Glu5) (Figure 17). Studies of small molecules as inhibitors of MDM2 have shown that a carboxylic acid moiety pointing out towards the solvent/hydrophilic surface of

MDM2 can facilitate additional interactions with His96 and Lys94 of MDM2 *via* hydrogen bonding and/or ionic interactions.²⁴

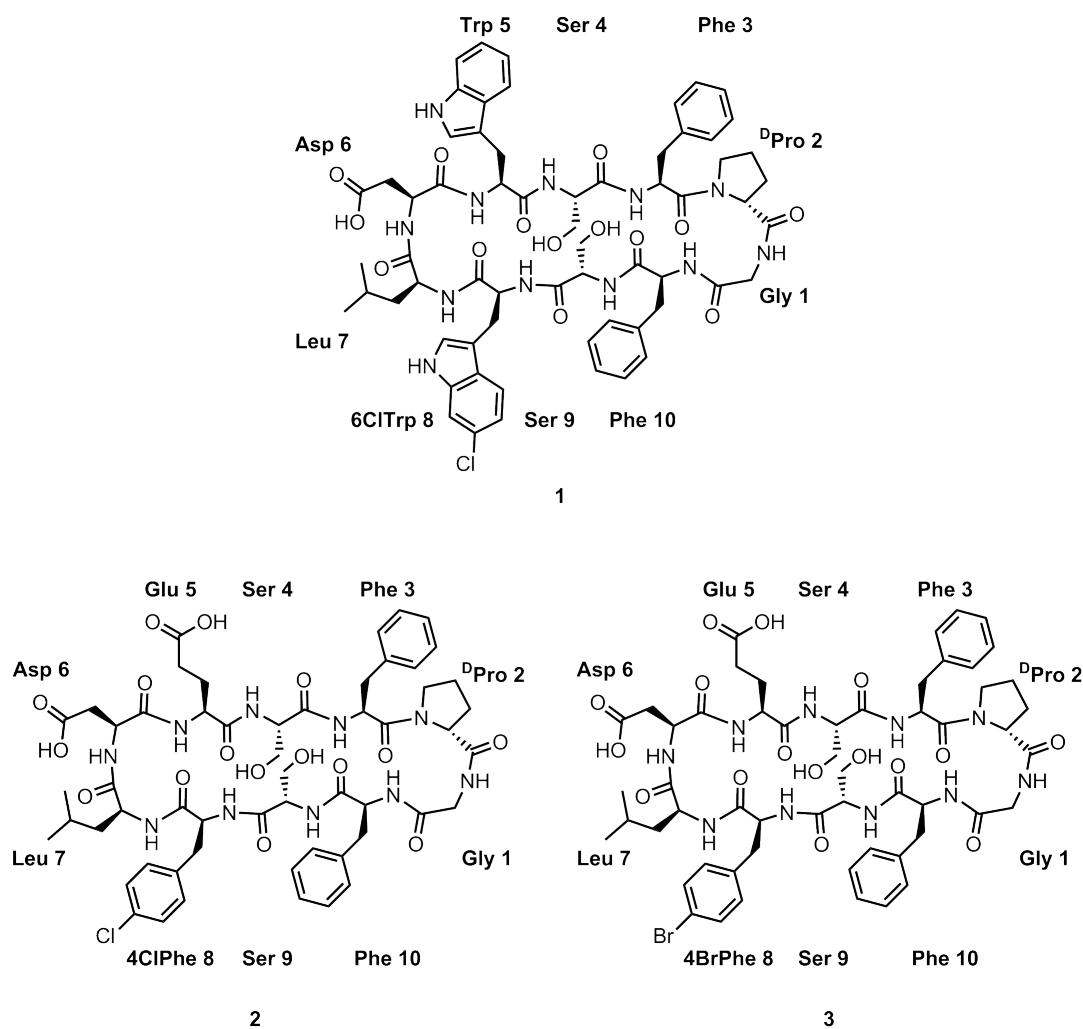


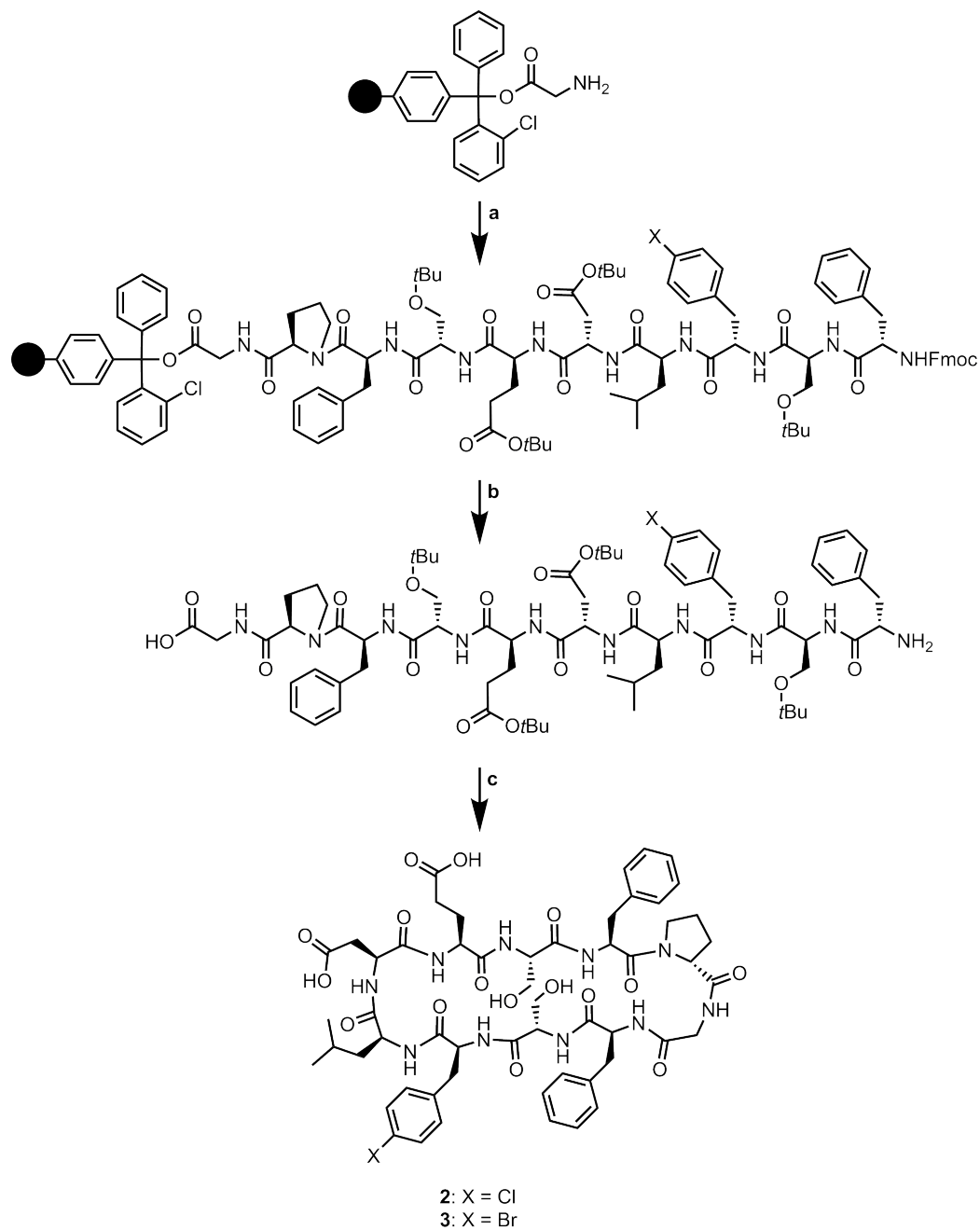
Figure 17. Structures of the investigated cyclic peptides **1-3**.

4.4.2. Synthesis of β -hairpins

Peptides **I** and **1-3** (Figure 16A and 17) were synthesised using combined solid phase and solution phase peptide synthesis. Synthesis of **2** and **3** is outlined in Scheme 3. The

linear peptides were first synthesised on a 2-chlorotrityl resin (starting from glycine-2-chlorotrityl) following the Fmoc/*t*Bu strategy (see section 4.2) using a PS3 Peptide Synthesizer. Double peptide couplings were performed using TBTU as coupling reagent and DIPEA as base in DMF. In a double coupling protocol two sequential couplings with the same amino acid are performed, to ensure high yields in the peptide synthesis. Piperidine in DMF was used for the Fmoc deprotection. The linear peptide was cleaved from the resin using 1% TFA in DCM. The linear peptide was cyclised following a previously published procedure by Malesevic *et al.*⁹⁶ Peptide cyclisation is often performed under high dilution conditions (10^{-3} to 10^{-4} M) in order to avoid polymerisation and as a result large solvent volumes are necessary. In the cyclisation protocol used the coupling reagent (HATU) and the linear peptide are added simultaneously from two separate syringes using a syringe pump (rate 0.03 ml/min) to a reaction vessel containing the base (DIPEA). The slow addition resulted in a low *in situ* concentration of the linear peptide and hence reduced the risk of polymerisation. Next the side chain protecting groups (*t*Bu and Boc) were cleaved using a mixture of TFA, distilled water and TIPS. The trialkylsilane is used to scavenge the formed *t*Bu carbocation in the deprotection.⁹⁷⁻⁹⁸ Peptide **2** and **3** were obtained after purification using RP-HPLC.

Peptides **1** and **I** were synthesised starting from serine-2-chlorotrityl and glutamine-2-trityl resins, respectively, using the same protocol as for **2** (see Appendix 3 and 4). Peptide **I** was synthesised in order to be used as a reference in both the biological evaluation and solution conformational analysis.



Scheme 3. Synthesis of **2** and **3**. Reagents and reaction conditions: **(a)** (i) Fmoc-AA-OH, TBTU, DIPEA. (ii) Acetic anhydride. (iii) 20% piperidine in DMF. Nine consecutive cycles with: Fmoc-D-Pro, Fmoc-Phe, Fmoc-Ser(*t*Bu)-OH, Fmoc-Glu(*t*Bu)-OH, Fmoc-Asp(*t*Bu)-OH, Fmoc-Leu, Fmoc-4-X-Phe, Fmoc-Ser(*t*Bu)-OH, Fmoc-Phe. **(b)** (i) 20% piperidine in DMF. (ii) 1% TFA in DCM. **(c)** (i) HATU, DIPEA, DMF. (ii) TFA:H₂O:TIPS (95:2.5:2.5)

4.4.3 Conformational analysis of peptides I and 1-3

The structures were assigned using TOCSY-NOESY sequential backbone walking.⁹⁹ Amide temperature coefficients ($\Delta\delta_{\text{NH}}/\Delta T$), scalar couplings ($^3J_{\text{CH}\alpha,\text{NH}}$) and H α proton chemical shifts were determined for peptides **I** and **1-3** (Table 1). The temperature dependence of DMSO- d_6 was accounted for when determining the amide temperature coefficients.¹⁰⁰ An amide temperature coefficient <3 indicates strong intramolecular hydrogen bonding, whereas an amide temperature coefficient >5 indicates that the amide protons are solvent exposed. Amide protons that are in equilibrium between solvent exposed and intramolecular hydrogen bonding have coefficients between 3 and 5.¹⁰¹

Table 1. Amide proton temperature coefficients ($\Delta\delta_{\text{NH}}/\Delta T$, 298-318 K), scalar couplings ($^3J_{\text{CH}\alpha,\text{NH}}$) and chemical shifts ($\delta_{\text{H}\alpha}$) for peptides **I** and **1-3**

Residue ^a	Peptide											
	$\Delta\delta_{\text{NH}}/\Delta T$ (ppb/K) ^b				$^3J_{\text{CH}\alpha,\text{NH}}$				$\delta_{\text{H}\alpha}$			
	I	1	2	3	I	1	2	3	I	1	2	3
1	-	10.0	9.3	8.1	-	-	-	-	4.22	3.52/3.60	3.58	3.52
2	-	-	-	-	-	-	-	-	4.46	4.20	4.22	4.22
3	5.7	8.1	7.4	7.6	-	-	7.8	7.5	4.90	4.68	4.78	4.79
4	8.8	11.8	9.4	9.6	-	7.4	-	7.3	4.83	4.83	4.85	4.86
5	4.8	5.5	3.2	3.1	8.4	-	7.4	8.2	4.76	4.67	4.56	4.56
6	10.0	8.2	7.1	7.2	7.7	5.4	6.1	8.0	4.27	4.33	4.37	4.37
7	8.2	10.1	9.3	8.6	5.2	-	-	-	3.48	3.64	3.65	3.64
8	6.7	8.5	6.2	6.1	7.3	7.3	7.4	8.6	4.67	4.57	4.54	4.54
9	9.1	8.5	10.5	9.8	7.9	6.6	-	7.3	5.02	4.80	4.70	4.71
10	3.7	3.7	3.5	3.7	8.9	8.5	7.5	9.2	4.82	4.77	4.78	4.78

^aFor residue identity see Figure 16 and 17. ^b $\Delta\delta_{\text{NH}}/\Delta T$ were obtained from $(\delta_{\text{T,high}} - \delta_{\text{T,low}}) / (T_{\text{high}} - T_{\text{low}})$ as negative values, but are reported as positive signals in analogy with literature.¹⁰¹

Lower amide temperature coefficients are observed from the NH of residue 5 and 10 of all peptides which is expected in a β -hairpin conformation. The scalar couplings ($^3J_{\text{CH}\alpha,\text{NH}}$) and H α proton chemical shifts obtained for peptide **I** and **1-3** are in agreement with expected for β -sheets.^{93,102-103}

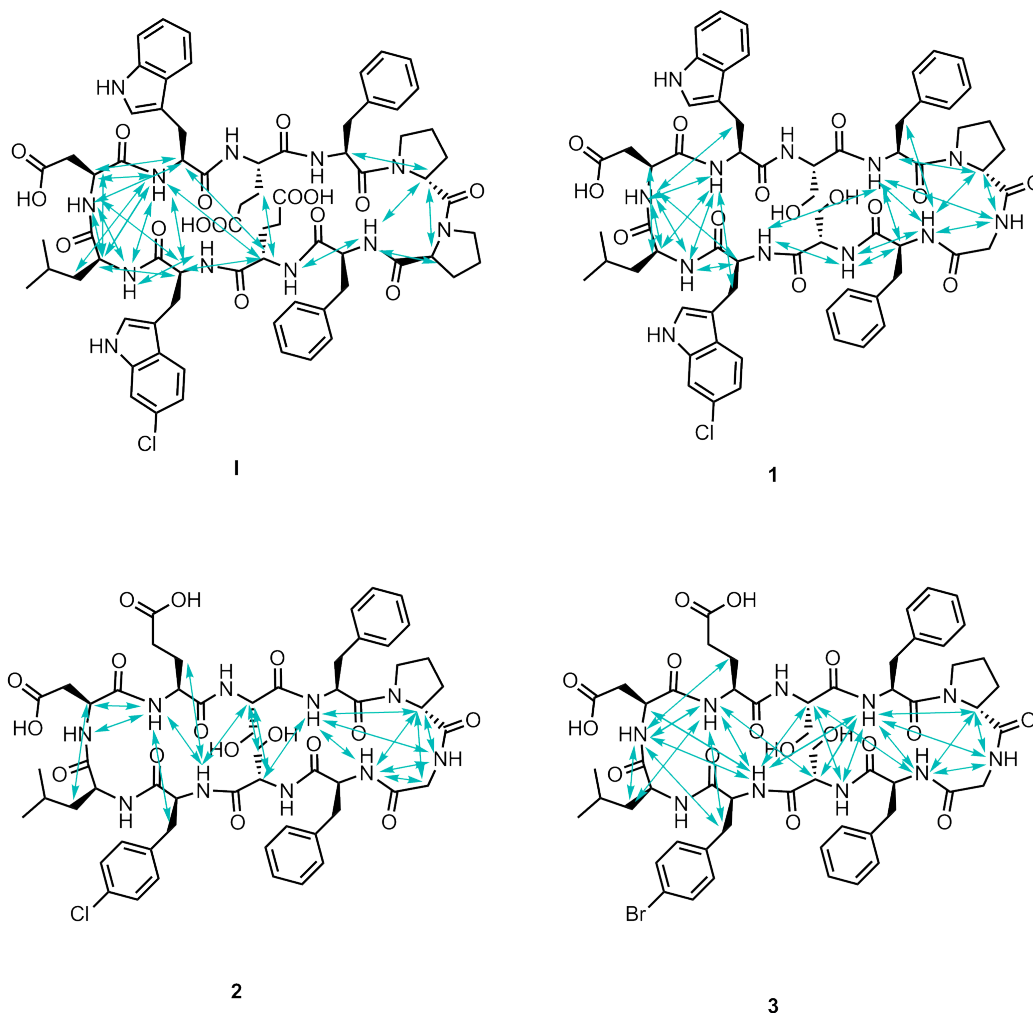


Figure 18. Key NOE correlations observed for peptides **I** and **1-3**.

NOE patterns for peptides **I** and **1-3** are shown in Figure 18. Peptides **2-3** display NOE patterns that are in good agreement with the expected β -hairpin conformation having interstrand NOE correlations. For peptide **I** and **1** fewer interstrand NOE

correlations were observed (Figure 18), which might indicate less β -hairpin folding in solution.

NOESY build-ups were derived by running NOESY experiments in DMSO- d_6 with different mixing times (200, 300, 400, 500, 600 and 700 ms). Experimental average interproton distances (r_{ij}) between protons i and j were calculated according to the initial rate approximation using $r_{ij} = r_{\text{ref}}(\sigma_{\text{ref}}/\sigma_{ij})^{(1/6)}$ where r_{ref} is the internal distance reference which in this case are geminal protons ($r_{\text{ref}} = 1.78\text{\AA}$), σ_{ij} is the NOE build-up rate and σ_{ref} is the build-up rate for the reference. σ_{ij} were obtained from plotting the mixing times against the normalised NOE peak areas using at least five mixing times yielding a linear ($R^2 \geq 0.98$) initial NOE build-up rate. Normalised NOE peak areas were calculated using normalisation of both cross peaks (xpeak) with both diagonal peaks (diagpeak) according to $([(\text{xpeak1} \times \text{xpeak2})/(\text{diagpeak1} \times \text{diagpeak2})]^{0.5})$.^{78,89} Dihedral angles were derived from $^3J_{\text{CH}\alpha,\text{NH}}$ scalar coupling constants utilising a Karplus equation developed for peptides.⁹²⁻⁹³

The theoretical conformational ensemble of the peptides was identified by performing two separate restraint-free Monte Carlo conformational searches with intermediate torsion sampling using OPLS-2005 and Amber* as force fields. The Born water solvation model was used in both conformational analyses. Conformations within 42 kJ/mol from the global minimum conformation were collected. The obtained conformations were combined and in order to identify the conformational ensemble needed for the NAMFIS analysis a redundant conformation elimination with the root-mean-square cutoff (RMSD) of 2.5 \AA for heavy atoms was performed and ensembles of 100-150 conformations of each peptide was obtained. Back-calculated interproton distances and dihedral angles were obtained from these ensembles and used as inputs in NAMFIS.

For peptides **I** and **1-3**, the set of conformations that best fitted the experimental data (NOE and $^3J_{\text{CH}\alpha,\text{NH}}$) was derived from the NAMFIS analyses and the obtained results are summarised in Table 2. Peptide **I** was found to have least folded β -hairpin solution conformation in DMSO (entry 1). Exchanging the turn sequence to D-Pro-Gly from D-Pro-Pro and introducing interstrand hydrogen bond possibilities (Ser4 and Ser9) of peptide **I** to **1** resulted a higher population of folded β -hairpin solution conformations (entry 2). Peptides **2** and **3** were found to have the highest probability for folded β -hairpin solution conformation (entries 3 and 4).

Table 2. Result of the NAMFIS analysis of peptide **I** and **3-4**.

Entry	Peptide	% β -hairpin
1	I	6
2	1	28
3	2	66
4	3	65

4.4.4 Evaluation of β -hairpins as MDM2 inhibitors

All four β -hairpins were evaluated for MDM2/p53 inhibitory activity using a FP-assay.¹⁰⁴ The displacement of a Texas Red labelled wild-type p53 peptide bound to MDM2 was measured. Peptide **I** was used as a reference displaying an IC_{50} of 2.86 μM (Table 3). Peptides **1-3** all displayed lower inhibitory activity towards MDM2, where the most active was β -hairpin **1** having an IC_{50} of 7.56 μM .

Table 3. MDM2/p53 inhibitory activity of peptides **I** and **1-3** as observed in FP- and SPR-assays.

Entry	Peptide	IC_{50} (μM)	95% CI ^a	K_D (μM)
		FP-assay	FP-assay	SPR-assay
1	I	2.86	1.16–5.10	0.127 ± 0.001
3	1	7.56	3.42–16.69	2.50 ± 0.02
3	2	23.94	7.72–74.30	7.0 ± 0.1
4	3	10.10	5.67–17.99	5.73 ± 0.09

^aCI = confidence interval

To confirm binding to MDM2, all peptides were also assayed for MDM2 binding using an SPR assay (Table 3) which supported the order of inhibitory activity observed in the FP-assay, i.e. **I** > **1** > **3** > **2**.

The obtained results from the biological evaluations and solution conformational analyses indicate that more stable β -hairpin results in less active MDM2 inhibitors. The conformational analyses showed an increasing stability of folding into β -hairpin in the order **I** < **1** < **3** \approx **2** in solution, which is inversely correlated to the inhibitory activity observed, **I** > **1** > **3** > **2**.

4.5 Summary paper I

Three β -hairpin-based MDM2 inhibitors were designed aiming for a more stable β -hairpin conformation. Syntheses of the peptides were performed using automated SPPS applying the Fmoc/*t*Bu strategy followed by a head to tail cyclisation.

The inhibitory activities for all peptides were determined by running both FP- and SPR assays using the previously published peptide **I** as a reference. NAMFIS analyses provided the possible conformations in solution for peptides **I** and **1-3**. The obtained results showed that the molecular flexibility of the peptides is important for the inhibitory activity, since the inhibitory activity was inversely correlated to the degree of observed β -hairpin conformations in solution. Furthermore, the conformational analyses revealed that incorporation of two serine residues (Ser4 and Ser9), enabling interstrand hydrogen bonding, and replacing the D-Pro-Pro turn with D-Pro-Gly in peptides **1-3** stabilised β -hairpin folding in solution.

5 8-(Triazolyl)purines as Inhibitors of the MDM2/p53 PPI (Paper II and III)

8-(Triazolyl)purines have previously been developed as fluorescent nucleic acid base analogues and stable analogues of acyl-AMP within the group.¹⁰⁵⁻¹⁰⁸ Pyrrolopyrimidine derived α -helix mimetics with an amide functionality in the C8-position (see Figure 6 section 1.3.3) have been reported as inhibitors of MDM2/p53.⁵⁵ Triazoles are known bioisosteres of the amide bond.¹⁰⁹⁻¹¹² Inspired by these facts it was decided to evaluate 2,9-disubstituted 8-(triazolyl)purines as α -helix mimetics and hence inhibitors of the MDM2/p53 PPI. Further, since 8-(triazolyl)purines previously have shown fluorescent properties it was expected that the 2,9-disubstituted 8-(triazolyl)purines should display similar characteristics. Fluorescent small molecule α -helix mimetics could be useful as probes to study PPIs.

5.1 Purines

A purine (imidazo[4,5-d]pyrimidine) is a heterocyclic compound constructed from a pyrimidine ring fused with an imidazole ring (Figure 19). The purine ring is the most common nitrogen containing heterocycle found in nature and is an acknowledged privileged structure as it is recognised by numerous proteins including protein kinases, reductases, polymerases and purine receptors.¹¹³⁻¹¹⁵ The purine framework is the core structure of adenine and guanine, two out of five bases in DNA and RNA. Purine derivatives are involved in many metabolic processes. One important example is adenosine 5'-triphosphate (ATP) which is used as the energy storage by all living cells (Figure 19). Potential applications of purine derivatives include treatment of cancer, Parkinson's disease, Alzheimer's disease, asthma, depression, viral infections and many more.¹¹⁵ Currently, purine derived drugs approved by U.S Food and Drug

Administration (FDA) are either intended for the treatment of cancer or for use as antiretroviral agents. For example abacavir and cladribine which are used for the treatment of HIV/AIDS and leukaemia, respectively (Figure 19).¹¹⁶

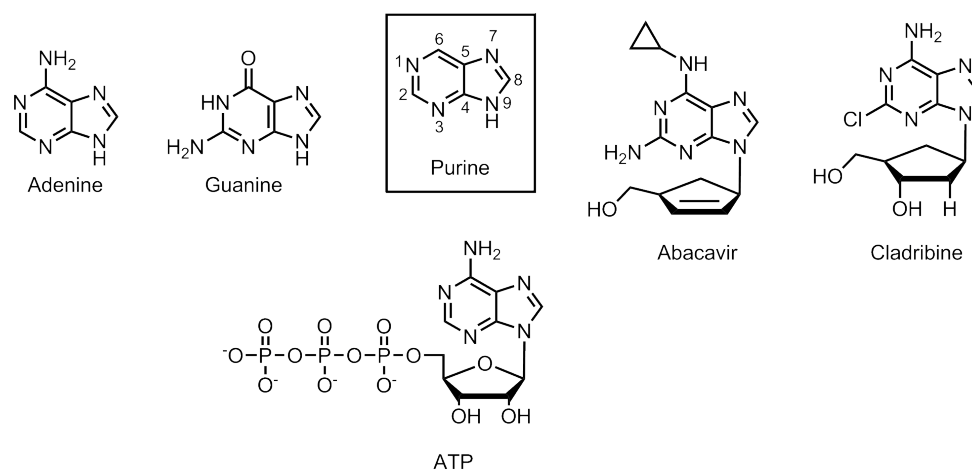


Figure 19. The purine ring system with numbering of atoms and examples of purine derivatives found in nature and in drugs.

A large set of structurally diverse purines derivatives are accessible since the purine ring can be substituted in the *N*1, C2, *N*3, C6, *N*7, C8 and *N*9 positions.¹¹⁷ There are two main synthetic strategies used for the synthesis of functionalised purines. The first strategy utilises a purine ring substituted with reactive functional groups that can be modified or replaced. In the second strategy the purine ring system is synthesised starting from substituted pyrimidine and/or imidazole precursors.¹¹⁷ In this thesis the first strategy has been utilised for the synthesis of 2,6,8,9-tetrasubstituted purines and will be further discussed in section 5.2.2.

5.2 8-(Triazolyl)purines as MDM2 inhibitors (Paper II)

5.2.1 Design of 8-(triazolyl)purines as type III inhibitors

Type III inhibitors (see also section 1.3.3) mimic the topography of an α -helix and for the MDM2/p53 PPI they should have the ability to position substituents in the same spatial orientation as the amino acid side chains of one face of an α -helix (i , $i+4$ and $i+7$) (see section 1.2). One alternative to investigate if the 8-(triazolyl)purine scaffold could be used in type III mimetics is to compare the scaffold with an idealized α -helix using computational methods.

Low energy conformations of the 8-(triazolyl)purine scaffold were obtained from conformational searches by MCMM using MacroModel.⁹³ The OPLS-2005 force field and a Born water solvation model were used. Identified low energy conformations were then compared to an α -helix consisting of alanine residues (Figure 20).

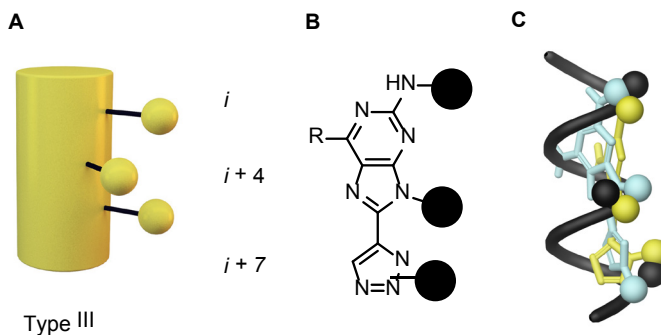
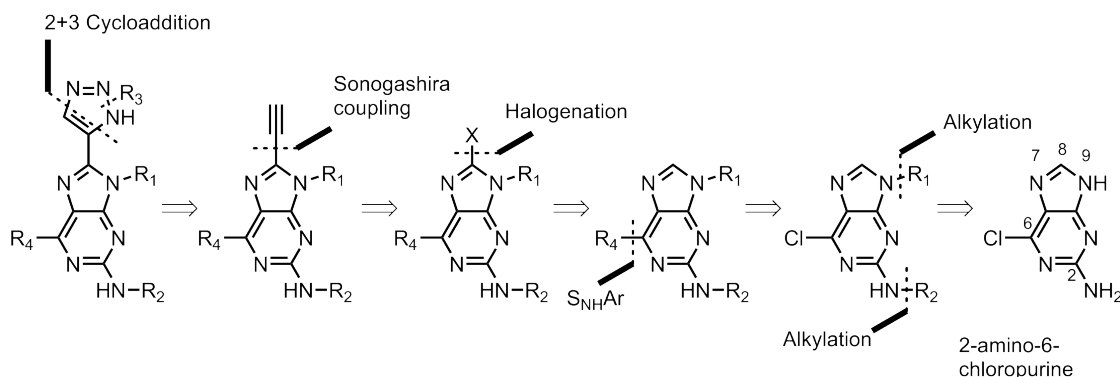


Figure 20. (A) Schematic illustration of a type III mimetic; (B) The 8-(triazolyl)purine scaffold with the appropriate substitution pattern; (C) Superimposition of an Ala-helix (black), with low energy conformations of 8-(1,4-triazolyl)purine (turquoise) and 8-(1,5-triazolyl)purine (yellow). Only the i , $i+4$ and $i+7$ residues of the Ala-helix are shown.

The obtained results showed that 2,9-disubstituted 8-(triazolyl)purine derivatives illustrated in Figure 20B could place the substituents in positions corresponding the i , $i+4$ and $i+7$ residues of the Ala-helix (Figure 20C).

5.2.2 Synthesis of 8-(triazolyl)purines

Retrosynthetic analysis of the 2,6,9-trisubstituted 8-(triazolyl)purine scaffold (Scheme 4) reveals the 2+3 cycloaddition as a convenient final step.



Scheme 4. Retrosynthetic analysis of 2,6,9-trisubstituted 8-(triazolyl)purine.

The choice of catalyst in the cyclisation controls the regiochemistry of the triazole ring. The use of a Cu(I)-catalyst results in formation of the 1,4-triazole, this reaction is often referred to as copper catalysed azide-alkyne cycloaddition (CuAAC).¹¹⁸ The reaction can be run under mild conditions and the reaction is compatible with a selection of different solvents. Sodium ascorbate is often added as a reducing agent and has been shown to accelerate the rate of conversion catalysed by the Cu(I) catalyst. Two methods for the synthesis of the 1,5-triazole are available, the first using a Ru(II)-catalyst¹¹⁹⁻¹²¹ and the second being a metal free method using KOH or tetramethylammonium hydroxide in DMSO.¹²² The alkyl- and benzyl azides can be formed prior to use or *in situ* from alkyl or aryl halides and sodium azide.^{121,123-124} The large number of commercially available alkyl and aryl halides enables a large chemical variation in the position of the R₃ substituent (Scheme 4). The palladium catalysed

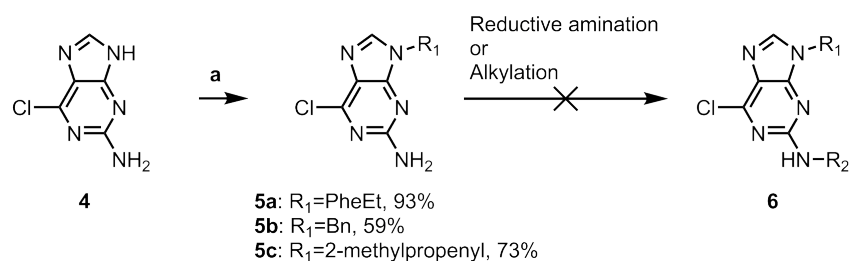
Sonogashira C-C coupling is a standard protocol for aryl-alkyne couplings¹²⁵ and can be used to introduce the terminal alkyne needed for the triazole formation in the C8-position of the purine. Before the C-C coupling the C8-position needs to be activated, generally through introduction of a halide, most often bromine. This reaction sequence, bromination, Sonogashira coupling followed by triazole cyclisation has previously been described for the synthesis of 8-(triazolyl)purines.^{105,107-108} The R₄ substituents (Scheme 4) can be introduced *via* nucleophilic aromatic substitution from the corresponding halide.¹²⁶⁻¹²⁷ The R₁ and R₂ substituents can be introduced *via* N9 alkylation followed by reductive amination or alkylation of the 2-amino group (2N).¹²⁸⁻¹³⁰ Alkylation in the N9-position can be accomplished using alkyl halides under basic conditions e.g. potassium carbonate in DMF.¹²⁸ A Mitsunobu protocol for the introduction of substituents in the N9 and 2N-positions has been reported and could serve as an alternative route.¹³¹⁻¹³² The commercial availability of 6-chloropurines makes this a suitable synthetic strategy for the synthesis of 2,6,9-trisubstituted 8-(triazolyl)purines.

5.2.3 Synthesis of 8-(triazolyl)purines as type III inhibitors

A series of hydrophobic substituents (R₁₋₃) was selected since the hot spot residues (Phe19, Trp23, Leu29) of the p53 helix are all hydrophobic and interact with a hydrophobic pockets of MDM2 (see section 1.2).

The initial route for the synthesis of 2,6,8,9-tetrasubstituted purines is outlined in Scheme 5. Starting from 2-amino-6-chloro purine (**4**), alkylation at N9 using an alkyl bromide, and potassium carbonate as base in DMF afforded **5a-c** in reasonable isolated yields (59-73%). Unfortunately, the introduction of the R₂ substituent at 2N using a previously published reductive amination protocol using NaCNBH₃ as the

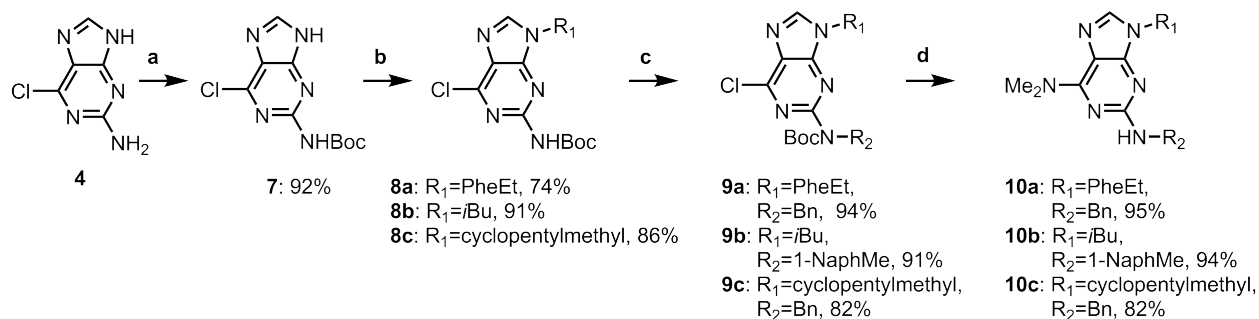
reducing agent proved unsuccessful as only trace of product could be observed by LCMS analysis.¹²⁹ The main product obtained was the alcohol derived from the reduction of the aldehyde. Other conditions and reducing agents (e.g. NaBH(OAc)₃) was evaluated but did not improve the outcome in this reaction, the low reactivity of the 2*N* amino group might be an explanation.



Scheme 5. Initial route towards 2,6,8,9-tetrasubstituted purines. Reagents and reaction conditions: (a) K₂CO₃ (1-1.2 eq.), R₁-Br (1-1.5 eq.), r.t., DMF.

Attempts to introduce R₂ by alkylation with at 2*N* benzyl halides, potassium iodide and potassium carbonate as base resulted in a mixture of mono- and di-substituted products. Therefore, alternative routes for the 2,9 substitution were investigated.

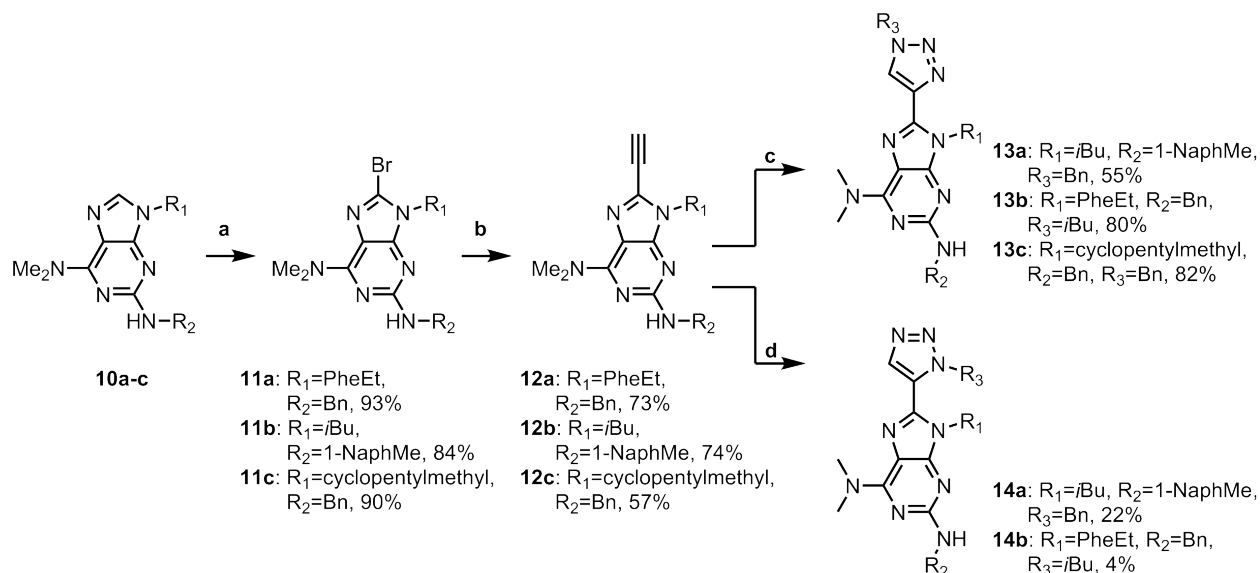
Fletcher *et al.*¹³¹⁻¹³² have published a protocol that involves two sequential Mitsunobu reactions, first at the *N*9- followed by the 2*N*-position, as the key steps. It was found that Boc protection at 2*N* improves the solubility in organic solvents and also activates the amine for a Mitsunobu reaction. Regioselectivity is believed to be obtained from the difference in acidity of the amines in 2- and 9-position as well as from the steric hindrance that the Boc group provides. Starting from 2-amino-6-chloropurine (**4**) the Boc group was introduced and **7** was isolated in 92% yield (Scheme 6).



Scheme 6. Synthesis of compound **7-10**. Reagents and reaction conditions: **(a)** (i) Boc₂O (1.1 eq.), DMAP (0.05 eq.), 0 °C – r.t., DMSO. (ii) NaH (1.4 eq.), r.t., THF. **(b)** R₁OH, DIAD, Ph₃P, r.t., THF. **(c)** R₂OH, ADDP, *n*Bu₃P, r.t., THF. **(d)** MW, 180 °C, DMF.

Applying the method by Fletcher *et al.* **8a-c** were isolated in 74-91% yield after the first Mitsunobu reaction and **9a-c** in 82-94% yield after the second Mitsunobu reaction (Scheme 6). The dimethylamino group was introduced in the 6-position by a nucleophilic aromatic substitution using microwave heating in DMF at 180 °C. Under these conditions dimethylamine is formed *in situ* from decomposition of DMF.¹²⁶ Furthermore, the Boc protecting group is also cleaved under these reaction conditions affording **10a-c** in 82-95% yield.

In order to activate C8 for C-C-cross coupling it was decided to brominate the C8-position. Standard protocols for the introduction of a bromine (e.g. *N*-bromosuccinimide (NBS) or Br₂) in the C8-position resulted in low yields and difficult purifications. It was found that pyridinium tribromide (PyrBr₃) could be used and **11a-c** could be isolated in 84-93% yields (Scheme 7). The findings concerning bromination with pyridinium tribromide will be discussed separately in section 5.3.



Scheme 7. Synthesis of compounds **11-14**. Reagents and reaction conditions: **(a)** PyrBr₃, DCM. **(b)** (i) Pd(II)Cl₂(PPh₃)₂, Cu(I)I, Amberlite IRA-67, TMS-acetylene, MW, 110 °C. (ii) PS-F, r.t., THF. **(c)** NaN₃, R₃-X, Cu(I)I, NaAsc, DMEDA, DMF. **(d)** NaN₃, R₃-X, Cp^{*}RuCl(PPh₃)₂, MW, 120 °C, DMF.

The terminal alkyne was introduced in the C8-position of **11a-c** using trimethylsilyl (TMS) acetylene in a Sonogashira type C-C-cross coupling catalysed by PdCl₂(PPh₃)₂ and CuI. TMS deprotection of the crude product using polymer supported fluoride provided **12a-c** in 57-74% yield over two synthetic steps.

As mentioned above in section 5.2.2 the regiochemistry of the triazole can be controlled by the choice of catalyst. The 1,4-triazole (**13a-c**) were obtained in 55-82% yield in the CuAAC. To avoid isolation of low molecular weight alkyl azides, which are potentially explosive, *isobutyl* azide was pre-formed by microwave heating of *isobutyl* bromide and sodium azide in DMF at 100 °C for 30 min followed by addition of alkyne, sodium ascorbate, CuI and DMEDA. Ruthenium catalysed cyclisation afforded the 1,5-triazoles **14a-b** in 4-22% yield. Full conversion of the starting material could be observed by TLC and/or LCMS analysis, the obtained products were difficult to purify and therefore low yields were obtained.

5.2.4 Evaluation of the purine type III mimetics as MDM2 inhibitors

The type III mimetics **13a-c** and **14a-b** were evaluated as MDM2 inhibitors in an FP-assay (section 1.2 and 4.4.4) in concentrations up to 47 μM . Unfortunately, all compounds were found to be inactive at the tested concentrations. The aqueous solubility of **13c** was determined to 0.3 μM at pH 7.4 which is too low to be practical for biological studies making it difficult to run the FP-assay at higher concentrations. To further investigate why this series did not show any inhibitory activity against the MDM2/p53 interaction it was decided to investigate the solution conformations by a NAMFIS analysis.

5.2.5 Conformational analysis of **13a** and **14a**

A NAMFIS analysis provides information of probable conformations present in solution (see section 4.3.1 and 4.4.3 for details about the NAMFIS analysis) and it was decided to use this method to further investigate if the 8-(triazolyl)purine scaffold could place the substituent in the same spatial orientation as an α -helix. The conformation of the triazole ring in relation to the purine ring determines the relative positions of the R_1 and R_3 substituents and is therefore suitable to investigate in a NAMFIS analysis. The solution conformation in DMSO of **13a** and **14a** was investigated and the distances were determined by running NOESY build-up experiments. The obtained key NOE correlations are shown in Figure 21.

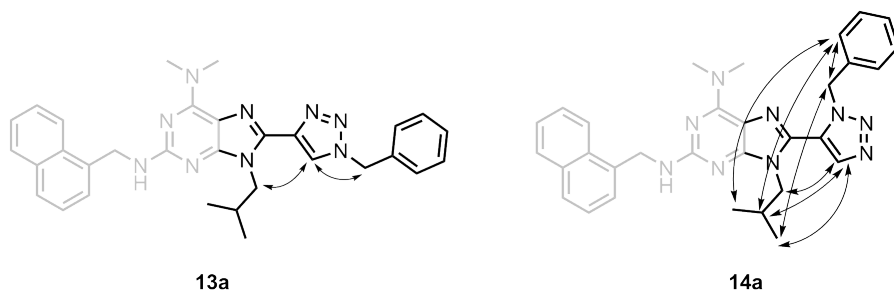


Figure 21. Key NOE-correlations observed for **14a** and **13a** indicated by the bent arrows.

The experimentally obtained distances (NOE) were fitted to the theoretical distances from the calculated conformations of **14a** and the NAMFIS analysis resulted in six possible conformations in solution (Figure 22).

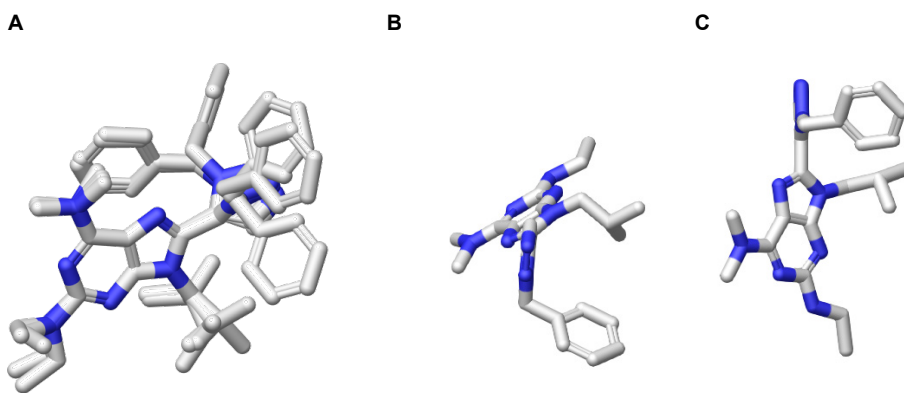


Figure 22. Conformations of **14a** found by the NAMFIS analysis. **(A)** An overlay of the six identified conformations; **(B)** Side view and **(C)** top view of one of the conformations. For clarification the naphthyl substituent has been removed in these figures.

The ensemble includes conformations that can place the substituents mimicking the $i+4$ and $i+7$ side chains of an idealized α -helix. The R_3 substituent (naphthylmethyl) in position $2N$ was excluded from the analysis since the goal of the conformational analysis was to determine the distance and orientation of the $R_1 = isobutyl$ and $R_3 = benzyl$ substituents relative to each other.

Only two NOEs were observed describing the conformation of the triazole ring in relation to the purine ring for **13a** (Figure 21). In this case, two correlations were not sufficient for a NAMFIS analysis. There are no alternative NOE correlations observed from **13a** that could describe the conformation of the triazole ring in relation to the purine ring.

In summary, the results from the NAMFIS analysis showed that the 8-(triazolyl)purine scaffold should be able to place the R₁ and R₃ substituent in the same spatial orientation as the *i*+4 and *i*+7 residues of an idealised α -helix and hence be suitable as α -helix mimetics (type III inhibitor). Since the compounds were inactive as inhibitors of the MDM2/p53 interaction at the concentrations evaluated in the FP-assay and they showed solubilities unsuitable for biological testing it was decided to design a second series of 8-(triazolyl)purines that could address the solubility issues.

5.2.6 Design of a second series of 8-(triazolyl)purines

During the work with the type III mimetics new potent MDM2 inhibitors co-crystallised with MDM2 were published,^{62,133-135} e.g. AMG 232 (Figure 7 section 1.3.3). As a result, docking studies could be used to optimise the design towards a type II mimetic. As discussed in section 1.3.3 AMG 232 is classified as a type II mimetic and the scaffold is not mimicking the topography of an α -helix as in the type III mimetics. Investigation of these new inhibitors in combination with docking studies using Glide as implemented in the Schrödinger package¹³⁶ revealed two major changes in the design. First, it was decided to decrease the size of the hydrophobic substituents making the inhibitor smaller, a typical type II inhibitor is generally not as extended as type III inhibitors. The docking results showed that changing the R₁ substituent from phenethyl to the more rigid indanyl and decreasing the size of the R₂ and R₃ substituents to a propyl and methyl group, respectively, improved the fit of the 8-

(triazolyl)purines in the MDM2 pockets (Figure 23). Second, as also discussed in section 4.4.1 several of the published binders of MDM2 have a hydrophilic substituent that can interact with the His96 and Lys94 residues of MDM2 *via* hydrogen bonding and/or ionic interactions. Introduction of a more hydrophilic substituent could also address problems with solubility. The docking model showed that introduction of a more hydrophilic group such as a carboxylic acid or ester in the 6-position could allow hydrogen bonding and/or ionic interactions. An example of an 8-(triazolyl)purine with $R_1 = \text{indanyl}$, $R_2 = \text{propyl}$, $R_3 = \text{methyl}$ and $R_4 = \text{NHCH}_2\text{CO}_2\text{H}$ is shown in Figure 23.

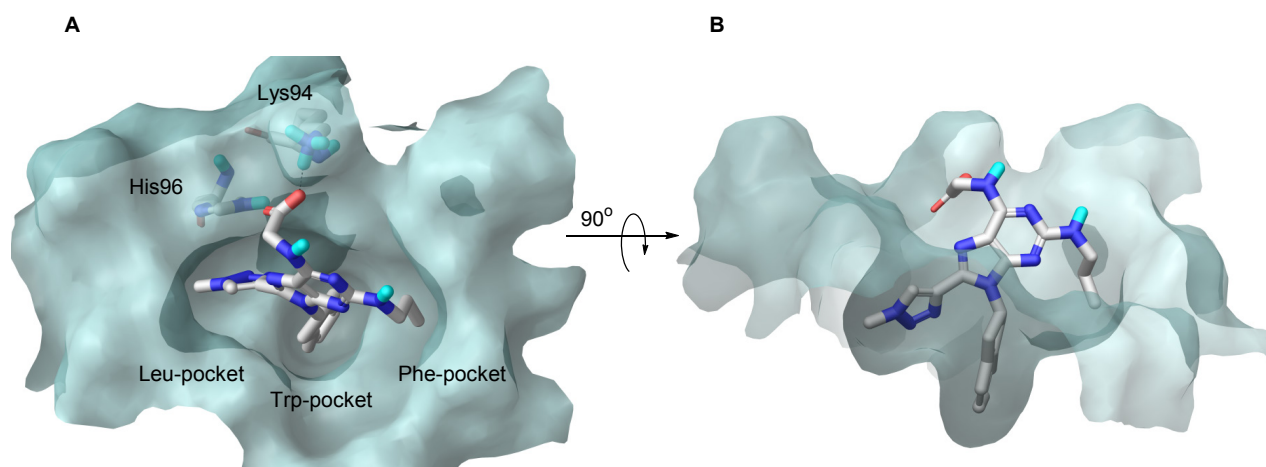


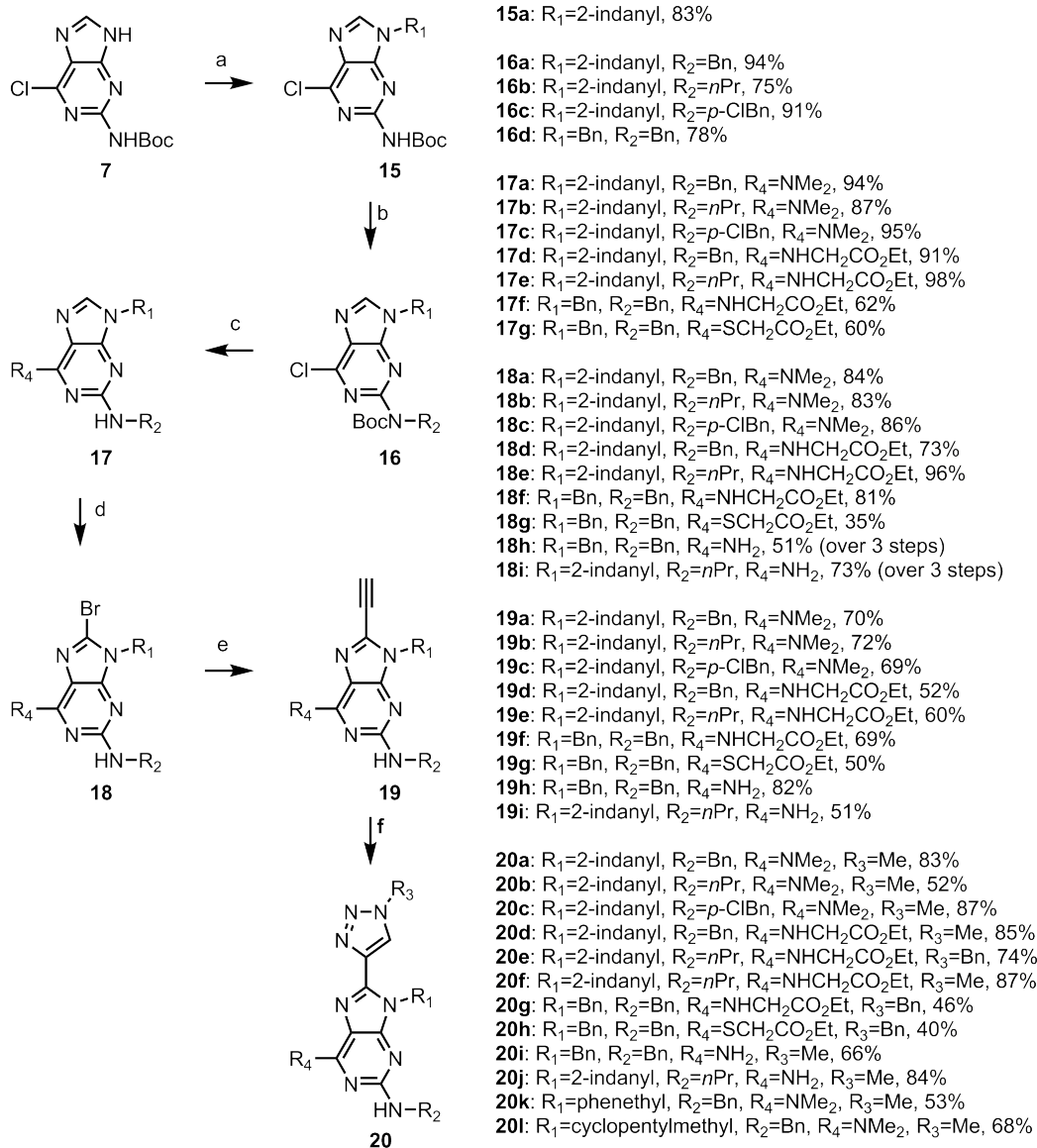
Figure 23. Docking of 8-(triazolyl)purine derivatives to MDM2 (PDB code: 4HBM), the protein surface is shown in turquoise. (A) The carboxylic acid moiety in position 6 makes an ionic interaction with the Lys94 residue of MDM2; (B) 90° rotation of A.

5.2.7 Synthesis of 8-(triazolyl)purines as type II mimetics

The synthesis of the series of type II mimetic series is outlined in Scheme 8. The introduction of R_1 and R_2 and the dimethylamino moiety in the 6-position (R_4) were performed as described above. Target compounds **15a** and **16a-d** were isolated in 83% and 75-94% yield, respectively. In order to introduce a more hydrophilic group in the

6-position, the 6-chloropurine derivatives (**16a,b,d**) were reacted with thioglycol ethyl ester or glycine ethyl ester under basic conditions. After Boc deprotection with TFA in DCM **17d-g** could be isolated in 60-98% yields over two steps. The bromine was introduced utilising PyrBr₃ to afford **18a-g** in 35-96% yield, where the lower yield of 35% was obtained for bromination of **17g** having a sulphur in the 6-position which gave lower yield compared to nitrogen in the same position.

Introduction of a primary amine in the 6-position was investigated since it could reduce the lipophilicity and hence improve the solubility. Compounds **16b** and **16d** were treated with ammonium hydroxide and the corresponding 6-amino derivative could be isolated. Bromination of the 6-amino derivatives with PyrBr₃ in DCM proved unsuccessful which was assumed to be due to the electron withdrawing effect of the Boc group in the 2*N*-position. After removal of the Boc group using TFA in DCM the bromination reaction was successful. The amination, deprotection and bromination sequence could be run without purification between each step and **18h** and **18i** were isolated in 51 and 73% yield over three synthetic steps, respectively. Compound **19a-i** were isolated in 50-82% yield employing the same Sonogashira coupling protocol as used in Scheme 7. Only the 1,4-triazole was considered in this series since the synthesis of the 1,5-triazole resulted in poor yields. The same cyclisation protocol used for the synthesis of the type III mimetics was employed and compounds **20a-l** were isolated in 40-87% yield.



Scheme 8. Synthesis of compounds **15-20**. Reagents and reaction conditions: **(a)** R₁OH, DIAD, Ph₃P, r.t., THF. **(b)** R₂OH, ADDP, *n*Bu₃P, r.t., THF. **(c)** R₄=NMe₂, DMF, MW, 180 °C. R₂=*p*-ClBn, R₄=NMe₂, (i) 5.6 M NMe₂ in EtOH. (ii) TFA/DCM. R₄=NHCH₂CO₂Et, (i) H₂NCH₂CO₂Et, Et₃N, EtOH, 100 °C. (ii) TFA/DCM, R₄=SCH₂CO₂Et, (i) HSCH₂CO₂Et, NaH, toluene, 70 °C. (ii) TFA/DCM. **(d)** PyrBr₃, DCM. For R₄=NH₂, (i) NH₄OH (aq.), dioxane, 100 °C. (ii) TFA/DCM. (iii) PyrBr₃, DCM. **(e)** (i) Pd(II)Cl₂(PPh₃)₂, Cu(I)I, Amberlite IRA-67, TMS-acetylene, MW, 110 °C, THF (ii) PS-F, THF. **(f)** NaN₃, R₃-X, Cu(I)I, NaAsc, DMEDA, DMF.

As described for the synthesis of *isobutyl* azide, methyl azide was formed prior to use by mixing methyl iodide and sodium azide in DMF which was then added as a solution to a mixture of the alkyne, CuI, sodium ascorbate and DMEDA. The highest yields in the cyclisation were obtained when the azide formation was run at room temperature followed by cyclisation at 60 °C. For the synthesis of **20k-l**, **10a**, and **10c** were used as starting materials (for synthesis of **10a** and **10c** see Scheme 6).

5.2.8 Evaluation of the 8-(triazolyl)purines type II mimetics as MDM2 inhibitors

The new purine-based derivatives, **20a-l**, were evaluated as inhibitors against the MDM2/p53 interaction using the standard FP-assay. Of the 12 evaluated compounds two of the purines showed activity (**20f** and **20j**) with IC₅₀ values of 10 μM and 56 μM, respectively (Figure 24A). The IC₅₀ curve of **20f** is shown in Figure 24B.

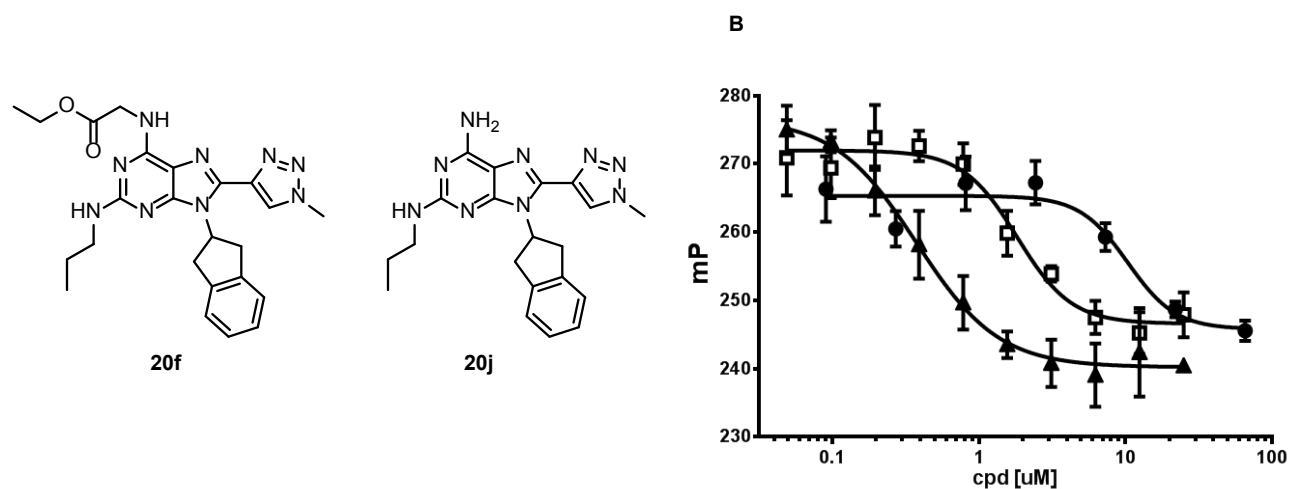


Figure 24. (A) 8-(triazolyl)purine type II inhibitors against the MDM2/p53 interaction; (B) Inhibition curves for nutlin-3a (▲) the natural p53 peptide (□) (positive controls) and for **20f** (●) (IC₅₀ = 10.4 μM [95% CI, 6.02–17.95]).

To confirm activity a secondary assay was run. The ability of **20f** to bind to MDM2 was investigated in a WaterLOGSY experiment (see section 2.3) which confirmed binding to MDM2 (for spectra see Figure A3, Appendix 5).

5.2.9 Photophysical characterisation of 8-(triazolyl)purines

Inherently fluorescent α -helix mimetics could potentially be used for imaging and localisation of compounds in cells. Examples of inherently fluorescent compounds include compounds that bind to specific cell types and allow their identification by the fluorescent properties of the molecule¹³⁷ as well as fluorescent inhibitors of kinases¹³⁸ and glutathione *S*-transferase.¹³⁹ UV/vis absorption and fluorescence measurements were performed and the data obtained are presented in Table 4 and a selection of absorption and emission spectra is shown in Figure 25.

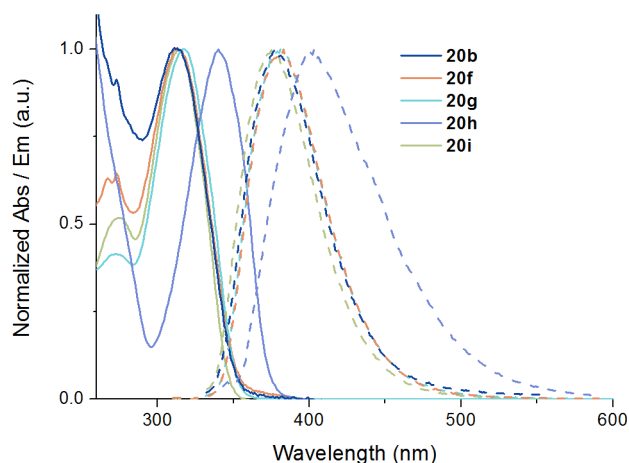
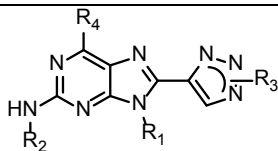


Figure 25. Photophysical characterisation of **20b**, **20f**, **20g**, **20h** and **20i**. Spectra of a selection of 8-(triazolyl)purines, normalised absorption (solid lines) and emission (dashed lines).

All the 8-triazolyl compounds have absorption maxima between 310 and 322 nm (entries 1-15) except **20h** (entry 16) which has a red shifted absorption maximum of 340 nm. In general low fluorescence quantum yields (1-2%) were obtained for compounds having tertiary amines in the 6-position ($R_4 = NMe_2$) and $R_3 = 1,4$ triazole (entries, 1-5 and 12) except for compound **13b** which had a quantum yield of 5% (entry 13). Replacing the tertiary amine in the 6-position with a primary amine or secondary amines increased the quantum yield to 4-7% (entries 6-7) and 4-10% (entries 8-11), respectively. Changing substituents at $N9$ or $2N$ did not affect the quantum yield to any greater extent. However, changing from 1,4- to 1,5-triazole did increase the fluorescence quantum yields, from 2-5% for the 1,4- to 37-51% for the 1,5-triazoles (entries 12-15). In order to confirm the effect of the triazole ring on the fluorescent properties compounds with a proton, bromine and alkyne in the 8-position were also investigated (entries 17-19). However, no quantum yield could be determined for these compounds since the emission was too low.

Table 4. Absorption and fluorescent properties of 8-(triazolyl)purine derivatives in MeOH solution. $\lambda_{\text{abs, max}}$ and $\lambda_{\text{em, max}}$ are the wavelengths of absorption and emission maxima, respectively, and Φ_F is the fluorescence quantum yield.



Entry	Cmp ^a	R ₁	R ₂	R ₃	R ₄	$\lambda_{\text{abs,max}}$ (nm)	$\lambda_{\text{em,max}}$ (nm)	Φ_F (%)
1	20a	2-Indanyl	Bn	1,4-Me	NMe ₂	310	376	2
2	20k	Phenethyl	Bn	1,4-Me	NMe ₂	315	376	2
3	13c	Cyclopentyl- methyl	Bn	1,4-Bn	NMe ₂	317	377	2
4	20b	2-Indanyl	<i>n</i> Pr	1,4-Me	NMe ₂	311	378	1
5	20l	Cyclopentyl- methyl	Bn	1,4-Me	NMe ₂	316	376	2
6	20i	Bn	Bn	1,4-Me	NH ₂	314	375	7
7	20j	2-Indanyl	<i>n</i> Pr	1,4-Me	NH ₂	311	377	4
8	20d	2-Indanyl	Bn	1,4-Me	NHCH ₂ CO ₂ Et	311	377	8
9	20g	Bn	Bn	1,4-Bn	NHCH ₂ CO ₂ Et	318	381	10
10	20e	2-Indanyl	<i>n</i> Pr	1,4-Bn	NHCH ₂ CO ₂ Et	316	382	4
11	20f	2-Indanyl	<i>n</i> Pr	1,4-Me	NHCH ₂ CO ₂ Et	313	380	5
12	13a	1-Naphtyl methyl	<i>i</i> Bu	1,4-Bn	NMe ₂	318	378	2
13	13b	Phenethyl	Bn	1,4- <i>i</i> Bu	NMe ₂	316	378	5
14	14a	1-Naphtyl methyl	<i>i</i> Bu	1,5-Bn	NMe ₂	322	437	37
15	14b	Phenethyl	Bn	1,5- <i>i</i> Bu	NMe ₂	320	422	51
16	20h	Bn	Bn	1,4-Bn	SCH ₂ CO ₂ Et	340	398	2
17	21	Phenethyl	Bn	ξ-H	NMe ₂	292	351	<1
18	11a	Phenethyl	Bn	ξ-Br	NMe ₂	294	412	<1
19	12a	Phenethyl	Bn	ξ≡	NMe ₂	319	391	<1

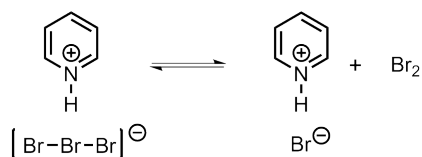
^aCmp = Compound

5.3 8-Bromination of purines (Paper III)

Looking through the literature there is no obvious standard procedure for the introduction of bromine in the C8-position of purines. However, Br_2 ¹⁴⁰ and NBS¹⁴¹⁻¹⁴² are reagents that are more frequently used. In addition, sodium monobromoisocyanurate¹⁴³ and 1,3-dibromo-5,5-dimethylhydantoin¹⁴⁴ have also been reported for the bromination of nucleobases including adenosine.

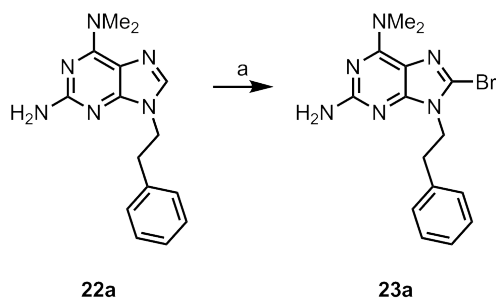
During the synthesis of 8-(triazolyl)purines described in section 5.2.3 commonly used methods for the bromination were examined, i.e. NBS in acetonitrile¹⁴⁵ or Br_2 in NaOAc/HOAc buffer in THF/MeOH.^{108,140} Both methods resulted in poor yields, 25% and 30% respectively, and in the case of NBS *para*-bromination of the phenethyl substituent could also be observed by ¹H NMR spectroscopy.

Pyridinium tribromide (PyrBr_3) has previously been used for the α -bromination of ketones,¹⁴⁶⁻¹⁴⁸ different aryl compounds¹⁴⁹⁻¹⁵¹ and alkenes.¹⁵²⁻¹⁵³ It is a crystalline solid and is much easier to handle than elemental bromine which is a liquid with high viscosity and low vapour pressure. PyrBr_3 is in equilibrium with pyridinium bromide and Br_2 in solution (Scheme 9) and both PyrBr_3 and Br_2 have been reported to act as brominating agents.¹⁵⁴



Scheme 9. Pyridinium tribromide (PyrBr_3) in equilibrium with pyridinium bromide and bromine in solution

When **22a** was treated with PyrBr_3 in DCM at room temperature for 5 h **23a** was isolated in 93% yield (Scheme 10).



Scheme 10. 8-Bromination of **22a** using PyrBr_3 . Reagents and reaction conditions: (a) PyrBr_3 , DCM, r.t., 5 h.

In addition to the higher yield, the workup procedure and purification are considerably simplified using PyrBr_3 compared with the use of elemental bromine. Furthermore, the need of brominating reagent in large excess is avoided as only 1.2 equivalents of PyrBr_3 is required to convert **22a** to **23a**.

Based on this result it was decided to explore if PyrBr_3 could be used as a general method for the bromination of purines in the C8-position. Since the bromination of **22a** was run in DCM at room temperature using 1.2 equivalents of PyrBr_3 , all reactions were run using these conditions. The obtained results are summarised in Table 5. Bromination of electron rich 2,6,9-trisubstituted purine derivatives using PyrBr_3 (entries 2-5) afforded the brominated products in high yields (80-91%). Due to the general poor solubility of several purines in DCM, alternative solvents were explored. Running the bromination reaction in DMF resulted in lower yields and the use of MeCN afforded the brominated product in comparable yields but slowed down the reaction (see e.g. entries 2, 7 and 9). Removing the substituent in the N9-position or the amino group in the C2-position resulted in no reaction or low yields in the bromination (entries 10-16). To investigate if the poor solubility of the starting materials were the reason for the low yield, the reactions were also run in DMF. However, bromination of **22i** with PyrBr_3 in DMF gave comparable yield to when the

reaction was run in DCM (entries 12-13). Electron withdrawing substituents in the 6-position were not tolerated (entry 21).

Table 5. 8-Bromination of purines using PyrBr₃.^a

Entry	Starting material	R ⁶	R ²	R ⁹	Solvent	Time (h)	Product	Yield (%) ^b
1	22a	N(Me) ₂	NH ₂	Phenethyl	DCM	5	23a	93
2	22b	N(Me) ₂	NH ₂	Bn	DCM	3	23b	90
3	22c	NHBn	NH ₂	Bn	DCM	3	23c	87
4	22d	N(Me) ₂	NH ₂	<i>i</i> Bu	DCM	2.5	23d	80
5	22e	N(Me) ₂	NHBn	Phenethyl	DCM	1	23e	91
6	22f	NH ₂	NH ₂	Bn	DMF	5	23f	27
7	22b	N(Me) ₂	NH ₂	Bn	DMF	3	23b	47
8	22a	N(Me) ₂	NH ₂	Phenethyl	DMF	3	23a	59
9	22b	N(Me) ₂	NH ₂	Bn	MeCN	o.n	23b	80
10	22g	Cl	H	H	DCM	24	23g	nr ^c
11	22h	Cl	NH ₂	H	DCM	o.n ^d	23h	trace ^e
12	22i	N(Me) ₂	NH ₂	H	DMF	6	23i	38
13	22i	N(Me) ₂	NH ₂	H	DCM	55	23i	46
14	22j	NH ₂	H	Bn	DCM	48	23j	nr
15	22k	Cl	H	Bn	DCM	o.n	23k	nr
16	22l	OMe	H	Bn	DCM	o.n	23l	nr
17	22m	N(Me) ₂	H	Bn	DCM	o.n	23m	trace
18	22n	NHBn	NHBoc	Bn	DCM	3	23n	36
19	22o	OMe	NH ₂	Bn	DCM	o.n	23o	37
20	22o	OMe	NH ₂	Bn	DCM	o.n	23o	43 ^f
21	22p	Cl	NH ₂	Bn	DCM	16	23p	nr
22	22b	N(Me) ₂	NH ₂	Bn	DCM	4	22b	93 ^g

^aReagents and reaction conditions: Purine (1.0 eq.), PyrBr₃ (1.1-1.4 eq.), DCM (0.05 M), r.t. ^bIsolated yield. ^cnr = no reaction, i.e., only starting material was observed by LCMS and/or TLC. ^do.n = overnight. ^eOnly a trace amount of the product was observed by LCMS. ^f3 equivalents of PyrBr₃ were used. ^gPyrBr₃ on polymer support was used.

5.4 Summary of papers II and III

Two series of 2,6,9-trisubstituted 8-(triazolyl)purines have been synthesised and evaluated as inhibitors of the MDM2/p53 PPI. The first series, type III inhibitors, proved inactive as MDM2 inhibitors in the FP-assay. The possible conformations in solution for two of the compounds were evaluated by a NAMFIS analysis. The result showed that the scaffold should be able to mimic the topography of an α -helix and could be potentially useful as α -mimetics. However, the analysis could not reveal why this series was inactive as inhibitors. The design was re-evaluated and based on docking studies a new series was synthesised and evaluated. Two out of fourteen compounds (**20f** and **20j**) from the second series showed micromolar IC₅₀ values in the FP-assay. Binding of **20f** to MDM2 was confirmed by WaterLOGSY experiments. The fluorescent properties of the obtained compounds were determined as quantum yields ranging from 1-51%. Interestingly changing the regioisomerism of the triazole from 1,4 to 1,5 resulted in a 10-fold increase of the quantum yield. In addition, an efficient bromination protocol using PyrBr₃ for the bromination of electron rich purines was developed.

6 2,5-Diketopiperazines as Inhibitors of the MDM2/p53 PPI (Paper IV)

Previous work in the group has been focused on development of efficient methods for the synthesis of 2,5-diketopiperazines (2,5-DKPs).¹⁵⁵⁻¹⁵⁸ In the following chapter the development of 2,5-DKP based inhibitors against the MDM2/p53 PPI will be discussed.

6.1 2,5-Diketopiperazines

A 2,5-DKP is a cyclic dipeptide (Figure 26). The DKP motif can be found in numerous natural products and pharmacologically active compounds that display a spectrum of biological activities, examples include anticancer, antibacterial, antiviral, antifungal and anti-inflammatory agents (Figure 26).¹⁵⁹

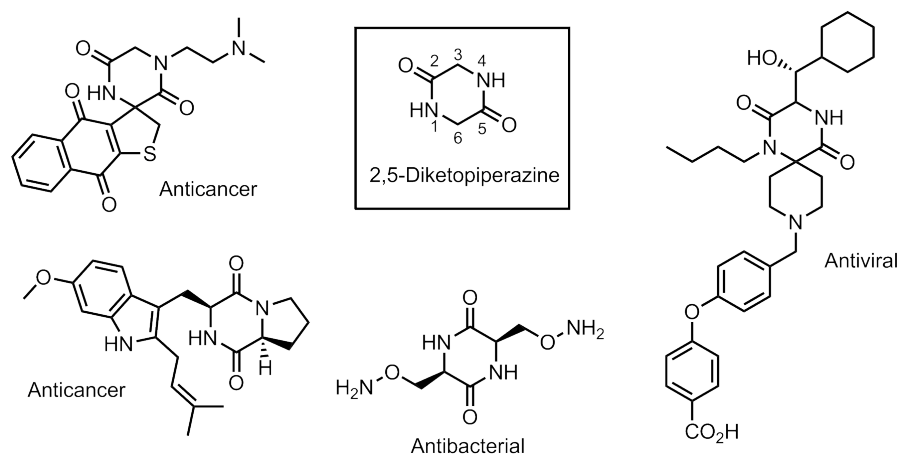
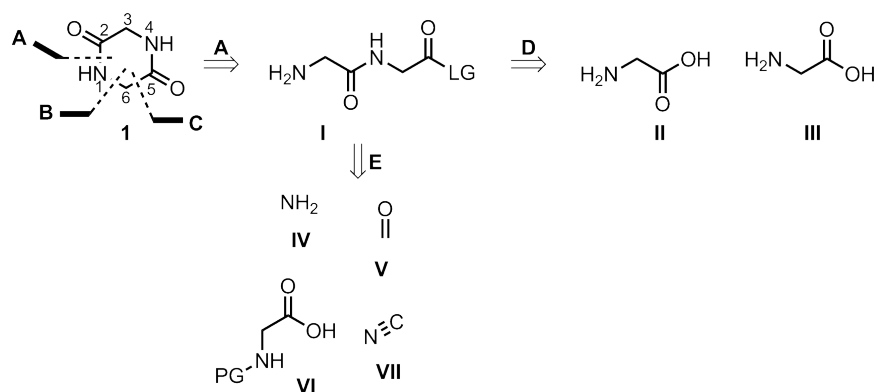


Figure 26. Structure of a 2,5-DKP with numbering of atoms and examples of biologically active 2,5-DKPs.

The 2,5-DKP scaffold is useful since it is small and conformationally rigid, it has up to six positions where diversity can be introduced with defined stereochemistry and it has functional groups that can act as both H-bond acceptors and H-bond donors.¹⁵⁹ In addition, 2,5-DKPs are attractive as starting material for the synthesis of other heterocyclic systems.¹⁶⁰

6.1.1 Synthesis of 2,5-DPKs

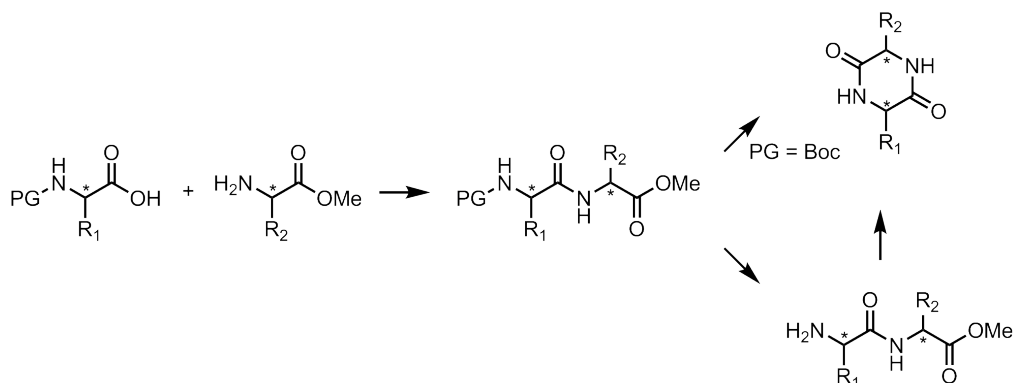
Retrosynthetic analysis of the 2,5-DKP ring system gives three disconnections: the amide bond (A), the C–N bond (B), and the C–C bond (C) (Scheme 11).¹⁵⁹ The most common strategy is to use disconnection A and only this will be further discussed in this work. The dipeptide I can be derived from either peptide coupling of the two amino acids (II and III, path D) or from a multicomponent Ugi reaction (path E) using an amine (IV), a carbonyl compound (aldehyde or ketone) (V), a carboxylic acid (Boc protected amino acid) (VI) and an isonitrile (VII).



Scheme 11. Retrosynthetic analysis of 2,5-DKP, LG = leaving group, PG = protecting group.

6.1.1.1 Synthesis of 2,5-DKPs via dipeptides derived from two amino acids

Synthesis of 2,5-DKPs *via* dipeptides is used routinely, the dipeptide can easily be obtained by peptide coupling of two amino acids (Scheme 12).¹⁵⁹ A large selection of commercially available protected amino acid derivatives as well as coupling agents makes this an attractive strategy (for peptide coupling reagents see Figure 14 section 4.2). Dipeptides can spontaneously cyclise under a range of both basic and acidic conditions to form a 2,5-DKP. Depending on the choice of protecting group (PG) direct cyclisation of the dipeptide is possible as is cyclisation *via* a separate deprotection step (Scheme 12).



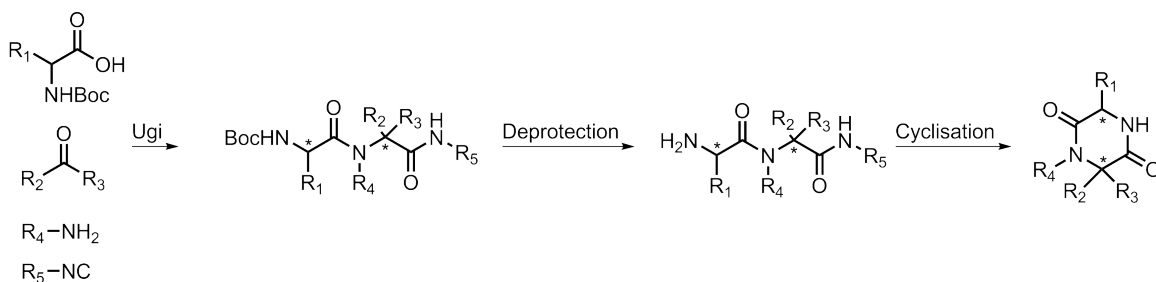
Scheme 12. 2,5-DKPs *via* dipeptides obtained from peptide coupling of two amino acids.

For the cyclisation to proceed spontaneously the amide bond needs to be in the *cis*-conformation. When the *cis*-conformation is prevented by steric or electronic hindrance, heat or catalysis by acid or base can facilitate the cyclisation.^{156,161-163}

6.1.1.2 Synthesis of 2,5-DKPs *via* the Ugi multicomponent reaction

The Ugi reaction¹⁶⁴ offers a complementary method to form the dipeptide and has proven useful in drug discovery, natural product synthesis and combinatorial chemistry as a source of peptidomimetic scaffolds.¹⁶⁵⁻¹⁶⁷

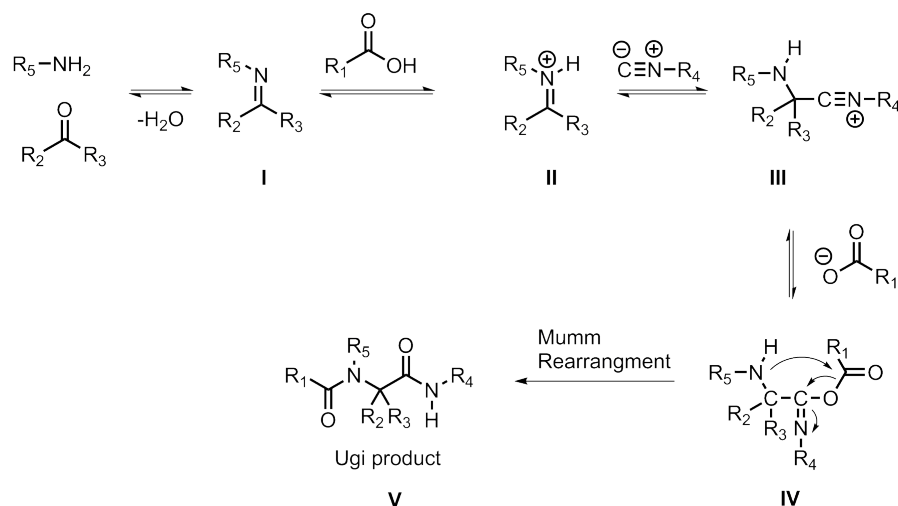
One variation of the Ugi reaction, the so called Ugi/Deprotection/Cyclisation (UDC) reaction, has been used for the synthesis of 2,5-DKPs (Scheme 13).¹⁶⁸⁻¹⁷¹ The Ugi reaction provides access to chemically diverse peptides since the required reactants (amines, carboxylic acids, aldehydes and isonitrile) are readily available. It should be noted that although commercial access to isonitriles is more limited than for the other three components, the terminal amide produced from this moiety often serves as a leaving group during formation of the 2,5-DKP ring (*vid infra*), and therefore, this does not affect the potential for diversity. Examples of isonitriles often used in UDC reactions include cyclohexenylisonitrile¹⁷² and *n*-butylisonitrile¹⁷³ and 2-(morpholin-1-yl)ethylisonitrile¹⁷¹.



Scheme 13. General reaction scheme of the UDC reaction used for the synthesis of 2,5-DKPs.

The proposed reaction pathway for the multicomponent Ugi reaction is illustrated in Scheme 14.¹⁷⁴⁻¹⁷⁵ In the first step an imine (I) is formed from condensation of the amine and an aldehyde or ketone, this is believed to be the rate determining step. The

imine is then protonated by the acid and a more reactive iminium ion (II) is formed which is attacked by the isonitrile. The obtained nitrilium intermediate (III) is trapped by the carboxylate forming an α -adduct (IV). The α -adduct is often unstable and can decompose to starting material or irreversibly rearrange *via* a so called Mumm rearrangement. The acyl moiety is transferred from the oxygen onto the nitrogen atom of the starting imine, to form a stable α -acylamino amide or the so called Ugi product (V).



Scheme 14. Reaction pathway for the multicomponent Ugi reaction.¹⁷⁴

6.2 2,5-DKPs as MDM2 inhibitors (Paper IV)

6.2.1 Design of 2,5-DKPs as type III mimetics

To evaluate if the spiro-2,5-DKP (spiro-1-DKP) derivatives (Figure 27B) could be used as α -helix mimetics, a range of energy minimised substituted spiro-1-DKPs were compared against an α -helix made up of alanine residues as described for the purine derivatives (section 5.2.1). The results indicated that the spiro-1-DKP scaffold with the substitution pattern illustrated in Figure 27B has the ability to arrange the

substituents as the i , $i+4$, $i+7$ residues of an Ala-helix (Figure 28C). The model also showed that the S -configuration in position C3 is preferred and that the exocyclic amino group should be in an equatorial position for optimal positioning of the substituent. A representative example is shown in Figure 27D where **I** (Figure 27C) is superimposed onto an Ala-helix.

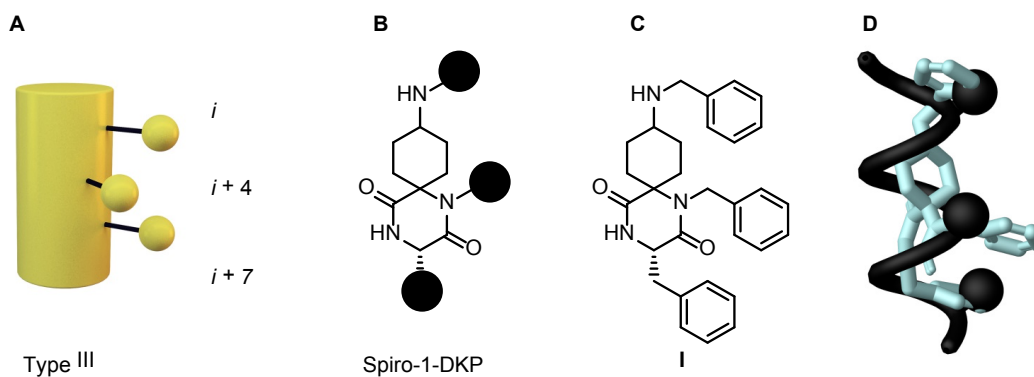
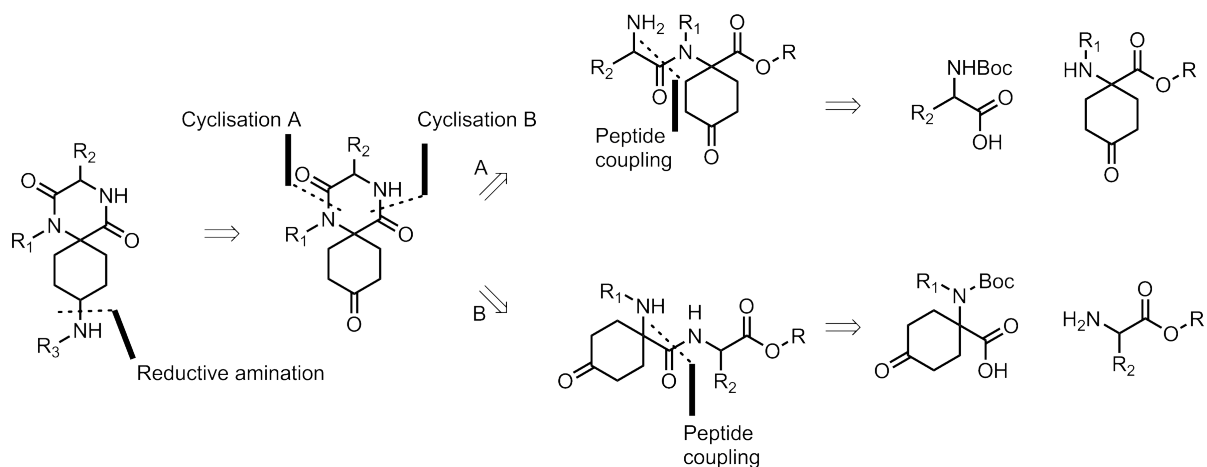


Figure 27. (A) Schematic illustration of a type III mimetic; (B) General structure of spiro-1-DKP; (C and D) Superimposition of an Ala-helix (black) with a low energy conformation of compound **I**. Only the i , $i+4$ and $i+7$ residues of the Ala-helix are shown.

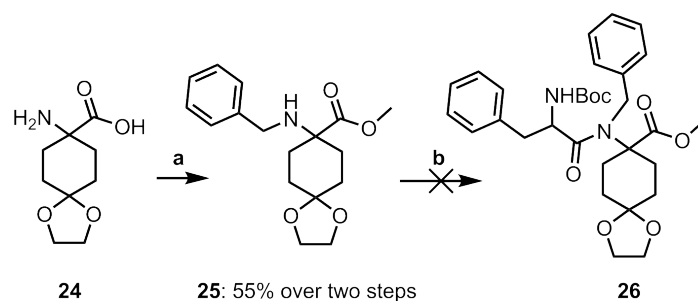
Retrosynthetic analysis of the spiro-1-DKPs is outlined in Scheme 15. The introduction of the R_3 substituent last in the synthesis makes it possible to introduce diversity late in the synthesis, R_3 could be introduced by reductive amination. Two possible routes for the cyclisation were considered here, either *via* cyclisation of an N -alkylated dipeptide (A) or an N -terminally alkylated dipeptide (B). The dipeptide can be obtained *via* peptide coupling of the appropriate amino acids shown in Scheme 15.



Scheme 15. Retrosynthetic analysis of spiro-1-DKPs.

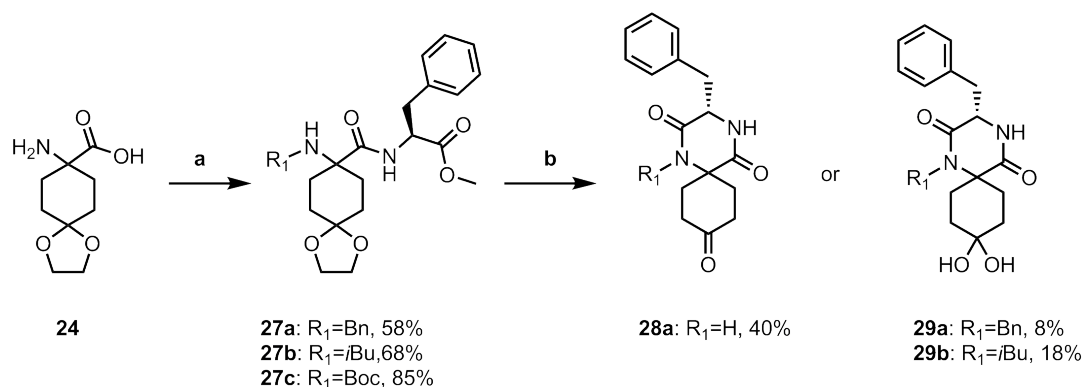
6.2.2 Synthesis of 2,5-DKPs as type III mimetic

The initial synthetic route towards spiro-1-DKPs involved cyclisation method A (Scheme 16). Since the key residues (Phe19, Trp23, Leu29) of the p53 helix interacting with MDM2 are all hydrophobic, hydrophobic substituents (R_{1-3}) were selected. The commercially available 8-amino-1,4-dioxaspiro[4.5]decane-8-carboxylic acid (**24**) was used as starting material. First the R_1 (benzyl) substituent was introduced using a reductive amination protocol with benzaldehyde, NaCNBH_3 and Et_3N ,¹⁷⁶ followed by protection of the carboxylic acid as the corresponding methyl ester using trimethylsilyl diazomethane (TMS-CHN_2) (Scheme 16).¹⁷⁷ Compound **25** was isolated in 55% yield over two synthetic steps. Several peptide coupling protocols such as HATU, EDC/HOBt and T3P were explored but they all failed to provide **26** and only starting material could be recovered after the reaction. The steric hindrance and the low nucleophilicity of the amine were believed to be the main reasons for the outcome of the reaction.



Scheme 16. Synthesis of compound **25**. Reagents and reaction conditions: **(a)** (i) PhCHO (1.2 eq.), Et₃N (1.2 eq.), NaCNBH₃ (1.0 eq.), MeOH, r.t. (ii) (CH₃)₃SiCHN₂ (6.4 eq.), MeOH, toluene (1:3), r.t.

It was then decided to explore the alternative cyclisation route B (Scheme 17). If the R₁ substituent would be introduced first no amine protecting group would be necessary, since, as observed using the cyclisation route A, an *N*-terminally alkylated amine did not participate in the peptide coupling (see Scheme 16). The R₁ substituent was introduced by reductive amination, followed by a peptide coupling using HATU as coupling reagent.



Scheme 17. Synthesis of compounds **27-29**. Reagents and reaction conditions: **(a)** For **27a** and **27b**: (i) R₁CHO (1.2-1.5 eq.), Et₃N (1.2 eq.), NaCNBH₃ (1.0 eq.), MeOH, r.t. (ii) Phe-OMe (2.0 eq.), HATU (2.0 eq.), DIPEA (12 eq.), DMF, 60 °C, 30 min. For **27c**: (i) Boc₂O, 3 M NaOH and 1,4-dioxane (1:2, pH ~12), r.t. (ii) Phe-OMe (2.0 eq.), HATU (2.0 eq.), DIPEA (6.0 eq.), DMF, 60 °C, 30 min. **(b)** **28a**: water, MW, 160 °C, 30 min; **29a**: water, MW, 160 °C, 90 min. **29b**: 1 M HCl (aq.) and acetone (1:1), 55 °C, 72 h.

Compound **27a** and **27b** could be isolated in 58-68% yield over two synthetic steps. Synthesis of spiro-DKPs *via* cyclisation of Boc-protected dipeptide methyl esters using water as solvent and microwave irradiation have previously been reported.¹⁵⁸ It was anticipated that these reaction conditions would result in cyclisation of the dipeptide, and also cleave both the Boc and the acetal protecting groups, to the corresponding spiro-1-DKP. Microwave heating of **27a** using water as solvent at 100 °C for 30 min resulted in a mixture of products and only trace amounts of the expected **29a** could be observed by LCMS. The major mass ions observed by LCMS correspond to side products derived from hydrolysis of the ester and/or acetal. Compound **29a** could be isolated in 8% yield after increasing both the temperature to 160 °C and the reaction time to 90 min. Attempts to increase the temperature or reaction time further did not improve the outcome of the reaction. Since the dipeptide with a free carboxylic acid was unable to cyclise to the corresponding 2,5-DKP reaction conditions that would minimise ester hydrolysis were explored. Using a 1:1 mixture of 1 M HCl (aq.) and acetone as the solvent under thermal heating at 55 °C for 72 h provided **29b** in 18% yield. LCMS analysis of the reaction mixture revealed that ester hydrolysis was still a major problem. In order to examine the impact of the secondary amine in the cyclisation **27c** (R₁=H) was synthesised. Boc-protection of **24** using Boc anhydride followed by peptide coupling with Phe-OMe using HATU as coupling reagent gave **27c** in 85% yield over two steps. Compound **27c** was heated in the microwave at 160 °C for 30 min using distilled water as solvent, whereupon **28a** was isolated in 40% yield (Scheme 17). Changing solvent to a 1:1 mixture of 1 M HCl (aq.) and acetone did not improve the yield. ¹³C NMR analysis of **29a** and **29b** revealed that instead of the expected ketone on the cyclohexyl ring the major product in solution was the geminal diol, which could be identified by peaks at 93.0 and 92.9 ppm for **29a** and **29b**, respectively. HRMS analysis of **29b** confirmed the diol formation. In comparison,

6.2.3 Biological evaluation of 2,5-DKPs as type III inhibitors

The obtained 2,5-DKPs, **28a**, **28b**, **29a**, **29b**, **32a**, **32b** and **32c**, were evaluated as type III inhibitors for the MDM2/p53 interaction in the standard FP-assay (see section 2.1). None of the seven evaluated compounds showed activity at the concentrations tested, up to 100 μ M. In analogy with the 8-(triazolyl)purines a re-evaluation of the original design was undertaken aiming for type II mimetics. Since the utilised synthetic route failed to provide trisubstituted 2,5-DKPs, an alternative synthetic route was also investigated.

6.2.4 Design of 2,5-DKPs as type II inhibitors

In analogy with the design of 8-(triazolyl)purines as type II inhibitors described in section 5.2.6 two major changes in the design based primarily on docking studies of 2,5-DKPs were made. The size of the scaffold was decreased and hydrophilic substituents were introduced that could participate in additional interactions with MDM2 and possibly improve solubility of the new series. The docking results also showed that a cyclohexyl group in the C6-position could serve as a substituent interacting with the Phe-pocket of MDM2 (Figure 29), as compared to the type III spiro-1-DKP where the cyclohexyl group is part of the scaffold. Furthermore, the C3 and N1 substituents could interact with the Leu- and Trp-pockets, respectively (Figure 28A and B). A hydrophilic substituent such as a carboxylic acid, ester, amide or alcohol could be introduced in the N4- or the C3-position enabling an additional interaction with MDM2. The model showed that the *S*-configuration at position C3 was preferred. Replacing the cyclohexyl group to a phenyl group in the C6-position also fitted in the Trp-pocket of MDM2 (Figure 28C). The model showed that the DKP ring system is rotated switching place of the C3 and C6 substituents, so that they now interact with the Phe- and Leu-pockets, respectively (Figure 28A compared to

28C). In addition, the isomer with *R*-configuration at C3 and *S*-configuration at C6 was now preferred. The *N*1 substituent could also be exchanged to a phenyl with good results (Figure 28D). Halogenated phenyl rings interacting in the Trp- and Leu-pockets have been shown to improve the inhibitory activity to MDM2.¹⁷⁹ The docking model showed that both chlorinated benzyl and phenyl substituents in the *N*1-position as well as chlorinated phenyls in the C6-position fitted well in MDM2 pockets (Figure 28A and B).

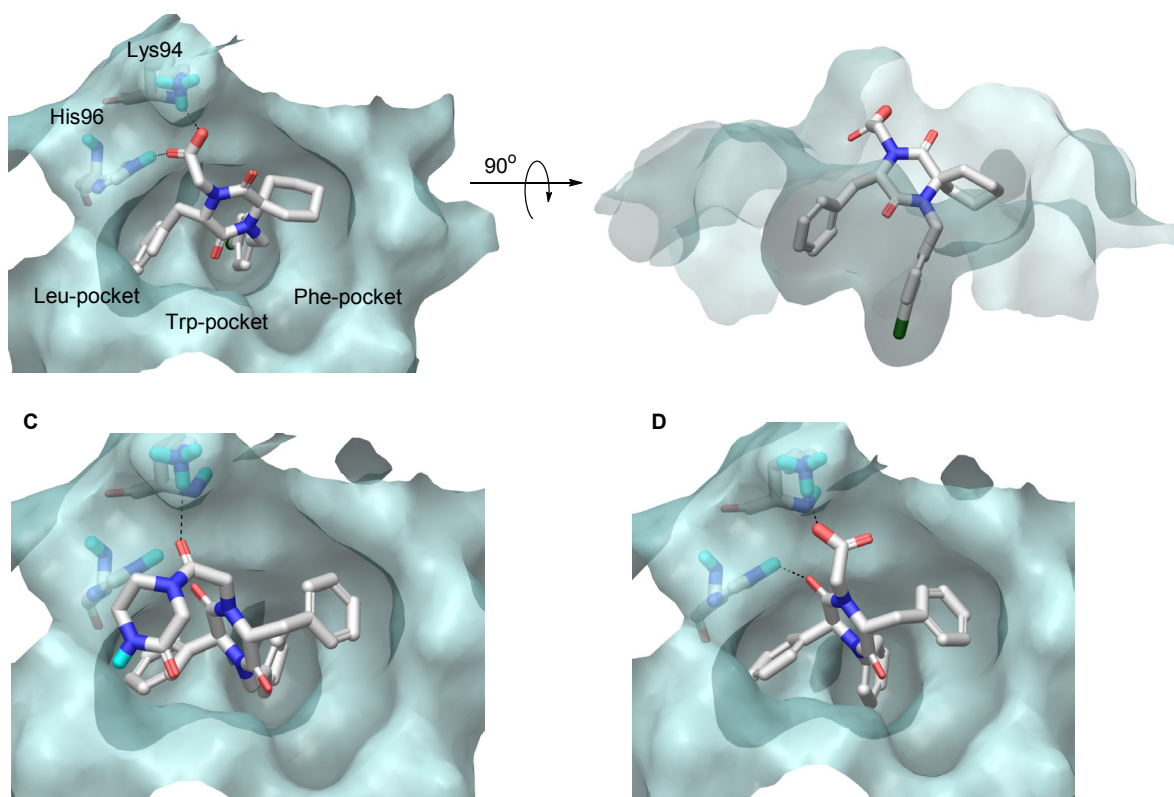


Figure 28. Docking of 2,5-DKPs to MDM2 (PDB code: 4HBM), the MDM2 surface is shown in turquoise. Hydrogen bonding and/or ionic interactions with His96 and Lys94 are shown as dashed black lines. **(A)** A cyclohexyl substituent in the C6-position interacts with the Trp-pocket, the carboxylic acid in the *N*4-position makes an ionic interaction with Lys94 and a hydrogen bond with His96; **(B)** 90° rotation of **A**; **(C)** A phenyl group in the C6-position rotates the 2,5-DKPs ring 90° and places the C6 substituent in the Leu-pocket of MDM2, an amide in the *N*4-position makes hydrogen bonding with Lys94; **(D)** A 2,5-DKP with a benzyl group in the C3 and phenyl groups in the *N*1- and C6-positions docked into MDM2.

Two series of 2,5-DKPs, spiro-2-DKP and non-spiro-DKP, were selected for synthesis and evaluation as type II inhibitors. The general structures are illustrated in Figure 29.

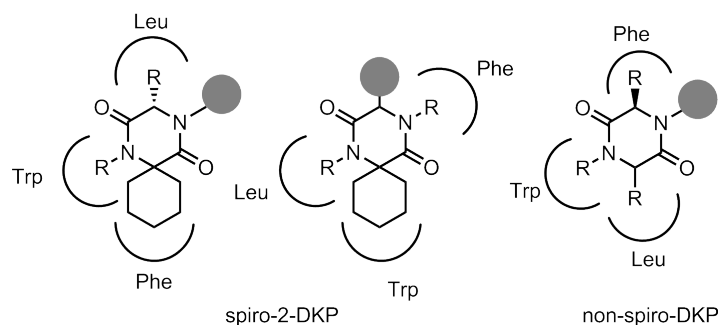


Figure 29. General structures of spiro-2- and non-spiro-DKPs, the curved lines represent the Phe-, Trp- and Leu-pockets of MDM2. ● = hydrophilic substituent.

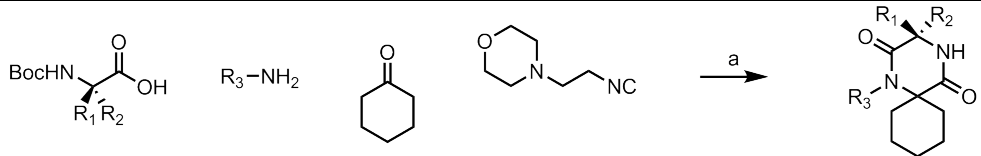
6.2.5 Synthesis of 2,5-DKPs as type II inhibitors

An Ugi/Deprotection/Cyclisation (UDC) protocol was used for the synthesis of spiro-2-DKP and non-spiro-DKP derivatives. The protocol has previously been used for the synthesis of 2,5-DKPs and the general reaction scheme is outlined in Scheme 13 section 6.1.1.2. The Ugi reaction was run by mixing the appropriate amine, Boc-protected amino, acid, ketone or aldehyde and 2-(morpholin-1-yl)ethylisonitrile in MeOH and running the reaction using thermal heating at 55 °C. In order to facilitate cyclisation of the dipeptide the Boc protecting group was cleaved under acidic conditions by addition of aqueous concentrated HCl. After a simple work up the cyclisation of the dipeptide was completed using acetic acid and toluene under thermal heating at 80 °C. The obtained 2,5-DKPs and isolated yields are presented in Table 6 and Table 7. The stereochemistry at the C3-position is controlled by the choice of amino acid. The stereochemistry at C6 cannot be controlled during the Ugi reaction

and when an aldehyde or a asymmetrical ketone is used a diastereomeric mixture is obtained.

Compounds **33-35** (Table 6, entries 1-4) were isolated in 43-61% yield. Compound **33R** was synthesised to validate the docking results that the *S*-enantiomer would fit better than the *R*-enantiomer in the MDM2 pocket (entry 2). A slightly lower yield was obtained when 4-chlorobenzylamine was used as the amine component (entry 4).

Table 6. Synthesis and isolated yields of compounds **33-37**.^a



Entry	R ₁	R ₂	R ₃	Product	Yield (%)
1	H	Bn	Bn	33S	53
2	Bn	H	Bn	33R	56
3	H	Bn	Phenethyl	34S	61
4	H	Bn	4ClBn	35S	43
5	H	CH ₂ COO ₂ tBu	Bn	36S	24 ^b
6	H	CH ₂ COO ₂ CH ₃	Bn	37S	37

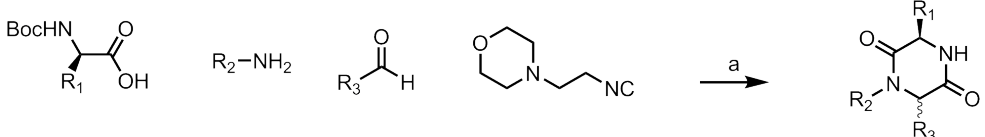
^aReagents and reaction conditions: (a) (i) Substrate (Boc-protected amino acid, cyclohexanone, amine and 2-(morpholin-1-yl)ethylisocyanide) (1 eq. of each), 55 °C, MeOH (ii) Conc. HCl (25 vol%) in MeOH, 55 °C. (iii) Toluene:acetic acid (1.25 M) (1:1), 80 °C. ^bBoc cleavage using TFA/DCM (1:1).

To further investigate the docking results, compound **36S** having a hydrophilic substituent in the C3-position was synthesised. Boc-L-aspartic acid 4-*tert*-butyl ester was used as the Boc-protected amino acid. To avoid hydrolysis of the *tert*-butyl ester, TFA in dry DCM was used for the Boc deprotection instead of HCl. Unfortunately the *tert*-butyl ester was unstable under these conditions, and the obtained carboxylic acid was lost during workup. Rerunning the reaction and changing the Boc deprotection procedure back to HCl in MeOH converted the *tert*-butyl ester to a methyl ester and the yield was improved from 24% to 37% of **36S** and **37S**, respectively (Table 6, entries 5-6).

Synthesis of non-spiro-DKPs was accomplished using the same UDC protocol to afford compounds **38-45** (Table 7). When the cyclic ketone was exchanged to benzaldehyde the total yield over three steps was lower (29-39%, Table 7, entries 1-2) compared with the synthesis of the spiro-2-DKP series (43-61%, Table 6, entries 1-4). The non-spiro-DKP products were obtained as approximately 1:1 diastereomeric mixtures, a result of exchanging cyclohexanone to benzaldehyde. However, the diastereoisomers could be separated by silica column chromatography.

The use of anilines as the amine component in the UDC reaction lowered the yields (Table 7, entries 3-4) compared to when using benzylamine (Table 7, entries 1-2). Combination of electron deficient anilines and benzaldehydes reduced the yield even more (Table 7, entries 5-7). Preformation of the imine could not improve the outcome of the reaction. The choice of components that facilitates iminium formation are beneficial in the Ugi. Weakly basic amine components with low nucleophilicity in combination with an electron-poor carbonyl component will disfavour the formation of the iminium ion even if the imine can be formed (see Scheme 14, section 6.1.1.2).¹⁷⁵ In addition to the low yield, some of the products were difficult to purify. In those cases the impurities could however be removed after the introduction of the *N*4 substituent (see Table 8).

In order to evaluate how the benzyl moiety at C3 affects the conformation and hence the inhibitory activity, the benzyl substituent was removed. First, the UDC was performed using Boc-Gly, 4-chloroaniline, 3-chlorobenzaldehyde and 2-(morpholino-1-yl)-ethylisonitrile but no product could be isolated. Exchanging the acid component to Boc-Ala afforded **45SS** and **45SR** in a total yield of 3% (Table 7, entry 8).

Table 7. Synthesis and isolated yields of compounds **38-45**.^a

Entry ^b	R ₁	R ₂	R ₃	Product	Yield (%) ^c
1	Bn	Bn	Ph	38RR	39
	Bn	Bn	Ph	38RS	
2	Bn	4ClBn	Ph	39RR	29
	Bn	4ClBn	Ph	39RS	
3	Bn	Ph	Ph	40RR	28
	Bn	Ph	Ph	40RS	
4	Bn	4ClPh	Ph	41RR	14
	Bn	4ClPh	Ph	41RS	
5	Bn	Ph	4ClPh	42RR	13
	Bn	Ph	4ClPh	42RS	
6	Bn	Ph	3ClPh	43RR	18
	Bn	Ph	3ClPh	43RS	
7	Bn	4ClPh	4ClPh	44RR	8
	Bn	4ClPh	4ClPh	44RS	
8	Me ^d	4ClPh	3ClPh	45SS	3
	Me ^d	4ClPh	3ClPh	45SR	

^aReagents and reaction conditions: (a) (i) Substrate (Boc-D-Phe, aldehyde, amine and 2-(morpholin-1-yl)ethylisocyanide) (1 eq. of each), MeOH, 55 °C. (ii) Conc. HCl (25 vol%) in MeOH, 55 °C. (iii) Toluene:acetic acid (1.25 M) (1:1), 80 °C. ^bOne entry corresponds to one reaction. ^cIsolated combined yield of both diastereoisomers. ^dS-configuration in position C3.

The low yield obtained for **45SS** and **45SR** could be explained by both a slow Ugi reaction and a slow cyclisation. Analysis of the reaction mixture after the Ugi reaction by LCMS showed that beside the desired product a lot of starting material was still present. In addition, a product mass ion with a different retention time than the Ugi product was observed which could correspond to the α -adduct (IV, Scheme 14 section 6.1.1.2). In addition, full conversion in the cyclisation reaction was never observed in the LCMS analysis.

The stereochemistry of the obtained non-spiro-DKPs was determined by running NOESY experiments. As expected a NOE correlation between the C3 and C6

protons of **38RR** was observed for the *R,R*-diastereoisomer having the phenyl and benzyl substituent on the same side of the 2,5-DKP ring compared to the absence of a NOE correlation for the *R,S*-diastereoisomer (**38RS**) (Figure 30).

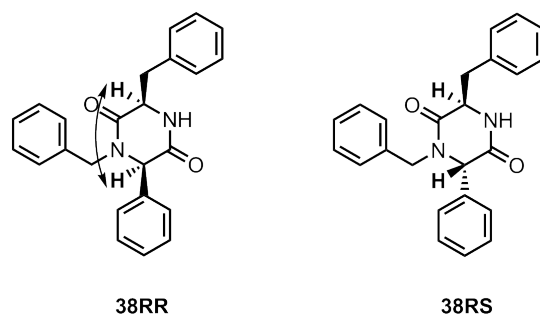


Figure 30. Stereochemistry assignment of non-spiro-DKPs. NOE correlations are shown by a double headed arrow.

A previously published protocol for amide alkylation in the *N4*-position of 2,5-DKPs was used.¹⁵⁵ Using the strong base 2-*tert*-butylimino-2-diethylamino-1,3-dimethylperhydro-1,3,2-diazaphosphorine (BEMP), different alkyl halides and DCM as solvent at room temperature afforded compounds **46-52** in good to excellent yields (Table 8). Introduction of an ester functionality in the *N4*-position would allow investigation of structure activity relationships (SARs) since esters can be converted to other functional groups including carboxylic acids, alcohols and amides. Generally, the alkylation reaction was completed within 12 h, except when ethyl 4-bromocrotonate was used as electrophile (Table 8, entries 10-11). Full consumption of the starting material could not be observed although the reaction time was prolonged to 2-3 days, the starting material could however be recovered (Table 8, entry 10). Introduction of a benzyl in the *N4*-position of **37S** was accomplished by activation of benzyl bromide using potassium iodide and DMF as solvent at room temperature, **49S** was isolated in 60% yield (Table 8, entry 5).

Table 8. Synthesis and isolated yields of compounds **46-52**.^a

Entry	Starting material	R ₁	R ₂	R ₃	R ₄	R ₅	R ₆	Product	Yield (%)
1	33S	H	Bn	Bn	Cyclohexyl			46S	91
2	33S	H	Bn	Bn	Cyclohexyl			47S	99
3	33R	Bn	H	Bn	Cyclohexyl			46R	87
4	33S	H	Bn	Bn	Cyclohexyl			48S	89
5	37S	H	CH ₂ CO ₂ CH ₃	Bn	Cyclohexyl			49S	60 ^b
6	38RR	Bn	H	Bn	Ph	H		50RR	93
7	38RS	Bn	H	Bn	H	Ph		50RS	80
8	39RR	Bn	H	4ClBn	Ph	H		51RR^c	68
9	39RS	Bn	H	4ClBn	H	Ph		51RS	96
10	38RR	Bn	H	Bn	Ph	H		52RR	40 ^d
11	38RS	Bn	H	Bn	H	Ph		52RS	73

^aReagents and reaction conditions: R₄-Br (1.5 eq.), BEMP (2 eq.), DCM, r.t. ^bR₄-Br (1.5 eq.), BEMP (2.1 eq.), KI (2.0 eq.), DMF, r.t. ^cExperimental procedure for **51RR** can be found in Appendix 6. ^d20 mg (29%) starting material was recovered.

The BEMP alkylation protocol was also used for the synthesis of compounds **53-58** (Table 9). The lower yields obtained (<80%) can be explained by the use of impure starting material, impurities left from the UDC reaction, which could be removed by purification using silica column chromatography. Epimerisation of the product was observed when the N1 and C6 substituents were electron deficient (chloro substituted anilines and/or benzaldehydes). Compounds **55-57** were isolated as diastereomeric mixtures and the ratio was determined from ¹H NMR spectra (Table 9, entries 6-10).

The diastereoisomers could be separated on silica and **58SS** and **58SR** were isolated as pure diastereoisomers (Table 9, entries 11-12).

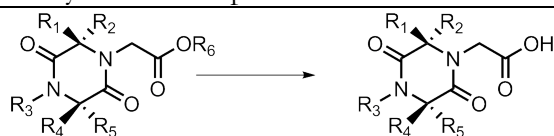
Table 9. Synthesis and isolated yields of compounds **53-58**.^a

Entry	Starting material	R ₁	R ₂	R ₃	R ₄	Product	Dr ^b	Yield (%)
1	40RR	Bn	Ph	Ph	H	53RR	99:1	94
2	40RS	Bn	Ph	H	Ph	53RS	99:1	94
3	41RR	Bn	4ClPh	Ph	H	54RR	99:1	60
4	41RS	Bn	4ClPh	H	Ph	54RS	99:1	54
5	42RR	Bn	Ph	4ClPh	H	55RR	99:1	86
6	42RS	Bn	Ph	H	4ClPh	55RS	3.33:1	70
7	43RR	Bn	Ph	3ClPh	H	56RR	5:1	93
8	43RS	Bn	Ph	H	3ClPh	56RS	2.8:1	63
9	44RR	Bn	4ClPh	4ClPh	H	57RR	4.3:1	87
10	44RS	Bn	4ClPh	H	4ClPh	57RS	1.7:1	36
11	45SS	Me ^c	4ClPh	H	3ClPh	58SS	99:1	55 ^d
12	45SR	Me ^c	4ClPh	3ClPh	H	58SR	99:1	37 ^e

^aReagents and reaction conditions: *tert*-Butyl 2-bromoacetate (2 eq.), BEMP (2 eq.), DCM, r.t.

^bDiastereomeric ratio according to ¹H NMR spectra. ^c*S*-configuration at C3. ^d28% of the other diastereoisomer was isolated. ^e43% of the other diastereoisomer was isolated.

The obtained esters were then converted to the corresponding carboxylic acids (Table 10). Initial attempts to hydrolyse the ester using LiOH in THF/water (1:1) resulted in epimerisation at the C3-position of the product as observed by ¹H NMR spectroscopy. The ethyl esters could be hydrolysed successfully using aqueous concentrated HCl at 70 °C and running the reaction for several hours, typically overnight (Table 10, entries 1 and 3-4). Exchanging the ethyl ester to a *tert*-butyl ester made it possible to run the reaction at 70 °C for a couple of hours or at room temperature overnight (Table 10, entries 2 and 5-17).

Table 10. Synthesis and isolated yields of compounds **59-67**.^a

Entry	Starting material	R ₁	R ₂	R ₃	R ₄	R ₅	R ₆	Product	Yield (%)
1	46S	H	Bn	Bn	Cyclohexyl		Et	59S	95
2	47S	H	Bn	Bn	Cyclohexyl		<i>t</i> Bu	59S	93
3	50RR	Bn	H	Bn	Ph	H	Et	60RR	87
4	50RS	Bn	H	Bn	H	Ph	Et	60RS	80
5	51RR	Bn	H	4ClBn	Ph	H	<i>t</i> Bu	61RR	98
6	51RS	Bn	H	4ClBn	H	Ph	<i>t</i> Bu	61RS	91
7	53RR	Bn	H	Ph	Ph	H	<i>t</i> Bu	62RR	99
8	53RS	Bn	H	Ph	H	Ph	<i>t</i> Bu	62RS	83
9	54RR	Bn	H	4ClPh	Ph	H	<i>t</i> Bu	63RR	98
10	54RS	Bn	H	4ClPh	H	Ph	<i>t</i> Bu	63RS	>99
11	55RS	Bn	H	Ph	H	4ClPh	<i>t</i> Bu	64RS	85
12	56RR	Bn	H	Ph	3ClPh	H	<i>t</i> Bu	65RR	77
13	56RS	Bn	H	Ph	H	3ClPh	<i>t</i> Bu	65RS	98
14	57RR	Bn	H	4ClPh	4ClPh	H	<i>t</i> Bu	66RR	71
15	57RS	Bn	H	4ClPh	H	4ClPh	<i>t</i> Bu	66RS	85
16	58SS	H	Me	4ClPh	H	3ClPh	<i>t</i> Bu	67SS	80
17	58SR	H	Me	4ClPh	3ClPh	H	<i>t</i> Bu	67SR	81

^aReagents and reaction conditions: Conc. HCl 70 °C for R₆ = ethyl and r.t. for R₆ = *tert*-butyl.

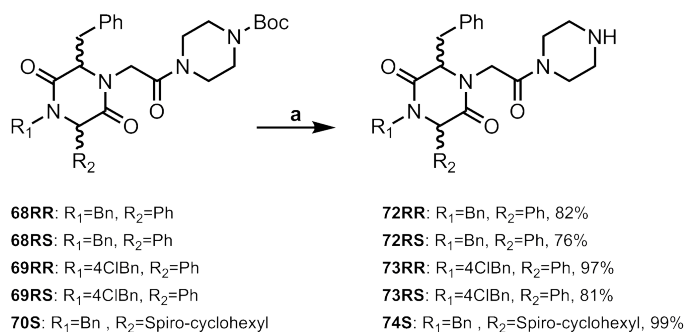
The obtained carboxylic acids were then further functionalised by amidations with 1-Boc-piperazine or 2-oxopiperazine (Table 11) to continue to investigate the SAR. The peptide coupling was performed using HATU as coupling reagent and Et₃N as base in DMF. Compounds **68-70** were obtained in moderate to excellent yields after coupling with 1-Boc-piperazine. The lower yield for **69RS** and **70S** (Table 11, entries 4-5) can be explained by loss of product during work-up and purification since LCMS analysis indicated full conversion of starting material.

Table 11. Synthesis and isolated yields of compounds **68-71**.^a

Entry	Starting material	R ₁	R ₂	R ₃	R ₄	R ₅	R ₆	Product	Yield (%)
1	60RR	Bn	H	Bn	Ph	H		68RR	89
2	60RS	Bn	H	Bn	H	Ph		68RS	78
3	61RR	Bn	H	4ClBn	Ph	H		69RR	85
4	61RS	Bn	H	4ClBn	H	Ph		69RS	59
5	59S	H	Bn	Bn	Spiro-cyclohexyl			70S	32
6	61RS	Bn	H	4ClBn	H	Ph		71RS	59

^aReagents and reaction conditions: Amine (1.5 eq.), HATU (1.3 eq.), Et₃N, 0 °C to r.t. overnight, DMF.

Cleavage of the Boc-protecting group on **68-70** was achieved using 50% TFA in DCM. Generally, the deprotection reaction was completed after 1 hour resulting in good to excellent yields (76-99%) of **72-74** (Scheme 19).

**Scheme 19.** Boc deprotection of **68-70**. Reagents and reaction conditions: (a) TFA:DCM (1:1), r.t.

2-Oxopiperazine was introduced in the *N*4-position of **61RS** and **71RS** could be isolated in a yield of 59% (Table 11, entry 6). Interestingly, double peaks were observed for several signals in both ^1H and ^{13}C NMR spectra. Since no epimerisation was observed in the introduction of 1-Boc-piperazine and the same reaction conditions were utilised it seemed unlikely that an epimerisation had occurred. It was assumed that a hindered rotation around the *N*4-C9 bond (Figure 31A) would result in two different low energy conformations of **71RS** in solution at room temperature explaining the double peaks observed. Studies of low energy conformations of **71RS** showed two major conformations, with the 2-oxopiperazine moiety pointing in opposite directions, with an energy difference of 12.5 kJ/mol between the conformations (Figure 31B). In order to confirm the presence of two conformations at room temperature NMR-analysis was performed at 25 °C and 55 °C. In the event of two low energy conformations the double peaks would coalesce at elevated temperatures since adding heat to the system will facilitate the rotation around the *N*4-C8 bond.¹⁸⁰⁻¹⁸¹ A clear difference was observed in the NMR spectra run at 25 °C and 55 °C confirming that **71RS** adopts two low energy conformations at 25 °C with a ratio of around 40:60 (Figure 31C).

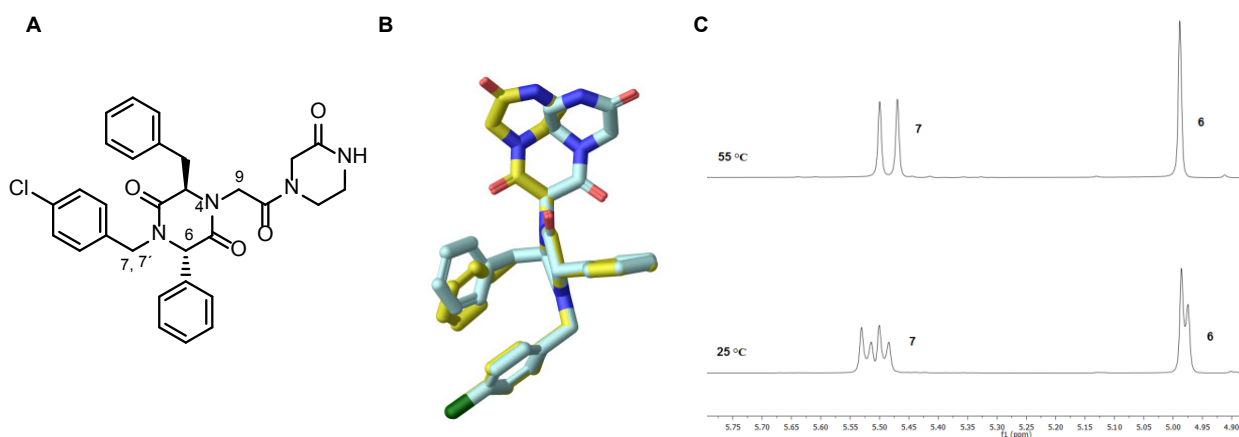
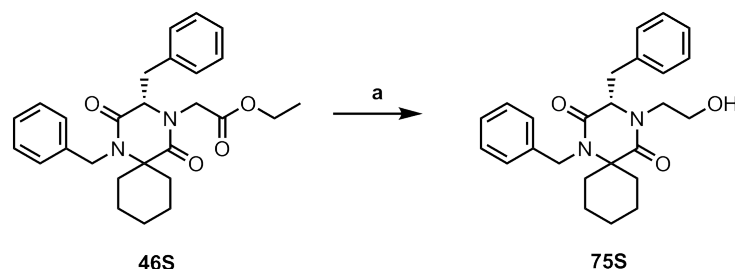


Figure 31. (A) Compound **71RS**; (B) Two of the major low energy conformations observed for **71RS** with a energy difference of 12.5 kJ/mol; (C) ^1H NMR peaks from H7 and H6 in **71RS** at 25 and 55 $^\circ\text{C}$, respectively.

Strategies for introduction of an alcohol at *N4* were also explored. First reduction of the ester functionality was investigated and treatment of **46S** with NaBH_4 as reducing agent afforded **75S** in 61% yield (Scheme 20).

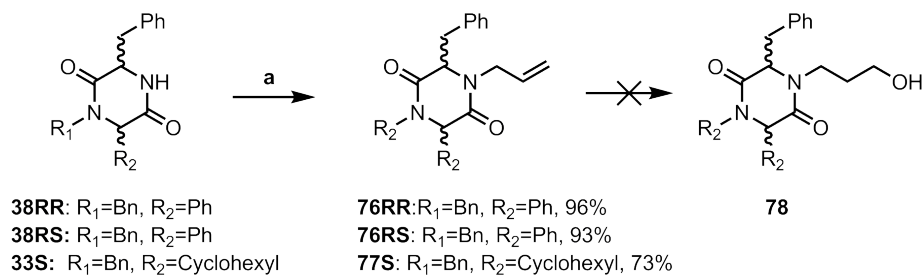


Scheme 20. Synthesis of **75S**. Reagents and reaction conditions: (a) NaBH_4 (3.0 eq.), r.t., 5 days, ethanol.

Reduction of **50RR** and **50RS** using NaBH_4 in EtOH resulted in epimerisation of the product at C6 which could be observed in ^1H NMR spectra. Attempts to reduce the carboxylic acid **60RR**, using $\text{BH}_3 \cdot \text{DMS}$ failed and several unidentified mass ions were observed by LCMS analysis of the reaction mixture and again epimerisation of the starting material was observed in ^1H NMR spectra.

An alternative route for the introduction of an alcohol in the *N4*-position of the 2,5-DKP ring was investigated. Hydroboration of alkenes followed by oxidation is a known strategy to convert alkenes to alcohols.¹⁸² Further, Tullberg *et al.* have reported a hydroboration/oxidation procedure of an *N4*-allyl of 2,5-DKPs to the corresponding alcohol using $\text{BH}_3 \cdot \text{THF}$ and H_2O_2 .¹⁵⁵

The allyl group could be introduced at the *N*4-position of **38RR** and **38RS** using allyl bromide and BEMP as base in DCM at room temperature (Scheme 21) and **76RR** and **76RS** were obtained in 96% and 93% isolated yield, respectively. Allylation of **33S** was slow at room temperature and required microwave heating whereupon **77S** could be isolated in 73% (Scheme 21).



Scheme 21. Synthesis of **76-77**. Reagents and reaction conditions: (a) For **38RR** and **38RS**: Allyl bromide (1.1-1.2 eq.), BEMP (1.3-1.4 eq.) r.t., 20-22 h, DCM and for **33S**: Allyl bromide (1.4 eq.), BEMP (0.9 eq.) MW, 150 °C, 45 min, DMF.

No product could be obtained after treatment of **76-77** with $\text{BH}_3 \cdot \text{THF}$, followed by H_2O_2 and NaOH . Attempts to optimise the reaction conditions proved unsuccessful. Running the hydroboration at $-40\text{ }^\circ\text{C}$ resulted in mainly starting material and only trace amounts of the product could be observed by LCMS. When the hydroboration was performed at room temperature a complex reaction mixture was observed and no product could be isolated. Other procedures were evaluated using $\text{BH}_3 \cdot \text{DMS}$ and 9-BBN as the borane sources but mostly unidentified side-products were observed by LCMS analysis and in ^1H NMR spectra.

To summarise the synthesis of 2,5-DKPs (spiro-2-DKP and non-spiro-DKP), the synthetic sequence starting with a UDC protocol followed by amide alkylation made it possible to synthesise a large set of different tetrasubstituted 2,5-DKPs. The obtained series was suitable for biological evaluation. In Figure 32 an overview of the

substituents introduced on the 2,5-DKP ring are illustrated. Note however that not all possible combinations have been synthesised.

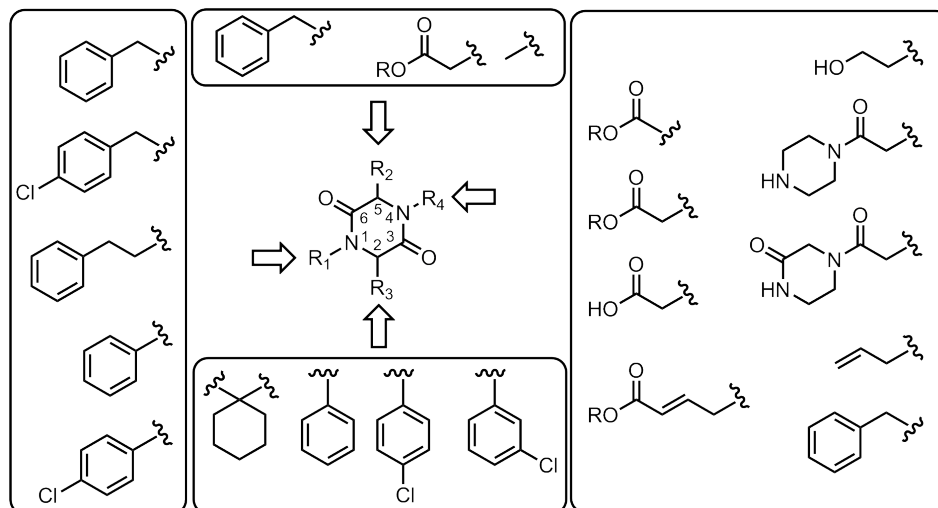


Figure 32. An overview of the different substituents that have been introduced on the 2,5-DKP ring using the UDC protocol followed by amide alkylation and further derivatisation. Not all possible combinations of substituents have been used.

6.2.6 Biological evaluation of 2,5-DKPs as type II inhibitors

The synthesised 2,5-DKPs (spiro-2-DKP and non-spiro-DKP) were evaluated for their inhibitory activity using the standard FP-assay. Two compounds, **66RR** and **66RS** from the non-spiro-DKP series showed activity as inhibitors and displayed IC_{50} -values of 31 μ M and 28 μ M, respectively (Figure 33).

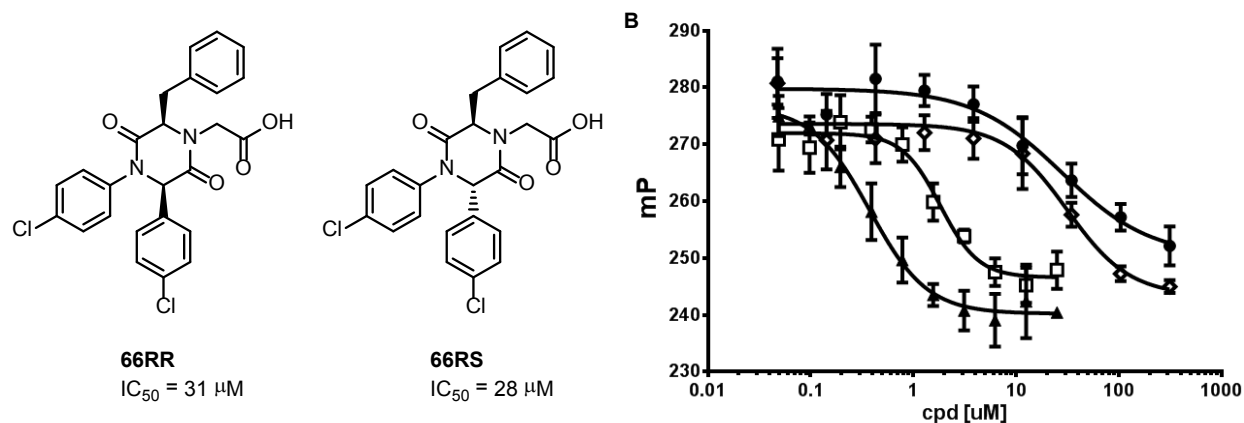


Figure 33. (A) Active 2,5-DKPs type II inhibitors against the MDM2/p53 interaction; (B) Inhibition curves for **66RR** (\diamond) (31.41 μ M [95% CI, 16.31–60.49]) and **66RS** (\bullet) (27.99 μ M [95% CI, 10.96–71.43]). Wild-type p53 peptide (\square , amino acids 15 – 29: GSGSSQETFSDLWKLLPEN) and nutlin-3a (\blacktriangle) were used as positive controls.

The binding of **66RR** and **66RS** was confirmed by SPR with K_D -values of 224 μ M and 191 μ M, respectively. The lower activity observed in the SPR measurements could be a result of poor solubility of the compounds in the assay buffer. Binding to MDM2 of **66RR** and **66RS** could however be confirmed in WaterLOGSY experiments (for spectra Figure A4 and A5 in Appendix 5).

With only a few active compounds it is not possible to establish any SARs. However, the results indicate that 4-chlorophenyl substituents in the *N*1- and *C*6-position are necessary to gain activity. All other substituents (Figure 32) investigated in these positions proved inactive in the FP-assay. In analogy with the obtained results, chloro-substituted phenyls interacting with the Trp and Phe-pockets of MDM2 have been shown to be important for activity.¹⁷⁹ Further, these results indicate that the carboxylic acid at *N*4 is important for the activity, since the ester analogues, **57RR** and **57RS**, were inactive in the FP-assay. Furthermore, the stereochemistry of the tested compounds does not seem to be of major importance since similar IC_{50} values were

obtained for both compounds. It should be noted that the active compounds were tested as diastereomeric mixtures, 4.3:1 and 1.7:1 for **66RR** and **66RS**, respectively.

6.3 Summary of paper IV

Two series of 2,5-DKPs have been synthesised and evaluated as α -helix mimetics and inhibitors of the MDM2/p53 PPI. The first series of spiro-DKPs (type III inhibitors) was designed to directly mimic the topography of the α -helical part of p53. The synthetic protocol used for the first series failed to provide tri- or tetrasubstituted 2,5-DKPs and the obtained disubstituted 2,5-DKPs were inactive as MDM2 inhibitors in the FP-assay. The original design was re-evaluated and a second series aiming for type II inhibitors was synthesised. The use of the UDC protocol followed by amide alkylation provided a large set of tetrasubstituted 2,5-DKPs and out of 54 evaluated derivatives two compounds (**66RR** and **66RS**) showed micromolar IC_{50} -values in the FP-assay. Binding to MDM2 was confirmed by WaterLOGSY experiments. The obtained results are in agreement with the observation that many of the published potent inhibitors of the p53/MDM2 interaction are less extended than the model p53 α -helix, hence acting more as type II like inhibitors (see Figures 5 and 6 section 1.3 for type II and type III inhibitors, respectively.)

7 Concluding Remarks and Future Perspectives

This thesis describes the design, synthesis and evaluation of β -hairpins, 8-(triazolyl)purines and 2,5-diketopiperazines as inhibitors of the MDM2/p53 PPI. Their MDM2 inhibitory activities were determined and three peptides, one 8-(triazolyl)purine and two 2,5-DKPs were identified as MDM2/p53 interaction inhibitors with IC_{50} values in the micromolar to low micromolar range.

Further studies that would be of interest include:

- NAMFIS analyses on linear peptide and small molecule MDM2/p53 interaction inhibitors. Conformational studies of the β -hairpins revealed that the molecular flexibility of cyclic peptidomimetics influence the inhibitory activity against MDM2. It would therefore be relevant to investigate if the same trend is observed for linear peptides and small molecules. It might explain the low activities obtained for the purine and 2,5-DKP based type II inhibitors.
- Evaluation the synthesised type III inhibitors against other PPI targets. Although the purine and 2,5-DKP based type III inhibitors described in this thesis were unable to inhibit MDM2 they could be used as α -helix mimetics targeting other PPIs having an α -helix at the interface.
- Investigation of various applications of the identified fluorescent purine derivatives. One application of fluorescent inhibitors would be as displacement probes in assays.
- In order to investigate spiro-1-DKPs as type III inhibitors against other PPIs access to tri- or tetrasubstituted derivatives are necessary. The UDC protocol followed by BEMP alkylation could be used for the synthesis of spiro-1-DKP derivatives.

8 Acknowledgement

Det har varit mycket roliga, givande och lärorika år, som har gått väldigt fort. Men som man brukar säga, tiden går fort när man har roligt! Jag vill passa på att tacka alla som på något sätt bidragit med idéer, stöd, hjälp, uppmuntran och trevligt sällskap under de här åren.

Extra mycket tack riktas till:

Min handledare **Morten Grøtli**, för att du antog mig som doktorand, för din entusiasm, för att du alltid är positivt inställd till nya idéer och har gett mig möjligheten att lära mig så mycket.

Kristina Luthman, min biträdande handledare, för att du är en fin förebild och, förutom ovärderlig hjälp och stöd under åren, alltid har ett bra boktips nära till hands.

Mina examinatorer, först **Ann-Therese Karlberg** och senare **Johan Gottfries** för givande samtal.

Mina examensarbetare genom åren i kronologisk ordning, **Petra Båth**, **Mattias Bood**, **Maria Quant**, **Jimmy Jacobson** och **Matilda Bred**. Mycket av ert arbete är inkluderat i denna avhandling så tack för ert hårda arbete och trevliga umgänge på labbet.

Former and present members of the MedChem group who have contributed considerably so that these five years have been an incredible time. Thank you for all the fun, support, help, interest and encouragement during this time. Särskilt tack till, **Tina Seifert** och **David Bliman**. Vi startade doktorandutbildningen på samma dag och utan er hade den inte blivit så här bra. David, dessutom för fint samarbete i purinprojektet.

All the people associated with floor 8 and 9, you have contributed to a friendly, stimulating working environment and nice get-togethers like crayfish parties, Christmas dinners, pea-soup parties – the list goes on ... Några av er förtjänar ett extra tack – **Emma Danelius**, för att du är en så fin kollega (och vän). Jag är så glad över att vi lyckades starta "hairpin-projektet" tillsammans och utan din expertis om peptider och NMR, som du generöst delar med dig av, hade det aldrig gått. **Mate Erdelyi** för all NMR-relaterad hjälp och superbt samarbete i hairpin-projektet.

Supermycket tack till **korrekturläsarna** av avhandlingen, Kristina Luthman, Morten Grøtli, Emma Danelius och David Bliman och av manuskripten, Hanna Andersson, Chris Lawson och Tina Seifert.

Alla andra **medförfattare** och **samarbetspartners**. Extra thanks to our collaborators at St. Jude Children's Research Hospital for all the biological testing in this thesis. Professor **Kiplin Guy** for letting me be part of your research group for three months and **Jaeki Min** for taking care of me in the lab and for never giving up on our compounds. **Jesper Nilsson** för fluoruscence-mätningarna på purinerna men framförallt för de fina pastellfärgade spektra.

Matlaget (Emma, David, Marcus, Tobias och Jenny) för alla goda och supertrevliga luncher!

Noel Danelius, för att du har gjort så grymt fina figurer av de olika inhibitorerna.

Familjer och **vänner** som hejat på och stöttat mig under dessa år – det betyder jättemycket.

Sist men inte minst, **Alex** för allt du gjort och gör för mig, jag finner inte ord, tack!

9 Appendices

9.1 Appendix 1. The twenty endogenous amino acids

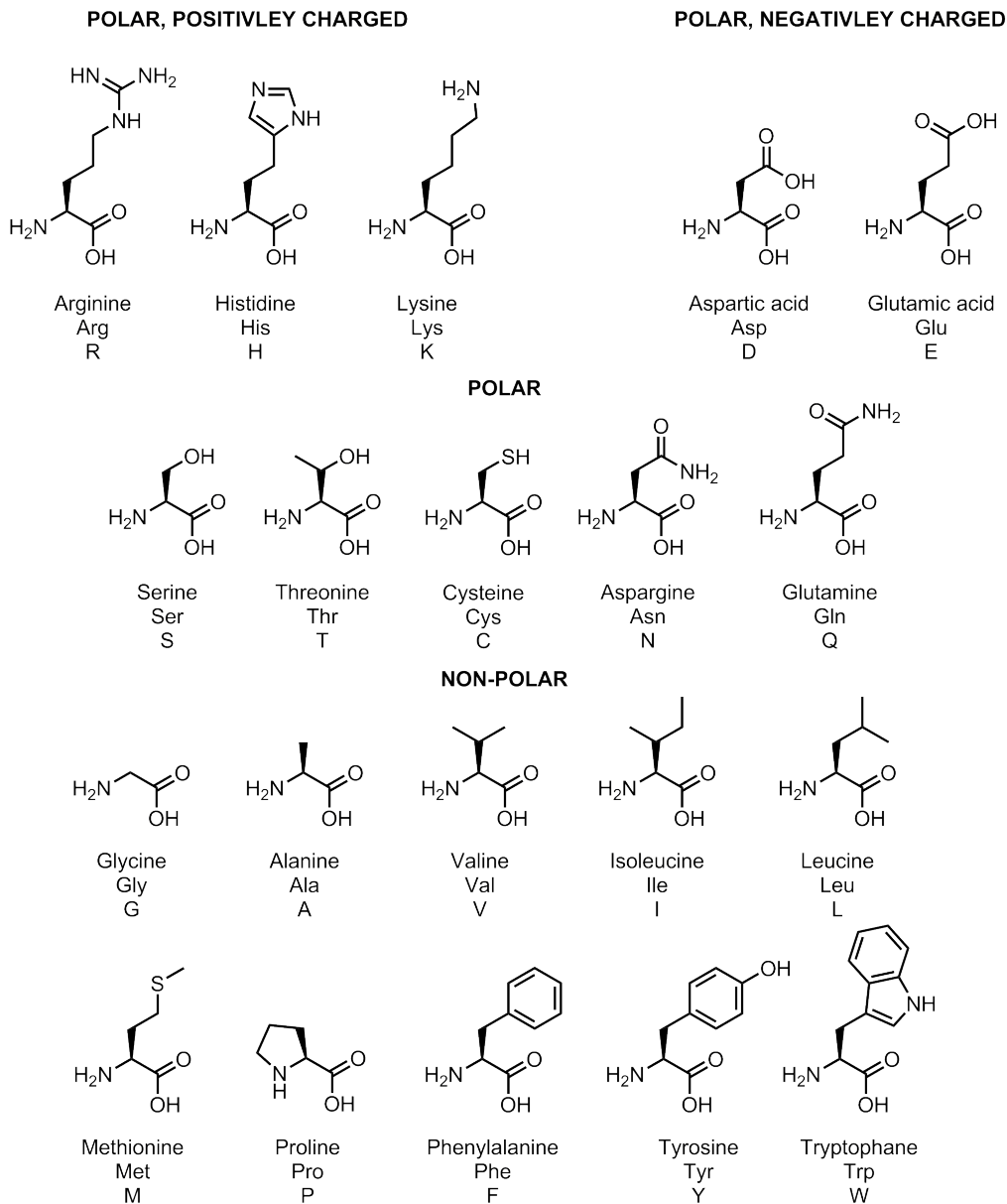


Figure A1. The twenty endogenous amino acids, divided into groups depending on their charge at physiological pH~7.4.

9.2 Appendix 2.

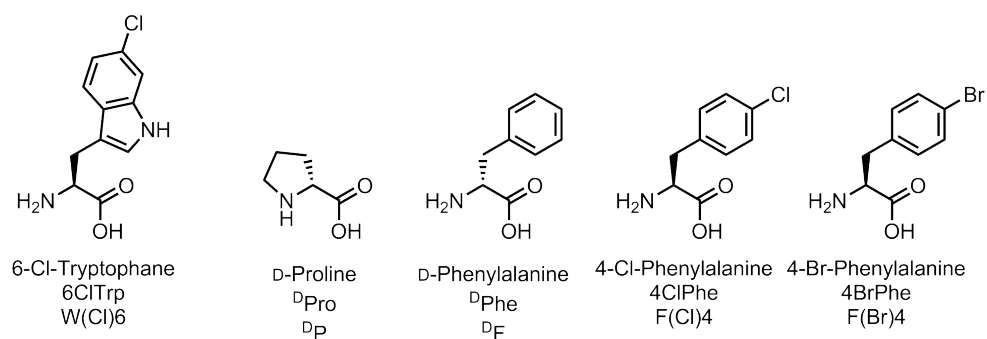
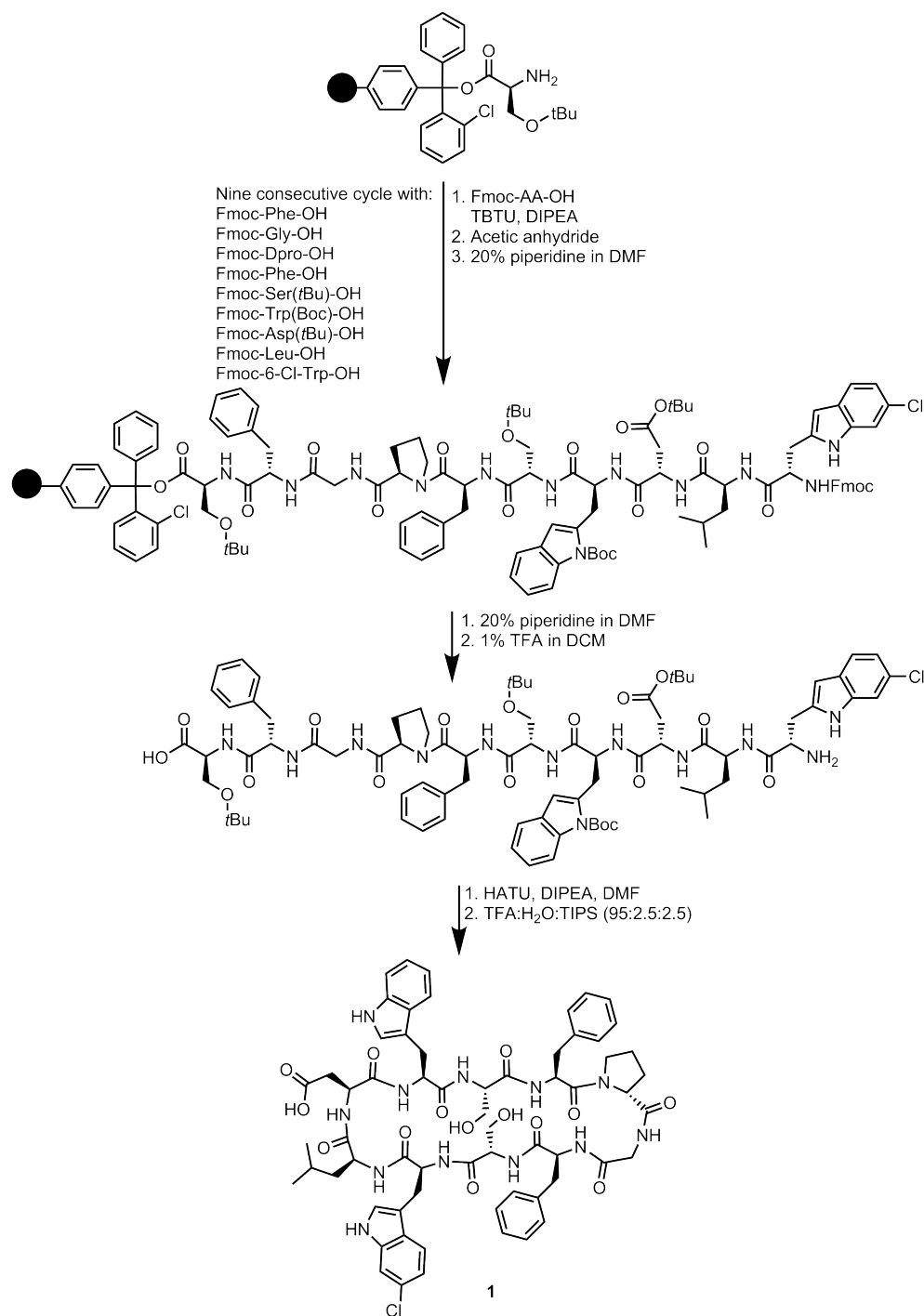
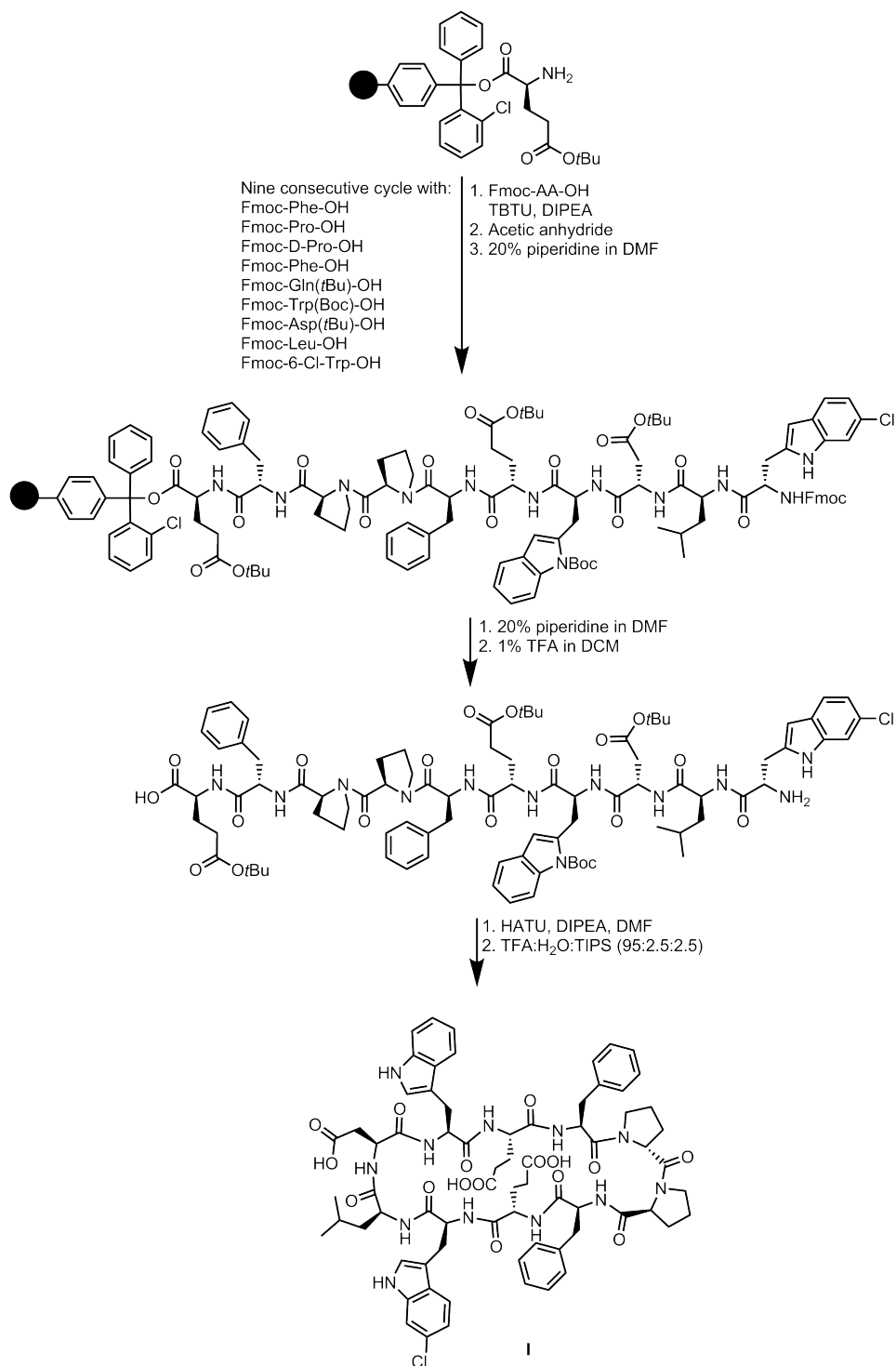


Figure A2. Additional amino acids used in this thesis.

9.3 Appendix 3. Synthetic scheme for the synthesis of 1



9.4 Appendix 4. Synthetic scheme for the synthesis of I



9.5 Appendix 5. WaterLOGSY spectra of 20f, 66RR and 66RS

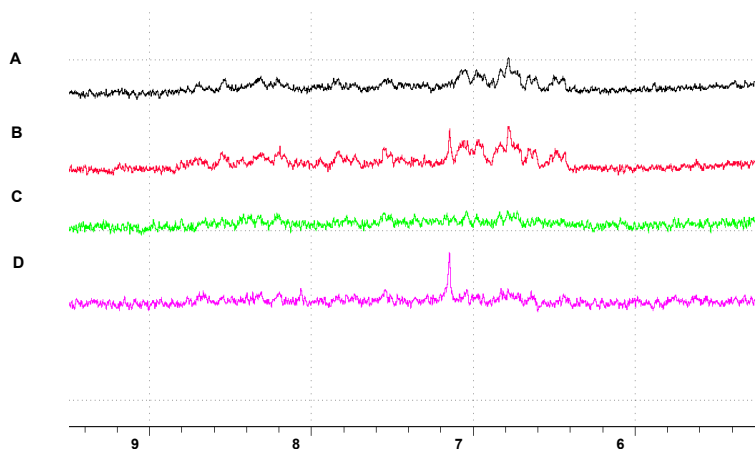


Figure A3. WaterLOGSY experiment. ^1H NMR spectra and WaterLOGSY spectra of the MDM2 protein in the absence of the compound (A = ^1H and C = WaterLOGSY) and in the presence of **20f** (B = ^1H and D = WaterLOGSY).

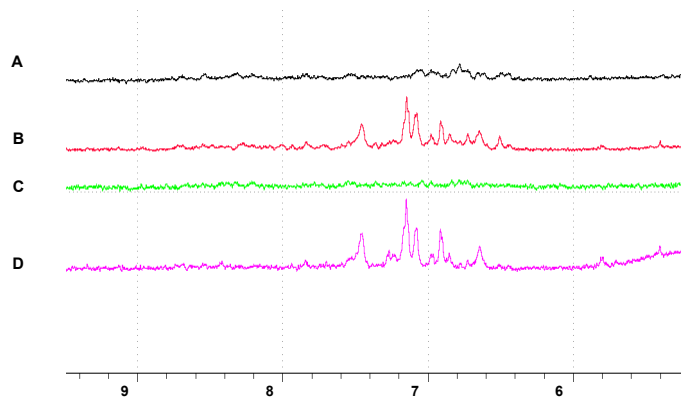


Figure A4. WaterLOGSY experiment. ^1H NMR spectra and WaterLOGSY spectra of the MDM2 protein in the absence of the compound (A = ^1H and C = WaterLOGSY) and in the presence of **66RR** (B = ^1H and D = WaterLOGSY).

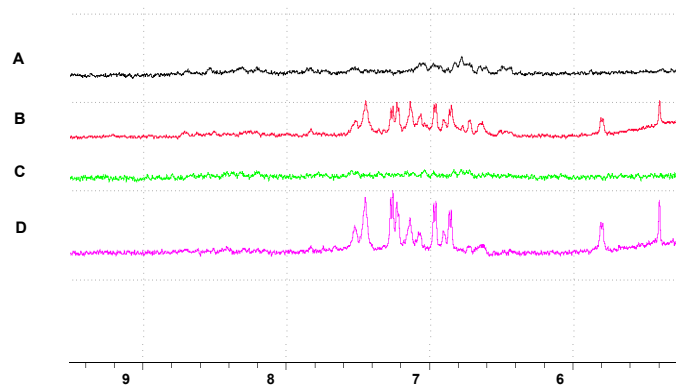
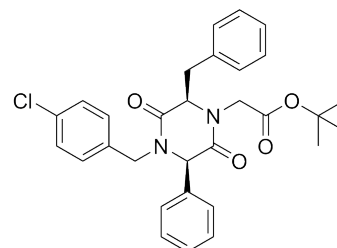


Figure A5. WaterLOGSY experiment. ^1H NMR spectra and WaterLOGSY spectra of the MDM2 protein in the absence of the compound (A = ^1H and C = WaterLOGSY) and in the presence of **66RS** (B = ^1H and D = WaterLOGSY).

9.6 Appendix 6

(3*R*,6*R*)-3-Benzyl-1-(4-chlorobenzyl)-4-(*tert*-butoxy-carbonyl-methyl)-6-phenylpiperazine-2,5-dione (**51RR**)

Compound **39RR** (150 mg, 0.371 mmol) and *tert*-butyl 2-bromoacetate (110 μ l, 0.745 mmol) were dissolved in dry CH_2Cl_2 (10 ml). BEMP (210 μ l 0.726 mmol) was added and the reaction was stirred at room temperature overnight. The reaction mixture was extracted with NaOH (0.5 M. aq.) and



HCl (0.5 M, aq.). The combined organic phases were washed with brine, dried over Na_2SO_4 and the solvent was removed under reduced pressure. Purification by flash column chromatography (10-20% ethyl acetate in pentane) provided **51RR** as a colourless oil (130 mg, 68%). ^1H NMR (CDCl_3): 7.34 – 7.18 (m, 6H), 7.15 – 7.04 (m, 6H), 6.61 – 6.56 (m, 2H), 5.06 (d, J 14.8 Hz, 1H), 4.84 (d, J 17.2 Hz, 1H), 4.69 (t, J 3.9 Hz, 1H), 4.10 (s, 1H), 3.63 (d, J 17.2 Hz, 1H), 3.46 (dd, J 14.4, 3.7 Hz, 1H), 3.40 (d, J 14.8 Hz, 1H), 3.25 (dd, J 14.4, 4.2 Hz, 1H), 1.42 (s, 9H). ^{13}C NMR (CDCl_3): 166.8, 165.8, 165.1, 136.4, 134.7, 133.5, 133.4, 130.1, 130.0, 129.0, 128.88, 128.87, 128.6, 128.3, 127.5, 82.7, 62.3, 60.8, 46.4, 45.9, 36.8, 28.1. HRMS m/z $[\text{M}+\text{H}]^+$ calculated for $\text{C}_{30}\text{H}_{31}\text{ClN}_2\text{O}_4$: 519.2050. Found: 519.2079.

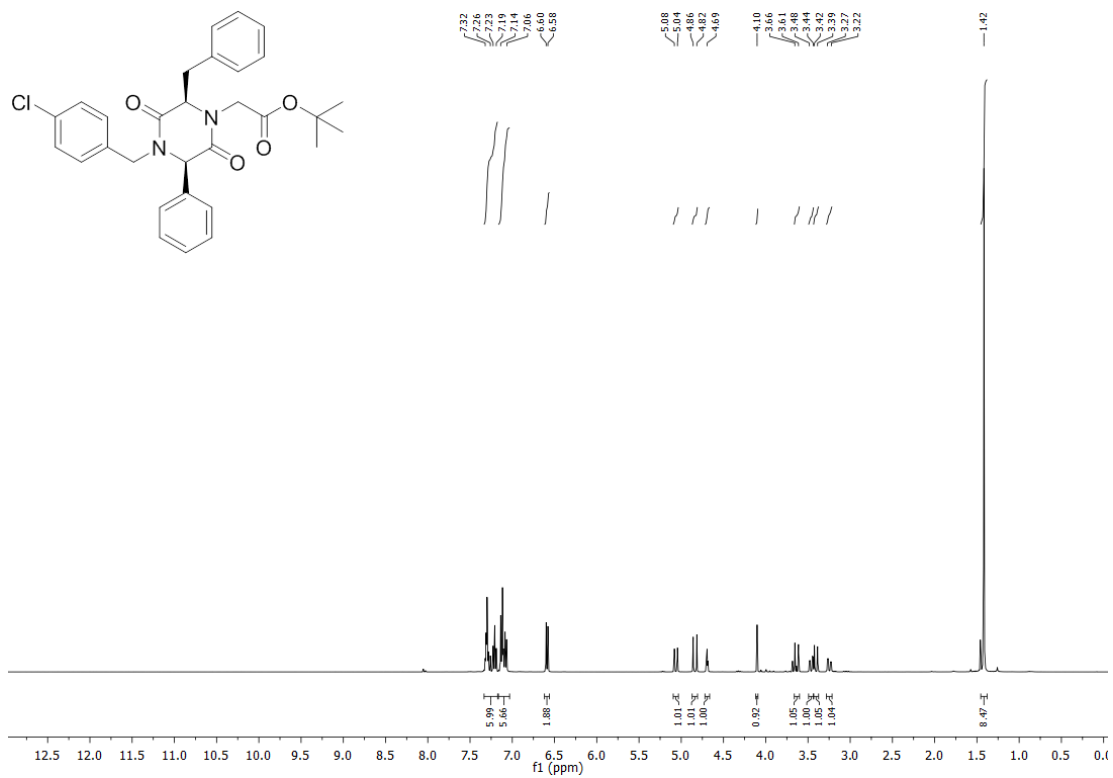


Figure A6. ¹H NMR spectrum of compound 51RR.

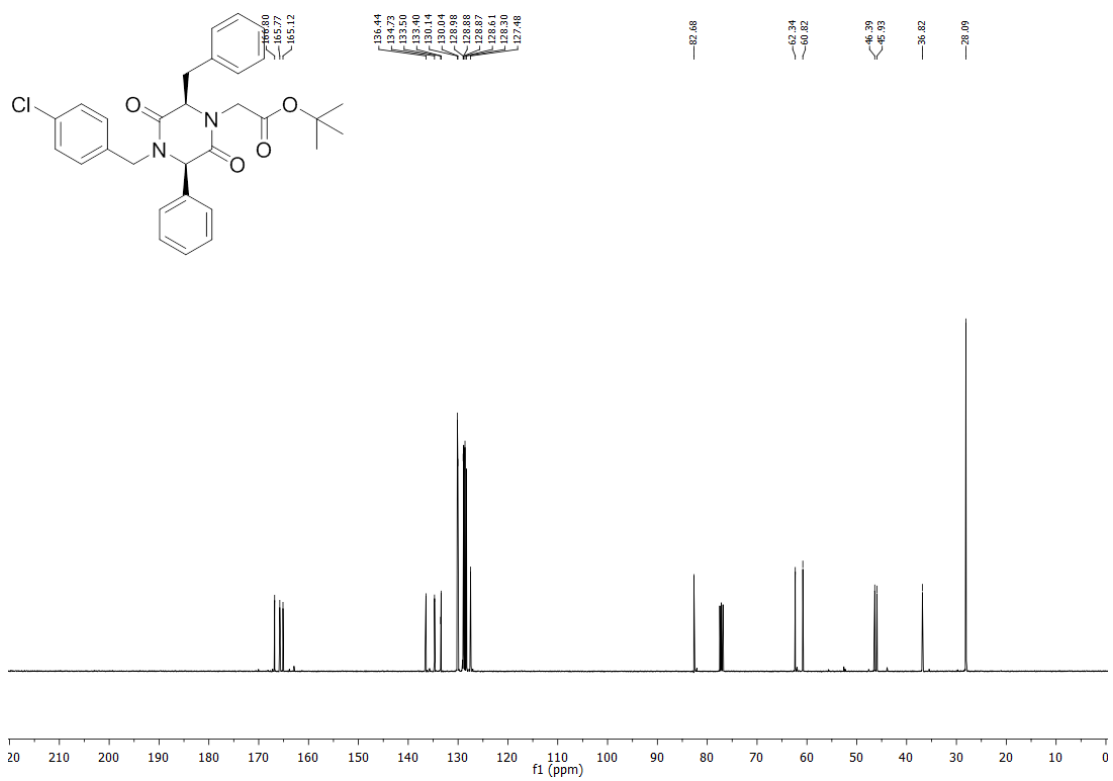


Figure A7. ¹³C NMR spectrum of compound 51RR.

10 References

1. Imming, P.; Sinning, C.; Meyer, A. *Drugs, their targets and the nature and number of drug targets*. *Nat. Rev. Drug Discov.* **2006**, *5*, 821-834.
2. Hopkins, A. L.; Groom, C. R. *The druggable genome*. *Nat. Rev. Drug Discov.* **2002**, *1*, 727-730.
3. Rognan, D. *Rational design of protein-protein interaction inhibitors*. *Med. Chem. Commun.* **2015**, *6*, 51-60.
4. Jin, L.; Wang, W.; Fang, G. *Targeting Protein-Protein Interaction by Small Molecules*. *Annu. Rev. Pharmacol. Toxicol.* **2014**, *54*, 435-456.
5. Zinzalla, G.; Thurston, D. E. *Targeting protein-protein interactions for therapeutic intervention: a challenge for the future*. *Future Med. Chem.* **2009**, *1*, 65-93.
6. Stites, W. E. *Protein-Protein Interactions: Interface Structure, Binding Thermodynamics, and Mutational Analysis*. *Chem. Rev.* **1997**, *97*, 1233-1250.
7. Smith, M. C.; Gestwicki, J. E. *Features of protein-protein interactions that translate into potent inhibitors: topology, surface area and affinity*. *Expert Rev. Mol. Med.* **2012**, *14*, e16.
8. Arkin, M. R.; Whitty, A. *The road less traveled: modulating signal transduction enzymes by inhibiting their protein-protein interactions*. *Curr. Opin. Chem. Biol.* **2009**, *13*, 284-290.
9. Thompson, A. D.; Dugan, A.; Gestwicki, J. E.; Mapp, A. K. *Fine-Tuning Multiprotein Complexes Using Small Molecules*. *ACS Chem. Biol.* **2012**, *7*, 1311-1320.
10. Fuller, J. C.; Burgoyne, N. J.; Jackson, R. M. *Predicting druggable binding sites at the protein-protein interface*. *Drug Discov. Today* **2009**, *14*, 155-161.
11. Wells, J. A.; McClendon, C. L. *Reaching for high-hanging fruit in drug discovery at protein-protein interfaces*. *Nature* **2007**, *450*, 1001-1009.
12. Clackson, T.; Wells, J. *A hot spot of binding energy in a hormone-receptor interface*. *Science* **1995**, *267*, 383-386.
13. Arkin, M. R.; Wells, J. A. *Small-molecule inhibitors of protein-protein interactions: progressing towards the dream*. *Nat. Rev. Drug Discov.* **2004**, *3*, 301-317.
14. Bogan, A. A.; Thorn, K. S. *Anatomy of hot spots in protein interfaces*. *J. Mol. Biol.* **1998**, *280*, 1-9.
15. Keskin, O.; Ma, B.; Nussinov, R. *Hot Regions in Protein-Protein Interactions: The Organization and Contribution of Structurally Conserved Hot Spot Residues*. *J. Mol. Biol.* **2005**, *345*, 1281-1294.
16. Hajduk, P. J.; Huth, J. R.; Fesik, S. W. *Druggability Indices for Protein Targets Derived from NMR-Based Screening Data*. *J. Med. Chem.* **2005**, *48*, 2518-2525.

17. Hajduk, P. J.; Huth, J. R.; Tse, C. *Predicting protein druggability*. *Drug Discov. Today* **2005**, *10*, 1675-1682.
18. Mattos, C.; Ringe, D. *Locating and characterizing binding sites on proteins*. *Nat. Biotech.* **1996**, *14*, 595-599.
19. Guo, W.; Wisniewski, J. A.; Ji, H. *Hot spot-based design of small-molecule inhibitors for protein-protein interactions*. *Bioorg. Med. Chem. Lett.* **2014**, *24*, 2546-2554.
20. Nero, T. L.; Morton, C. J.; Holien, J. K.; Wielens, J.; Parker, M. W. *Oncogenic protein interfaces: small molecules, big challenges*. *Nat. Rev. Cancer* **2014**, *14*, 248-262.
21. Jayatunga, M. K. P.; Thompson, S.; Hamilton, A. D. *α -Helix mimetics: Outwards and upwards*. *Bioorg. Med. Chem. Lett.* **2014**, *24*, 717-724.
22. Bullock, B. N.; Jochim, A. L.; Arora, P. S. *Assessing Helical Protein Interfaces for Inhibitor Design*. *J. Am. Chem. Soc.* **2011**, *133*, 14220-14223.
23. Richardson, J. S. *The Anatomy and Taxonomy of Protein Structure*. Academic Press: **1981**; Vol. 34, 167-339.
24. Zhao, Y.; Aguilar, A.; Bernard, D.; Wang, S. *Small-Molecule Inhibitors of the MDM2-p53 Protein-Protein Interaction (MDM2 Inhibitors) in Clinical Trials for Cancer Treatment*. *J. Med. Chem.* **2014**, [Article ASAP]. DOI: 10.1021/jm501092z.
25. Konopleva, M.; Contractor, R.; Tsao, T.; Samudio, I.; Ruvolo, P. P.; Kitada, S.; Deng, X.; Zhai, D.; Shi, Y.-X.; Sneed, T.; Verhaegen, M.; Soengas, M.; Ruvolo, V. R.; McQueen, T.; Schober, W. D.; Watt, J. C.; Jiffar, T.; Ling, X.; Marini, F. C.; Harris, D.; Dietrich, M.; Estrov, Z.; McCubrey, J.; May, W. S.; Reed, J. C.; Andreeff, M. *Mechanisms of apoptosis sensitivity and resistance to the BH3 mimetic ABT-737 in acute myeloid leukemia*. *Cancer Cell* **2006**, *10*, 375-388.
26. Oltersdorf, T.; Elmore, S. W.; Shoemaker, A. R.; Armstrong, R. C.; Augeri, D. J.; Belli, B. A.; Bruncko, M.; Deckwerth, T. L.; Dinges, J.; Hajduk, P. J.; Joseph, M. K.; Kitada, S.; Korsmeyer, S. J.; Kunzer, A. R.; Letai, A.; Li, C.; Mitten, M. J.; Nettesheim, D. G.; Ng, S.; Nimmer, P. M.; O'Connor, J. M.; Oleksijew, A.; Petros, A. M.; Reed, J. C.; Shen, W.; Tahir, S. K.; Thompson, C. B.; Tomaselli, K. J.; Wang, B.; Wendt, M. D.; Zhang, H.; Fesik, S. W.; Rosenberg, S. H. *An inhibitor of Bcl-2 family proteins induces regression of solid tumours*. *Nature* **2005**, *435*, 677-681.
27. Lawson, A. D. G. *Antibody-enabled small-molecule drug discovery*. *Nat. Rev. Drug Discov.* **2012**, *11*, 519-525.
28. Zeng, J.; Zhang, J.; Tanaka, T.; Rabbitts, T. *Single Domain Antibody Fragments as Drug Surrogates Targeting Protein-Protein Interactions inside Cells*. *Antibodies* **2013**, *2*, 306-320.
29. Zábřady, M.; Hrdinová, V.; Müller, B.; Conrad, U.; Hejátko, J.; Janda, L. *Targeted In Vivo Inhibition of Specific Protein-Protein Interactions Using Recombinant Antibodies*. *PLoS ONE* **2014**, *9*, e109875.

30. Hoe, K. K.; Verma, C. S.; Lane, D. P. *Drugging the p53 pathway: understanding the route to clinical efficacy*. *Nat. Rev. Drug Discov.* **2014**, *13*, 217-236.
31. Vousden, K. H.; Lu, X. *Live or let die: the cell's response to p53*. *Nat. Rev. Cancer* **2002**, *2*, 594-604.
32. Brooks, C. L.; Gu, W. *New insights into p53 activation*. *Cell Res.* **2010**, *20*, 614-621.
33. Harris, S. L.; Levine, A. J. *The p53 pathway: positive and negative feedback loops*. *Oncogene* **2005**, *24*, 2899-2908.
34. Nigro, J. M.; Baker, S. J.; Preisinger, A. C.; Jessup, J. M.; Hosteller, R.; Cleary, K.; Signer, S. H.; Davidson, N.; Baylin, S.; Devilee, P.; Glover, T.; Collins, F. S.; Weslon, A.; Modali, R.; Harris, C. C.; Vogelstein, B. *Mutations in the p53 gene occur in diverse human tumour types*. *Nature* **1989**, *342*, 705-708.
35. Momand, J.; Jung, D.; Wilczynski, S.; Niland, J. *The MDM2 gene amplification database*. *Nucleic Acids Res.* **1998**, *26*, 3453-3459.
36. Onel, K.; Cordon-Cardo, C. *MDM2 and Prognosis*. *Mol. Cancer Res.* **2004**, *2*, 1-8.
37. Rayburn, E.; Zhang, R.; He, J.; Wang, H. *MDM2 and Human Malignancies: Expression, Clinical Pathology, Prognostic Markers, and Implications for Chemotherapy*. *Curr. Cancer Drug Targets* **2005**, *5*, 27-41.
38. Moll, U. M.; Petrenko, O. *The MDM2-p53 Interaction*. *Mol. Cancer Res.* **2003**, *1*, 1001-1008.
39. Kussie, P. H.; Gorina, S.; Marechal, V.; Elenbaas, B.; Moreau, J.; Levine, A. J.; Pavletich, N. P. *Structure of the MDM2 Oncoprotein Bound to the p53 Tumor Suppressor Transactivation Domain*. *Science* **1996**, *274*, 948-953.
40. Aeluri, M.; Chamakuri, S.; Dasari, B.; Guduru, S. K. R.; Jimmidi, R.; Jogula, S.; Arya, P. *Small Molecule Modulators of Protein-Protein Interactions: Selected Case Studies*. *Chem. Rev.* **2014**, *114*, 4640-4694.
41. Azzarito, V.; Long, K.; Murphy, N. S.; Wilson, A. J. *Inhibition of α -helix-mediated protein-protein interactions using designed molecules*. *Nat. Chem.* **2013**, *5*, 161-173.
42. Lau, Y. H.; de Andrade, P.; Wu, Y.; Spring, D. R. *Peptide stapling techniques based on different macrocyclisation chemistries*. *Chem. Soc. Rev.* **2015**, *44*, 91-102.
43. Tyndall, J. D. A.; Nall, T.; Fairlie, D. P. *Proteases Universally Recognize Beta Strands In Their Active Sites*. *Chem. Rev.* **2005**, *105*, 973-1000.
44. Henchey, L. K.; Jochim, A. L.; Arora, P. S. *Contemporary strategies for the stabilization of peptides in the α -helical conformation*. *Curr. Opin. Chem. Biol.* **2008**, *12*, 692-697.
45. Schafmeister, C. E.; Po, J.; Verdine, G. L. *An All-Hydrocarbon Cross-Linking System for Enhancing the Helicity and Metabolic Stability of Peptides*. *J. Am. Chem. Soc.* **2000**, *122*, 5891-5892.
46. Bernal, F.; Wade, M.; Godes, M.; Davis, T. N.; Whitehead, D. G.; Kung, A. L.; Wahl, G. M.; Walensky, L. D. *A Stapled p53 Helix Overcomes HDMX-Mediated Suppression of p53*. *Cancer Cell* **2010**, *18*, 411-422.

47. Baek, S.; Kutchukian, P. S.; Verdine, G. L.; Huber, R.; Holak, T. A.; Lee, K. W.; Popowicz, G. M. *Structure of the Stapled p53 Peptide Bound to Mdm2*. J. Am. Chem. Soc. **2011**, *134*, 103-106.
48. Vassilev, L. T.; Vu, B. T.; Graves, B.; Carvajal, D.; Podlaski, F.; Filipovic, Z.; Kong, N.; Kammlott, U.; Lukacs, C.; Klein, C.; Fotouhi, N.; Liu, E. A. *In Vivo Activation of the p53 Pathway by Small-Molecule Antagonists of MDM2*. Science **2004**, *303*, 844-848.
49. Grasberger, B. L.; Lu, T.; Schubert, C.; Parks, D. J.; Carver, T. E.; Koblisch, H. K.; Cummings, M. D.; LaFrance, L. V.; Milkiewicz, K. L.; Calvo, R. R.; Maguire, D.; Lattanze, J.; Franks, C. F.; Zhao, S.; Ramachandren, K.; Bylebyl, G. R.; Zhang, M.; Manthey, C. L.; Petrella, E. C.; Pantoliano, M. W.; Deckman, I. C.; Spurlino, J. C.; Maroney, A. C.; Tomczuk, B. E.; Molloy, C. J.; Bone, R. F. *Discovery and Cocrystal Structure of Benzodiazepinedione HDM2 Antagonists That Activate p53 in Cells*. J. Med. Chem. **2005**, *48*, 909-912.
50. Allen, J. G.; Bourbeau, M. P.; Wohlhieter, G. E.; Bartberger, M. D.; Michelsen, K.; Hungate, R.; Gadwood, R. C.; Gaston, R. D.; Evans, B.; Mann, L. W.; Matison, M. E.; Schneider, S.; Huang, X.; Yu, D.; Andrews, P. S.; Reichelt, A.; Long, A. M.; Yakowec, P.; Yang, E. Y.; Lee, T. A.; Oliner, J. D. *Discovery and Optimization of Chromenotriazolopyrimidines as Potent Inhibitors of the Mouse Double Minute 2–Tumor Protein 53 Protein–Protein Interaction*. J. Med. Chem. **2009**, *52*, 7044-7053.
51. Orner, B. P.; Ernst, J. T.; Hamilton, A. D. *Toward Proteomimetics: Terphenyl Derivatives as Structural and Functional Mimics of Extended Regions of an α -Helix*. J. Am. Chem. Soc. **2001**, *123*, 5382-5383.
52. Yin, H.; Lee, G.-i.; Park, H. S.; Payne, G. A.; Rodriguez, J. M.; Sebti, S. M.; Hamilton, A. D. *Terphenyl-Based Helical Mimetics That Disrupt the p53/HDM2 Interaction*. Angew. Chem., Int. Ed. **2005**, *44*, 2704-2707.
53. Cummings, C. G.; Hamilton, A. D. *Disrupting protein–protein interactions with non-peptidic, small molecule α -helix mimetics*. Curr. Opin. Chem. Biol. **2010**, *14*, 341-346.
54. Plante, J. P.; Burnley, T.; Malkova, B.; Webb, M. E.; Warriner, S. L.; Edwards, T. A.; Wilson, A. J. *Oligobenzamide proteomimetic inhibitors of the p53-hDM2 protein–protein interaction*. Chem. Commun. **2009**, 5091-5093.
55. Lee, J. H.; Zhang, Q.; Jo, S.; Chai, S. C.; Oh, M.; Im, W.; Lu, H.; Lim, H.-S. *Novel Pyrrolopyrimidine-Based α -Helix Mimetics: Cell-Permeable Inhibitors of Protein–Protein Interactions*. J. Am. Chem. Soc. **2011**, *133*, 676-679.
56. Brown, Z. Z.; Akula, K.; Arzumanyan, A.; Alleva, J.; Jackson, M.; Bichenkov, E.; Sheffield, J. B.; Feitelson, M. A.; Schafmeister, C. E. *A Spiroligomer α -Helix Mimic That Binds HDM2, Penetrates Human Cells and Stabilizes HDM2 in Cell Culture*. PLoS ONE **2012**, *7*, e45948.

57. Fasan, R.; Dias, R. L. A.; Moehle, K.; Zerbe, O.; Vrijbloed, J. W.; Obrecht, D.; Robinson, J. A. *Using a β -Hairpin To Mimic an α -Helix: Cyclic Peptidomimetic Inhibitors of the p53–HDM2 Protein–Protein Interaction*. *Angew. Chem., Int. Ed.* **2004**, *43*, 2109-2112.
58. Fasan, R.; Dias, R. L. A.; Moehle, K.; Zerbe, O.; Obrecht, D.; Mittl, P. R. E.; Grütter, M. G.; Robinson, J. A. *Structure–Activity Studies in a Family of β -Hairpin Protein Epitope Mimetic Inhibitors of the p53–HDM2 Protein–Protein Interaction*. *Chembiochem* **2006**, *7*, 515-526.
59. Yin, H.; Lee, G.-i.; Sedey, K. A.; Kutzki, O.; Park, H. S.; Orner, B. P.; Ernst, J. T.; Wang, H.-G.; Sebt, S. M.; Hamilton, A. D. *Terphenyl-Based Bak BH3 α -Helical Proteomimetics as Low-Molecular-Weight Antagonists of Bcl-xL*. *J. Am. Chem. Soc.* **2005**, *127*, 10191-10196.
60. Vu, B.; Wovkulich, P.; Pizzolato, G.; Lovey, A.; Ding, Q.; Jiang, N.; Liu, J.-J.; Zhao, C.; Glenn, K.; Wen, Y.; Tovar, C.; Packman, K.; Vassilev, L.; Graves, B. *Discovery of RG7112: A Small-Molecule MDM2 Inhibitor in Clinical Development*. *ACS Med. Chem. Lett.* **2013**, *4*, 466-469.
61. Ding, Q.; Zhang, Z.; Liu, J.-J.; Jiang, N.; Zhang, J.; Ross, T. M.; Chu, X.-J.; Bartkovitz, D.; Podlaski, F.; Janson, C.; Tovar, C.; Filipovic, Z. M.; Higgins, B.; Glenn, K.; Packman, K.; Vassilev, L. T.; Graves, B. *Discovery of RG7388, a Potent and Selective p53–MDM2 Inhibitor in Clinical Development*. *J. Med. Chem.* **2013**, *56*, 5979-5983.
62. Sun, D.; Li, Z.; Rew, Y.; Gribble, M.; Bartberger, M. D.; Beck, H. P.; Canon, J.; Chen, A.; Chen, X.; Chow, D.; Deignan, J.; Duquette, J.; Eksterowicz, J.; Fisher, B.; Fox, B. M.; Fu, J.; Gonzalez, A. Z.; Gonzalez-Lopez De Turiso, F.; Houze, J. B.; Huang, X.; Jiang, M.; Jin, L.; Kayser, F.; Liu, J.; Lo, M.-C.; Long, A. M.; Lucas, B.; McGee, L. R.; McIntosh, J.; Mihalic, J.; Oliner, J. D.; Osgood, T.; Peterson, M. L.; Roveto, P.; Saiki, A. Y.; Shaffer, P.; Toteva, M.; Wang, Y.; Wang, Y. C.; Wortman, S.; Yakowec, P.; Yan, X.; Ye, Q.; Yu, D.; Yu, M.; Zhao, X.; Zhou, J.; Zhu, J.; Olson, S. H.; Medina, J. C. *Discovery of AMG 232, a Potent, Selective, and Orally Bioavailable MDM2–p53 Inhibitor in Clinical Development*. *J. Med. Chem.* **2014**, *57*, 1454-1472.
63. Lea, W. A.; Simeonov, A. *Fluorescence polarization assays in small molecule screening*. *Expert Opin. Drug Discov.* **2011**, *6*, 17-32.
64. Moerke, N. J. *Fluorescence Polarization (FP) Assays for Monitoring Peptide-Protein or Nucleic Acid-Protein Binding*. John Wiley & Sons, Inc.: **2009**;
65. Milroy, L.-G.; Grossmann, T. N.; Hennig, S.; Brunsveld, L.; Ottmann, C. *Modulators of Protein–Protein Interactions*. *Chem. Rev.* **2014**, *114*, 4695-4748.
66. Navratilova, I.; Hopkins, A. L. *Emerging role of surface plasmon resonance in fragment-based drug discovery*. *Future Med. Chem.* **2011**, *3*, 1809-1820.

67. Dalvit, C.; Fogliatto, G.; Stewart, A.; Veronesi, M.; Stockman, B. *WaterLOGSY as a method for primary NMR screening: Practical aspects and range of applicability*. J Biomol NMR **2001**, *21*, 349-359.
68. Fernandez-Alonso, M. d. C.; Alvaro Berbis, M.; Canales, A.; Arda, A.; Javier Canada, F.; Jimenez-Barbero, J. *New Applications of High-Resolution NMR in Drug Discovery and Development*. The Royal Society of Chemistry: **2013**; 7-42.
69. Fielding, L. *NMR methods for the determination of protein–ligand dissociation constants*. Prog. Nucl. Mag. Res. Sp. **2007**, *51*, 219-242.
70. Cooper, W. J.; Waters, M. L. *Molecular recognition with designed peptides and proteins*. Curr. Opin. Chem. Biol. **2005**, *9*, 627-631.
71. Lewandowska, A.; Oldziej, S.; Liwo, A.; Scheraga, H. A. *β -hairpin-forming peptides; models of early stages of protein folding*. Biophys. Chem. **2010**, *151*, 1-9.
72. Robinson, J. A. *β -Hairpin Peptidomimetics: Design, Structures and Biological Activities*. Acc. Chem. Res. **2008**, *41*, 1278-1288.
73. Yudin, A. K. *Macrocycles: lessons from the distant past, recent developments, and future directions*. Chem. Sci. **2015**, *6*, 30-49.
74. Wilmot, C. M.; Thornton, J. M. *Analysis and prediction of the different types of β -turn in proteins*. J. Mol. Biol. **1988**, *203*, 221-232.
75. Stotz, C. E.; Topp, E. M. *Applications of model β -hairpin peptides*. J. Pharm. Sci. **2004**, *93*, 2881-2894.
76. Cochran, A. G.; Skelton, N. J.; Starovasnik, M. A. *Tryptophan zippers: Stable, monomeric β -hairpins*. Proc. Natl. Acad. Sci. U.S.A **2001**, *98*, 5578-5583.
77. Minor, D. L.; Kim, P. S. *Measurement of the β -sheet-forming propensities of amino acids*. Nature **1994**, *367*, 660-663.
78. Danelius, E.; Brath, U.; Erdélyi, M. *Insight into β -Hairpin Stability: Interstrand Hydrogen Bonding*. Synlett **2013**, *24*, 2407-2410.
79. Erdélyi, M.; Karlén, A.; Gogoll, A. *A New Tool in Peptide Engineering: A Photoswitchable Stilbene-type β -Hairpin Mimetic*. Chem. Eur. J. **2006**, *12*, 403-412.
80. Merrifield, R. B. *Solid Phase Peptide Synthesis. I. The Synthesis of a Tetrapeptide*. J. Am. Chem. Soc. **1963**, *85*, 2149-2154.
81. Amblard, M.; Fehrentz, J.-A.; Martinez, J.; Subra, G. *Methods and protocols of modern solid phase peptide synthesis*. Mol Biotechnol **2006**, *33*, 239-254.
82. Chandrudu, S.; Simerska, P.; Toth, I. *Chemical Methods for Peptide and Protein Production*. Molecules **2013**, *18*, 4373-4388.
83. Isidro-Llobet, A.; Álvarez, M.; Albericio, F. *Amino Acid-Protecting Groups*. Chem. Rev. **2009**, *109*, 2455-2504.
84. Barany, G.; Merrifield, R. B. *A new amino protecting group removable by reduction. Chemistry of the dithiasuccinoyl (Dts) function*. J. Am. Chem. Soc. **1977**, *99*, 7363-7365.

85. Góngora-Benítez, M.; Tulla-Puche, J.; Albericio, F. *Handles for Fmoc Solid-Phase Synthesis of Protected Peptides*. ACS. Comb. Sci. **2013**, *15*, 217-228.
86. El-Faham, A.; Albericio, F. *Peptide Coupling Reagents, More than a Letter Soup*. Chem. Rev. **2011**, 6557–6602.
87. Cicero, D. O.; Barbato, G.; Bazzo, R. *NMR Analysis of Molecular Flexibility in Solution: A New Method for the Study of Complex Distributions of Rapidly Exchanging Conformations. Application to a 13-Residue Peptide with an 8-Residue Loop*. J. Am. Chem. Soc. **1995**, *117*, 1027-1033.
88. Koivisto, J. J.; Kumpulainen, E. T. T.; Koskinen, A. M. P. *Conformational ensembles of flexible β -turn mimetics in DMSO-*d*₆*. Org. Biomol. Chem. **2010**, *8*, 2103-2116.
89. Andersson, H.; Demaegdt, H.; Vauquelin, G.; Lindeberg, G.; Karlén, A.; Hallberg, M.; Erdélyi, M. t.; Hallberg, A. *Disulfide Cyclized Tripeptide Analogues of Angiotensin IV as Potent and Selective Inhibitors of Insulin-Regulated Aminopeptidase (IRAP)*. J. Med. Chem. **2010**, *53*, 8059-8071.
90. Grimmer, C.; Moore, T. W.; Padwa, A.; Prussia, A.; Wells, G.; Wu, S.; Sun, A.; Snyder, J. P. *Antiviral Atropisomers: Conformational Energy Surfaces by NMR for Host-Directed Myxovirus Blockers*. J. Chem. Inf. Model. **2014**, *54*, 2214-2223.
91. Fridén-Saxin, M.; Seifert, T.; Hansen, L. K.; Grøtli, M.; Erdelyi, M.; Luthman, K. *Proline-mediated formation of novel chroman-4-one tetrahydropyrimidines*. Tetrahedron **2012**, *68*, 7035-7040.
92. Kessler, H.; Griesinger, C.; Lautz, J.; Mueller, A.; Van Gunsteren, W. F.; Berendsen, H. J. C. *Conformational dynamics detected by nuclear magnetic resonance NOE values and J coupling constants*. J. Am. Chem. Soc. **1988**, *110*, 3393-3396.
93. Schmidt, J. M. *A versatile component-coupling model to account for substituent effects: Application to polypeptide ϕ and χ ₁ torsion related 3J data*. J. Magn. Reson. **2007**, *186*, 34-50.
94. Nevins, N.; Cicero, D.; Snyder, J. P. *A Test of the Single-Conformation Hypothesis in the Analysis of NMR Data for Small Polar Molecules: A Force Field Comparison*. J. Org. Chem. **1999**, *64*, 3979-3986.
95. MacroModel, version 9.9, Schrödinger, LLC, New York, NY, 2012.
96. Malesevic, M.; Strijowski, U.; Bächle, D.; Sewald, N. *An improved method for the solution cyclization of peptides under pseudo-high dilution conditions*. J. Biotechnol. **2004**, *112*, 73-77.
97. Pearson, D. A.; Blanchette, M.; Baker, M. L.; Guindon, C. A. *Trialkylsilanes as scavengers for the trifluoroacetic acid deblocking of protecting groups in peptide synthesis*. Tetrahedron Lett. **1989**, *30*, 2739-2742.
98. Mehta, A.; Jaouhari, R.; Benson, T. J.; Douglas, K. T. *Improved efficiency and selectivity in peptide synthesis: Use of triethylsilane as a carbocation scavenger in deprotection*

- of *t*-butyl esters and *t*-butoxycarbonyl-protected sites. *Tetrahedron Lett.* **1992**, *33*, 5441-5444.
99. Jacobsen, N. E. *NMR Spectroscopy Explained: Simplified Theory, Applications and Examples for Organic Chemistry and Structural Biology*. 1st ed.; John Wiley & Sons, Inc.: New Jersey, **2007**.
100. Hoffman, R. E.; Becker, E. D. *Temperature dependence of the ¹H chemical shift of tetramethylsilane in chloroform, methanol, and dimethylsulfoxide*. *J. Magn. Reson.* **2005**, *176*, 87-98.
101. Erdelyi, M.; Langer, V.; Karlen, A.; Gogoll, A. *Insight into β -hairpin stability: a structural and thermodynamic study of diastereomeric β -hairpin mimetics*. *New J. Chem.* **2002**, *26*, 834-843.
102. Wishart, D. S.; Sykes, B. D.; Richards, F. M. *Relationship between nuclear magnetic resonance chemical shift and protein secondary structure*. *J. Mol. Biol.* **1991**, *222*, 311-333.
103. Kessler, H. *Conformation and Biological Activity of Cyclic Peptides*. *Angew. Chem., Int. Ed. Engl.* **1982**, *21*, 512-523.
104. Reed, D.; Shen, Y.; Shelat, A. A.; Arnold, L. A.; Ferreira, A. M.; Zhu, F.; Mills, N.; Smithson, D. C.; Regni, C. A.; Bashford, D.; Cicero, S. A.; Schulman, B. A.; Jochemsen, A. G.; Guy, R. K.; Dyer, M. A. *Identification and Characterization of the First Small Molecule Inhibitor of MDMX*. *J. Biol. Chem.* **2010**, *285*, 10786-10796.
105. Dyrager, C.; Börjesson, K.; Dinér, P.; Elf, A.; Albinsson, B.; Wilhelmsson, L. M.; Grøtli, M. *Synthesis and Photophysical Characterisation of Fluorescent 8-(1H-1,2,3-Triazol-4-yl)adenosine Derivatives*. *Eur. J. Org. Chem.* **2009**, *2009*, 1515-1521.
106. Dierckx, A.; Dinér, P.; El-Sagheer, A. H.; Kumar, J. D.; Brown, T.; Grøtli, M.; Wilhelmsson, L. M. *Characterization of photophysical and base-mimicking properties of a novel fluorescent adenine analogue in DNA*. *Nucleic Acids Res.* **2011**, *39*, 4513-4524.
107. O'Mahony, G.; Ehrman, E.; Grøtli, M. *Synthesis and photophysical properties of novel cyclonucleosides—substituent effects on fluorescence emission*. *Tetrahedron* **2008**, *64*, 7151-7158.
108. Redwan, I. N.; Bliman, D.; Tokugawa, M.; Lawson, C.; Grøtli, M. *Synthesis and photophysical characterization of 1- and 4-(purinyl)triazoles*. *Tetrahedron* **2013**, *69*, 8857-8864.
109. Pedersen, D. S.; Abell, A. *1,2,3-Triazoles in Peptidomimetic Chemistry*. *Eur. J. Org. Chem.* **2011**, *2011*, 2399-2411.
110. Davis, M. R.; Singh, E. K.; Wahyudi, H.; Alexander, L. D.; Kunicki, J. B.; Nazarova, L. A.; Fairweather, K. A.; Giltrap, A. M.; Jolliffe, K. A.; McAlpine, S. R. *Synthesis of sansalvamide A peptidomimetics: triazole, oxazole, thiazole, and pseudoproline containing compounds*. *Tetrahedron* **2012**, *68*, 1029-1051.
111. Horne, W. S.; Yadav, M. K.; Stout, C. D.; Ghadiri, M. R. *Heterocyclic Peptide Backbone Modifications in an α -Helical Coiled Coil*. *J. Am. Chem. Soc.* **2004**, *126*, 15366-15367.

112. Valverde, I. E.; Bauman, A.; Kluba, C. A.; Vomstein, S.; Walter, M. A.; Mindt, T. L. *1,2,3-Triazoles as Amide Bond Mimics: Triazole Scan Yields Protease-Resistant Peptidomimetics for Tumor Targeting*. *Angew. Chem., Int. Ed.* **2013**, *52*, 8957-8960.
113. Horton, D. A.; Bourne, G. T.; Smythe, M. L. *The Combinatorial Synthesis of Bicyclic Privileged Structures or Privileged Substructures*. *Chem. Rev.* **2003**, *103*, 893-930.
114. Rosemeyer, H. *The Chemodiversity of Purine as a Constituent of Natural Products*. *Chem. Biodiversity* **2004**, *1*, 361-401.
115. Legraverend, M.; Grierson, D. S. *The purines: Potent and versatile small molecule inhibitors and modulators of key biological targets*. *Bioorg. Med. Chem.* **2006**, *14*, 3987-4006.
116. Vitaku, E.; Smith, D. T.; Njardarson, J. T. *Analysis of the Structural Diversity, Substitution Patterns, and Frequency of Nitrogen Heterocycles among U.S. FDA Approved Pharmaceuticals*. *J. Med. Chem.* **2014**, *57*, 10257-10274.
117. Legraverend, M. *Recent advances in the synthesis of purine derivatives and their precursors*. *Tetrahedron* **2008**, *64*, 8585-8603.
118. Meldal, M.; Tornøe, C. W. *Cu-Catalyzed Azide-Alkyne Cycloaddition*. *Chem. Rev.* **2008**, *108*, 2952-3015.
119. Zhang, L.; Chen, X. G.; Xue, P.; Sun, H. H. Y.; Williams, I. D.; Sharpless, K. B.; Fokin, V. V.; Jia, G. C. *Ruthenium-catalyzed cycloaddition of alkynes and organic azides*. *J. Am. Chem. Soc.* **2005**, *127*, 15998-15999.
120. Boren, B. C.; Narayan, S.; Rasmussen, L. K.; Zhang, L.; Zhao, H. T.; Lin, Z. Y.; Jia, G. C.; Fokin, V. V. *Ruthenium-catalyzed azide-alkyne cycloaddition: Scope and mechanism*. *J. Am. Chem. Soc.* **2008**, *130*, 8923-8930.
121. Johansson, J. R.; Lincoln, P.; Norden, B.; Kann, N. *Sequential One-Pot Ruthenium-Catalyzed Azide-Alkyne Cycloaddition from Primary Alkyl Halides and Sodium Azide*. *J. Org. Chem.* **2011**, *76*, 2355-2359.
122. Kwok, S. W.; Fotsing, J. R.; Fraser, R. J.; Rodionov, V. O.; Fokin, V. V. *Transition-Metal-Free Catalytic Synthesis of 1,5-Diaryl-1,2,3-triazoles*. *Org. Lett.* **2010**, *12*, 4217-4219.
123. Bräse, S.; Gil, C.; Knepper, K.; Zimmermann, V. *Organic Azides: An Exploding Diversity of a Unique Class of Compounds*. *Angew. Chem., Int. Ed.* **2005**, *44*, 5188-5240.
124. Ju, Y.; Kumar, D.; Varma, R. S. *Revisiting Nucleophilic Substitution Reactions: Microwave-Assisted Synthesis of Azides, Thiocyanates, and Sulfones in an Aqueous Medium*. *J. Org. Chem.* **2006**, *71*, 6697-6700.
125. Chinchilla, R.; Nájera, C. *The Sonogashira Reaction: A Booming Methodology in Synthetic Organic Chemistry*. *Chem. Rev.* **2007**, *107*, 874-922.
126. Čechová, L.; Jansa, P.; Šála, M.; Dračínský, M.; Holý, A.; Janeba, Z. *The optimized microwave-assisted decomposition of formamides and its synthetic utility in the amination reactions of purines*. *Tetrahedron* **2011**, *67*, 866-871.

127. Huang, L.-K.; Cherng, Y.-C.; Cheng, Y.-R.; Jang, J.-P.; Chao, Y.-L.; Cherng, Y.-J. *An efficient synthesis of substituted cytosines and purines under focused microwave irradiation*. *Tetrahedron* **2007**, *63*, 5323-5327.
128. Camaioni, E.; Costanzi, S.; Vittori, S.; Volpini, R.; Klotz, K.-N.; Cristalli, G. *New substituted 9-alkylpurines as adenosine receptor ligands*. *Bioorg. Med. Chem.* **1998**, *6*, 523-533.
129. Hirota, K.; Kazaoka, K.; Niimoto, I.; Sajiki, H. *Efficient synthesis of 2,9-disubstituted 8-hydroxyadenine derivatives*. *Org. Biomol. Chem.* **2003**, *1*, 1354-1365.
130. Chang, Y.-T.; Gray, N. S.; Rosania, G. R.; Sutherlin, D. P.; Kwon, S.; Norman, T. C.; Sarohia, R.; Leost, M.; Meijer, L.; Schultz, P. G. *Synthesis and application of functionally diverse 2,6,9-trisubstituted purine libraries as CDK inhibitors*. *Chem. Biol.* **1999**, *6*, 361-375.
131. Fletcher, S.; Shahani, V. M.; Gunning, P. T. *Facile and efficient access to 2,6,9-trisubstituted purines through sequential N9, N2 Mitsunobu reactions*. *Tetrahedron Lett.* **2009**, *50*, 4258-4261.
132. Fletcher, S.; Shahani, V. M.; Lough, A. J.; Gunning, P. T. *Concise access to N9-mono-, N2-mono- and N2,N9-di-substituted guanines via efficient Mitsunobu reactions*. *Tetrahedron* **2010**, *66*, 4621-4632.
133. Michelsen, K.; Jordan, J. B.; Lewis, J.; Long, A. M.; Yang, E.; Rew, Y.; Zhou, J.; Yakowec, P.; Schnier, P. D.; Huang, X.; Poppe, L. *Ordering of the N-Terminus of Human MDM2 by Small Molecule Inhibitors*. *J. Am. Chem. Soc.* **2012**, *134*, 17059-17067.
134. Rew, Y.; Sun, D.; Gonzalez-Lopez De Turiso, F.; Bartberger, M. D.; Beck, H. P.; Canon, J.; Chen, A.; Chow, D.; Deignan, J.; Fox, B. M.; Gustin, D.; Huang, X.; Jiang, M.; Jiao, X.; Jin, L.; Kayser, F.; Kopecky, D. J.; Li, Y.; Lo, M.-C.; Long, A. M.; Michelsen, K.; Oliner, J. D.; Osgood, T.; Ragains, M.; Saiki, A. Y.; Schneider, S.; Toteva, M.; Yakowec, P.; Yan, X.; Ye, Q.; Yu, D.; Zhao, X.; Zhou, J.; Medina, J. C.; Olson, S. H. *Structure-Based Design of Novel Inhibitors of the MDM2-p53 Interaction*. *J. Med. Chem.* **2012**, *55*, 4936-4954.
135. Gonzalez-Lopez de Turiso, F.; Sun, D.; Rew, Y.; Bartberger, M. D.; Beck, H. P.; Canon, J.; Chen, A.; Chow, D.; Correll, T. L.; Huang, X.; Julian, L. D.; Kayser, F.; Lo, M.-C.; Long, A. M.; McMinn, D.; Oliner, J. D.; Osgood, T.; Powers, J. P.; Saiki, A. Y.; Schneider, S.; Shaffer, P.; Xiao, S.-H.; Yakowec, P.; Yan, X.; Ye, Q.; Yu, D.; Zhao, X.; Zhou, J.; Medina, J. C.; Olson, S. H. *Rational Design and Binding Mode Duality of MDM2-p53 Inhibitors*. *J. Med. Chem.* **2013**, *56*, 4053-4070.
136. Schrödinger, Glide version 5.8, (2012) LLC, New York.
137. Yun, S.-W.; Kang, N.-Y.; Park, S.-J.; Ha, H.-H.; Kim, Y. K.; Lee, J.-S.; Chang, Y.-T. *Diversity Oriented Fluorescence Library Approach (DOFLA) for Live Cell Imaging Probe Development*. *Acc. Chem. Res.* **2014**, *47*, 1277-1286.

138. Kim, D.; Jun, H.; Lee, H.; Hong, S.-S.; Hong, S. *Development of New Fluorescent Xanthines as Kinase Inhibitors*. *Org. Lett.* **2010**, *12*, 1212-1215.
139. Son, J.; Lee, J.-J.; Lee, J.-S.; Schüller, A.; Chang, Y.-T. *Isozyme-Specific Fluorescent Inhibitor of Glutathione S-Transferase Omega 1*. *ACS Chem. Biol.* **2010**, *5*, 449-453.
140. Minetti, P.; Tinti, M. O.; Carminati, P.; Castorina, M.; Di Cesare, M. A.; Di Serio, S.; Gallo, G.; Ghirardi, O.; Giorgi, F.; Giorgi, L.; Piersanti, G.; Bartoccini, F.; Tarzia, G. *2-n-Butyl-9-methyl-8-[1,2,3]triazol-2-yl-9H-purin-6-ylamine and Analogues as A2A Adenosine Receptor Antagonists. Design, Synthesis, and Pharmacological Characterization*. *J. Med. Chem.* **2005**, *48*, 6887-6896.
141. Lambertucci, C.; Antonini, I.; Buccioni, M.; Ben, D. D.; Kachare, D. D.; Volpini, R.; Klotz, K.-N.; Cristalli, G. *8-Bromo-9-alkyl adenine derivatives as tools for developing new adenosine A2A and A2B receptors ligands*. *Bioorg. Med. Chem.* **2009**, *17*, 2812-2822.
142. Borrmann, T.; Abdelrahman, A.; Volpini, R.; Lambertucci, C.; Alksnis, E.; Gorzalka, S.; Knospe, M.; Schiedel, A. C.; Cristalli, G.; Müller, C. E. *Structure–Activity Relationships of Adenine and Deazaadenine Derivatives as Ligands for Adenine Receptors, a New Purinergic Receptor Family*. *J. Med. Chem.* **2009**, *52*, 5974-5989.
143. Maity, J.; Stromberg, R. *An Efficient and Facile Methodology for Bromination of Pyrimidine and Purine Nucleosides with Sodium Monobromoisocyanurate (SMBI)*. *Molecules* **2013**, *18*, 12740-12750.
144. Rayala, R.; Wnuk, S. F. *Bromination at C-5 of pyrimidine and C-8 of purine nucleosides with 1,3-dibromo-5,5-dimethylhydantoin*. *Tetrahedron Lett.* **2012**, *53*, 3333-3336.
145. Wu, T. Y. H.; Schultz, P. G.; Ding, S. *One-Pot Two-Step Microwave-Assisted Reaction in Constructing 4,5-Disubstituted Pyrazolopyrimidines*. *Org. Lett.* **2003**, *5*, 3587-3590.
146. Fridén-Saxin, M.; Seifert, T.; Landergren, M. R.; Suuronen, T.; Lahtela-Kakkonen, M.; Jarho, E. M.; Luthman, K. *Synthesis and Evaluation of Substituted Chroman-4-one and Chromone Derivatives as Sirtuin 2-Selective Inhibitors*. *J. Med. Chem.* **2012**, *55*, 7104-7113.
147. Inoue, T.; Morita, M.; Tojo, T.; Nagashima, A.; Moritomo, A.; Imai, K.; Miyake, H. *Synthesis and SAR study of new thiazole derivatives as vascular adhesion protein-1 (VAP-1) inhibitors for the treatment of diabetic macular edema: Part 2*. *Bioorg. Med. Chem.* **2013**, *21*, 2478-2494.
148. O'Brien, J. M.; Kingsbury, J. S. *A Practical Synthesis of 3-Acyl Cyclobutanones by [2 + 2] Annulation. Mechanism and Utility of the Zn(II)-Catalyzed Condensation of α -Chloroamines with Electron-Deficient Alkenes*. *J. Org. Chem.* **2011**, *76*, 1662-1672.
149. Gillmore, A. T.; Badland, M.; Crook, C. L.; Castro, N. M.; Critcher, D. J.; Fussell, S. J.; Jones, K. J.; Jones, M. C.; Kougoulos, E.; Mathew, J. S.; McMillan, L.; Pearce, J. E.; Rawlinson, F. L.; Sherlock, A. E.; Walton, R. *Multikilogram Scale-*

- Up of a Reductive Alkylation Route to a Novel PARP Inhibitor.* Org. Process Res. Dev. **2012**, *16*, 1897-1904.
150. Suzuki, S.; Nagata, A.; Kuratsu, M.; Kozaki, M.; Tanaka, R.; Shiomi, D.; Sugisaki, K.; Toyota, K.; Sato, K.; Takui, T.; Okada, K. *Trinitroxide-Trioxyltriphenylamine: Spin-State Conversion from Triradical Doublet to Diradical Cation Triplet by Oxidative Modulation of a π -Conjugated System.* Angew. Chem., Int. Ed. **2012**, *51*, 3193-3197.
151. Zhou, H.-B.; Lee, J. H.; Mayne, C. G.; Carlson, K. E.; Katzenellenbogen, J. A. *Imaging Progesterone Receptor in Breast Tumors: Synthesis and Receptor Binding Affinity of Fluoroalkyl-Substituted Analogues of Tanaproget.* J. Med. Chem. **2010**, *53*, 3349-3360.
152. Araki, T.; Ozawa, T.; Yokoe, H.; Kanematsu, M.; Yoshida, M.; Shishido, K. *Diastereoselective Intramolecular Carbamoylketene/Alkene [2 + 2] Cycloaddition: Enantioselective Access to Pyrrolidinoindoline Alkaloids.* Org. Lett. **2012**, *15*, 200-203.
153. Marks, I. S.; Kang, J. S.; Jones, B. T.; Landmark, K. J.; Cleland, A. J.; Taton, T. A. *Strain-Promoted "Click" Chemistry for Terminal Labeling of DNA.* Bioconjugate Chem. **2011**, *22*, 1259-1263.
154. Reeves, W. P.; Lu, C. V.; Russel, J. S. *Bromination of Aniline with Pyridinium Hydrobromide Perbromide: some Mechanistic Considerations.* Mendeleev Commun. **1994**, *4*, 223-224.
155. Tullberg, M.; Grötli, M.; Luthman, K. *Synthesis of Functionalized, Unsymmetrical 1,3,4,6-Tetrasubstituted 2,5-Diketopiperazines.* J. Org. Chem. **2007**, *72*, 195-199.
156. Tullberg, M.; Grötli, M.; Luthman, K. *Efficient synthesis of 2,5-diketopiperazines using microwave assisted heating.* Tetrahedron **2006**, *62*, 7484-7491.
157. Tullberg, M.; Luthman, K.; Grötli, M. *Microwave-Assisted Solid-Phase Synthesis of 2,5-Diketopiperazines: Solvent and Resin Dependence.* J. Comb. Chem. **2006**, *8*, 915-922.
158. Jam, F.; Tullberg, M.; Luthman, K.; Grötli, M. *Microwave assisted synthesis of spiro-2,5-diketopiperazines.* Tetrahedron **2007**, *63*, 9881-9889.
159. Borthwick, A. D. *2,5-Diketopiperazines: Synthesis, Reactions, Medicinal Chemistry, and Bioactive Natural Products.* Chem. Rev. **2012**, *112*, 3641-3716.
160. Gonzalez, J. F.; Ortin, I.; de la Cuesta, E.; Menendez, J. C. *Privileged scaffolds in synthesis: 2,5-piperazinediones as templates for the preparation of structurally diverse heterocycles.* Chem. Soc. Rev. **2012**, *41*, 6902-6915.
161. Sun, X.; Rai, R.; MacKerell Jr, A. D.; Faden, A. I.; Xue, F. *Facile one-step synthesis of 2,5-diketopiperazines.* Tetrahedron Lett. **2014**, *55*, 1905-1908.
162. Bull, S. D.; Davies, S. G.; Moss, W. O. *Practical synthesis of Schöllkopf's bis-lactim ether chiral auxiliary: (3S)-3,6-dihydro-2,5-dimethoxy-3-isopropyl-pyrazine.* Tetrahedron: Asymmetry **1998**, *9*, 321-327.
163. Woodard, R. W. *Stereochemistry of cyclic dipeptides. Assignment of the prochiral methylenes of 1-aminocyclopropane-1-carboxylic acid.* J. Org. Chem. **1985**, *50*, 4796-4799.

164. Ugi, I.; Steinbrückner, C. *Über ein neues Kondensations-Prinzip*. *Angew. Chem.* **1960**, *72*, 267-268.
165. Touré, B. B.; Hall, D. G. *Natural Product Synthesis Using Multicomponent Reaction Strategies*. *Chem. Rev.* **2009**, *109*, 4439-4486.
166. Dömling, A.; Wang, W.; Wang, K. *Chemistry and Biology Of Multicomponent Reactions*. *Chem. Rev.* **2012**, *112*, 3083-3135.
167. Dömling, A. *Recent Developments in Isocyanide Based Multicomponent Reactions in Applied Chemistry*. *Chem. Rev.* **2006**, *106*, 17-89.
168. Nishizawa, R.; Nishiyama, T.; Hisaichi, K.; Minamoto, C.; Murota, M.; Takaoka, Y.; Nakai, H.; Tada, H.; Sagawa, K.; Shibayama, S.; Fukushima, D.; Maeda, K.; Mitsuya, H. *Discovery of 4-[4-({(3R)-1-butyl-3-[(R)-cyclohexyl(hydroxy)methyl]-2,5-dioxo-1,4,9-triazaspiro[5.5]undec-9-yl}methyl)phenoxy]benzoic acid hydrochloride: A highly potent orally available CCR5 selective antagonist*. *Bioorg. Med. Chem.* **2011**, *19*, 4028-4042.
169. Nishizawa, R.; Nishiyama, T.; Hisaichi, K.; Hirai, K.; Habashita, H.; Takaoka, Y.; Tada, H.; Sagawa, K.; Shibayama, S.; Maeda, K.; Mitsuya, H.; Nakai, H.; Fukushima, D.; Toda, M. *Discovery of orally available spirodiketopiperazine-based CCR5 antagonists*. *Bioorg. Med. Chem.* **2010**, *18*, 5208-5223.
170. Nishizawa, R.; Nishiyama, T.; Hisaichi, K.; Hirai, K.; Habashita, H.; Takaoka, Y.; Tada, H.; Sagawa, K.; Shibayama, S.; Maeda, K.; Mitsuya, H.; Nakai, H.; Fukushima, D.; Toda, M. *Spirodiketopiperazine-based CCR5 antagonists: Improvement of their pharmacokinetic profiles*. *Bioorg. Med. Chem. Lett.* **2010**, *20*, 763-766.
171. Nishizawa, R.; Nishiyama, T.; Hisaichi, K.; Matsunaga, N.; Minamoto, C.; Habashita, H.; Takaoka, Y.; Toda, M.; Shibayama, S.; Tada, H.; Sagawa, K.; Fukushima, D.; Maeda, K.; Mitsuya, H. *Spirodiketopiperazine-based CCR5 antagonists: Lead optimization from biologically active metabolite*. *Bioorg. Med. Chem. Lett.* **2007**, *17*, 727-731.
172. Accounts of Chemical Research Strocker, A. M.; Keating, T. A.; Tempest, P. A.; Armstrong, R. W. *Use of a convertible isocyanide for generation of Ugi reaction derivatives on solid support: Synthesis of α -acylaminoesters and pyrroles*. *Tetrahedron Lett.* **1996**, *37*, 1149-1152.
173. Hulme, C.; Chappeta, S.; Dietrich, J. *A simple, cheap alternative to 'designer convertible isonitriles' expedited with microwaves*. *Tetrahedron Lett.* **2009**, *50*, 4054-4057.
174. Medeiros, G. A.; da Silva, W. A.; Bataglioni, G. A.; Ferreira, D. A. C.; de Oliveira, H. C. B.; Eberlin, M. N.; Neto, B. A. D. *Probing the mechanism of the Ugi four-component reaction with charge-tagged reagents by ESI-MS(/MS)*. *Chem. Commun.* **2014**, *50*, 338-340.
175. Marcaccini, S.; Torroba, T. *The use of the Ugi four-component condensation*. *Nat. Protocols* **2007**, *2*, 632-639.

176. Park, J. D.; Lee, K. J.; Kim, D. H. *A new inhibitor design strategy for carboxypeptidase A as exemplified by N-(2-chloroethyl)-N-methylphenylalanine*. *Bioorg. Med. Chem.* **2001**, *9*, 237-243.
177. Kühnel, E.; Laffan, D. D. P.; Lloyd-Jones, G. C.; Martínez del Campo, T.; Shepperson, I. R.; Slaughter, J. L. *Mechanism of Methyl Esterification of Carboxylic Acids by Trimethylsilyldiazomethane*. *Angew. Chem., Int. Ed.* **2007**, *46*, 7075-7078.
178. Burkhardt, E. R.; Coleridge, B. M. *Reductive amination with 5-ethyl-2-methylpyridine borane*. *Tetrahedron Lett.* **2008**, *49*, 5152-5155.
179. Fry, D. C.; Wartchow, C.; Graves, B.; Janson, C.; Lukacs, C.; Kammlott, U.; Belunis, C.; Palme, S.; Klein, C.; Vu, B. *Deconstruction of a Nutlin: Dissecting the Binding Determinants of a Potent Protein-Protein Interaction Inhibitor*. *ACS Med. Chem. Lett.* **2013**, *4*, 660-665.
180. Mutulis, F.; Erdélyi, M.; Mutule, I.; Kreicberga, J.; Yahorava, S.; Yahorau, A.; Borisova-Jan, L.; Wikberg, J. *2-(p-Hydroxybenzyl)indoles - Side Products Formed Upon Cleavage of Indole Derivatives from Carboxylated Wang Polymer - an NMR Study*. *Molecules* **2003**, *8*, 728-734.
181. Gasparro, F. P.; Kolodny, N. H. *NMR determination of the rotational barrier in N,N-dimethylacetamide. A physical chemistry experiment*. *J. Chem. Educ.* **1977**, *54*, 258.
182. Brown, H. C.; Zweifel, G. *A stereospecific cis hydration of the double bond in cyclic derivatives*. *J. Am. Chem. Soc.* **1959**, *81*, 247-247.